RESULTS AND INTERPRETATION OF PRELIMINARY AQUIFER TESTS IN BOREHOLES UE-25c #1, UE-25c #2, AND UE-25c #3, YUCCA MOUNTAIN, NYE COUNTY, NEVADA

by Arthur L. Geldon

U.S. GEOLOGICAL SURVEY

Water-Resources Investigations Report 94-4177

Prepared in cooperation with the
U.S. DEPARTMENT OF ENERGY,
NEVADA FIELD OFFICE, under
Interagency Agreement DE-AI08-92NV10874

Denver, Colorado
1996

U.S. DEPARTMENT OF THE INTERIOR

BRUCE BABBITT, Secretary

U.S. GEOLOGICAL SURVEY

Gordon P. Eaton, Director

For additional information write to:
Chief, Earth Science Investigations Program
Yucca Mountain Project Branch
U.S. Geological Survey
Box 25046, MS 421
Denver Federal Center
Denver, CO 80225

Copies of this report can be purchased from:
U.S. Geological Survey
USGS Information Services
Open-File Reports Section
Box 25286, MS 517
Denver Federal Center
Denver, CO 80225

CONTENTS

PLATES

[In pocket]

FIGURES

TABLES

CONVERSION FACTORS AND VERTICAL DATUM

Multiply inch-pound unit	By	To obtain metric unit
cubic foot per day (ft^3/d)	2.832×10^{-2}	cubic meter per day
foot	.3048	meter
foot per day (ft/d)	.3048	meter per day
foot squared per day (ft^2/d)	9.290×10^{-2}	meter squared per day
gallon (gal)	3.7854	liter
gallon per minute (gal/min)	6.309×10^{-2}	liter per second
inch (in.)	2.54	centimeter
inch of mercury (in. of mercury)	.3453	meter of water
mile	1.6093	kilometer
millidarcy (mD)	9.87×10^{-12}	square centimeter
minute per square foot (min/ft^2)	10.76	minute per square meter
pound per square inch ($lb/in.^2$)	6.895	Kilopascal
reciprocal foot (ft^{-1})	3.2808	reciprocal meter
square foot (ft^2)	9.290×10^{-2}	square meter

Degree Fahrenheit (°F) may be converted to degree Celsius (°C) by using the following equation:

$$°C = 5/9 (°F - 32).$$

Sea level: Altitudes in this report are referenced to the National Geodetic Vertical Datum of 1929 (NGVD of 1929), a geodetic datum derived from a general adjustment of the first-order level nets of the United States and Canada, formerly called the Sea Level Datum of 1929.

Results and Interpretation of Preliminary Aquifer Tests in Boreholes UE-25c #1, UE-25c #2, and UE-25c #3, Yucca Mountain, Nye County, Nevada

By Arthur L. Geldon

Abstract

Pumping and injection tests conducted in 1983 and 1984 in boreholes UE-25c #1, UE-25c #2, and UE-25c #3 (the c-holes) at Yucca Mountain, Nevada, were analyzed with respect to information obtained from lithologic and borehole geophysical logs, core permeameter tests, and borehole flow surveys. The three closely spaced c-holes, each of which is about 3,000 feet deep, are completed mainly in nonwelded to densely welded, ash-flow tuff of the tuffs and lavas of Calico Hills and the Crater Flat Tuff of Miocene age. Below the water table, tectonic and cooling fractures pervade the tuffaceous rocks but are distributed mainly in 11 transmissive intervals, many of which also have matrix permeability. Although steep to vertical, south-striking (west dipping) fractures predominate in rocks penetrated by the c-holes, fractures in transmissive intervals generally are oriented diversely. From the water table, at depths between 1,312 and 1,320 feet, to a depth of 1,700 feet, transmissive intervals are unconfined; transmissive intervals between 1,800 and 2,700 feet respond to pumping as fissure-block or nonleaky, confined aquifers; below 2,700 feet, transmissive intervals are recharged by water released from faults that have offset and brecciated the rocks in these intervals. Miocene tuffaceous rocks and Paleozoic carbonate rocks at the c-hole complex appear to be connected hydraulically.

Heat-pulse flowmeter surveys indicate a change from generally small, downward to large, upward flow with depth, that is disrupted by pumping. Flow from unconfined to confined intervals occurs in response to hydraulic gradients established during pumping tests. Diverse aquifer tests consistently indicate layered heterogeneity and the dependence of calculated hydrologic properties on the volume of aquifer being tested. For the entire thickness of rocks penetrated by the test holes, cross-hole pumping and injection tests indicated transmissivity between 20,000 and 35,000 feet squared per day; storativity between 0.002 and 0.004; horizontal hydraulic conductivity between 30 and 40 feet per day; and vertical hydraulic conductivity between 2 and 5 feet per day.

INTRODUCTION

Information contained in this report is presented as part of ongoing investigations by the U.S. Geological Survey (USGS) regarding the hydrologic and geologic suitability of Yucca Mountain, Nevada, as a potential site for the storage of high-level nuclear waste in an underground mined geologic repository. This investigation was conducted in cooperation with the U.S. Department of Energy under Interagency Agreement DE-AI08-78ET44802, as part of the Yucca Mountain Site Characterization Project.

Purpose and Scope

This report presents previously unpublished syntheses of geologic and hydrologic data from boreholes UE-25c #1, UE-25c #2, and UE-25c #3 (collectively called the c-holes) and descriptions, analyses, and interpretations of fluid-injection and withdrawal tests conducted in the c-holes. These tests were conducted between September 1983 and December 1984 to (1) help develop a conceptual model of the groundwater system at the c-hole complex; (2) provide a range in hydrologic properties for the rocks in tested intervals based on multiple analytical solutions applied to aquifer test data; and (3) provide information for designing hydraulic-stress tests and tracer tests within constraints imposed by initial test analyses. Analysis and interpretation of the preliminary aquifer tests at the c-holes were aided by published and unpublished data obtained between April 1985 and December 1992 that are listed

in table 1. Interpretations presented in this report should be considered tentative and subject to change, as optimally designed hydraulic-stress and tracer tests are conducted and analyzed. This report updates some hydrogeologic information and corrects some erroneous information about aquifer tests in U.S. Geological Survey Water-Resources Investigations Report 92-4016 (Geldon, 1993).

Acknowledgments

The author is indebted to many people currently or formerly with the USGS and Fenix and Scisson, Inc., who assisted with data collection, processing, and analysis, including but not limited to: Richard K. Waddell, Jr., James R. Erickson, Devin L. Galloway, Michael P. Chornack, Charles T. Warren, David H. Lobmeyer, Robert W. Craig, John B. Czarnecki, Brent Anderson, Jack Kume, William J. Oatfield, Charles S. Washington, and Geoffrey Miller (USGS); Robin L. Reed, Byron W. Cork, Sandy Waddell, Eric P. Eshom, Jennifer B. Warner, Daniel O. Blout, Kirstin A. Johnson, Lynn D. Parrish, Heather Huckins, Thomas M. Howard, Eric Larsen, and Russell G. Lahoud (Fenix and Scisson, Inc.).

PHYSICAL SETTING

Boreholes UE-25c #1, UE-25c #2, and UE-25c #3 are located in Nye County, Nevada, just east of the western boundary of the Nevada Test Site, approximately 90 miles northwest of Las Vegas. The c-holes are in the channel of an ephemeral stream that cuts through Bow Ridge parallel to and east of the main part of Yucca Mountain. The c-holes, other boreholes referred to in this report, and the potential high-level nuclear waste repository site are shown in figure 1. Yucca Mountain is situated in the arid Basin and Range physiographic province of the southwestern United States. Typical of the Basin and Range, the area around Yucca Mountain is characterized by narrow, predominantly northerly aligned mountain ranges separated by broad, alluvial basins (Frizzell and Shulters, 1990).

Borehole Construction

Boreholes UE-25c #1, UE-25c #2, and UE-25c #3 are 100 to 251 ft apart at the land surface (fig. 2). Lines connecting the boreholes delineate a triangle with an area of 11,050 ft^2. Because of borehole drift during drilling (fig. 2), interborehole distances at depth vary substantially from distances at the surface. For example, average horizontal distances between intervals monitored in some of the pumping tests conducted in the c-holes range from 92 to 280 ft (table 2). Cumulative borehole drift in a vertical plane for each of the c-holes was less than a foot. As a result, measured depths to features within the c-holes did not require a true-depth correction for the purposes of this report.

Borehole UE-25c #1 was completed in September 1983 (Fenix and Scisson, Inc., 1986). The top of the borehole is at an altitude of 3,709.28 ft (Grady O'Brien, U.S. Geological Survey, written commun., 1993). As indicated by television (TV) and caliper logs listed in table 1, casing and concrete extend 1,371 ft below the top of the borehole. The open part of the borehole was rotary-drilled with a 14.75-in.-diameter bit through the bottom of the concrete to a depth of 1,511 ft and a 9.875-in.-diameter bit from 1,511 to 2,990 ft. The borehole was cored with an 8.75-in.-diameter bit from 2,990 to 3,000 ft. Caliper logs indicate that the borehole walls are very irregular (plate 1). TV and caliper logs indicate that the bottom of the borehole has collapsed substantially since the borehole was completed. The bottom of the borehole was at a depth of 2,994 ft in September 1983, 2,962 ft in November 1983, and 2,945 ft in December 1990.

Borehole UE-25c #2 was completed in February 1984 (Fenix and Scisson, Inc., 1986). The top of the borehole is at an altitude of 3,715.25 ft (Grady O'Brien, U.S. Geological Survey, written commun., 1993). As indicated by TV and caliper logs listed in table 1, casing and concrete extend 1,365 ft below the top of the borehole. The open part of the borehole was rotary-drilled with a 14.75-in.-diameter bit through the bottom of the concrete to a depth of 1,515 ft and a 9.875-in.-diameter bit from 1,515 to 3,000 ft. Caliper logs indicate that the borehole walls are very irregular (pl. 2). In figure 3, a close relationship is shown between the location of open, near vertical to vertical (dip 70°–84°), southerly and northwesterly striking fractures and an enlarged, rugose section of borehole UE-25c #2. TV and acoustic televiewer logs in the c-holes indicate that prominent fractures with other orientations, partings at contacts between geologic units, and drilling-induced sloughing, also, are associated with enlargement and rugosity in the c-holes. TV and caliper logs indicate that the bottom of borehole UE-25c #2 has collapsed slightly since completion. The bottom of the borehole was at a depth of 2,999 ft in February 1984, 2,990 ft in August 1984, and 2,986 ft in June 1992.

Borehole UE-25c #3 was completed in April 1984 (Fenix and Scisson, Inc., 1986). The top of the borehole is at an altitude of 3,715.25 ft

Table 1. Information collected at the c-hole complex for determination of rock hydrologic properties[1]

Information	Source	Dates obtained
	Borehole UE-25c #1	
Caliper logs	Birdwell	09/18/83
	Atlas Wireline Services	12/11/90
	USGS	12/10/91
Gyroscopic (borehole deviation) survey	Eastman	09/18/83
Resistivity logs	Birdwell	09/20/83
Temperature logs (nonpumping)	Birdwell	09/20/83
	USGS	12/09/91
Miscellaneous geophysical logs	Nelson and others (1991)	08/21/83–11/20/83
Tracejector survey (pumping)	Gearhart-Owen	09/29/83
Television logs	Westech	09/17/83–11/18/83
Acoustic televiewer log	Richard K. Waddell (USGS, written commun., 1984)	10/31/83
Lithologic log	Richard E. Spengler (USGS, written commun., 1984)	2/84
Core permeability analyses (9)	Holmes and Narver, Inc.	03/14/84
Pumping tests (2)	USGS, assisted by REECo	09/27/83–10/02/83
Falling-head (slug) tests (16)	USGS, assisted by TAM International	10/06/83–10/12/83
Pressure-injection tests (9)	USGS, assisted by TAM International	10/08/83–10/12/83
Heat-pulse flowmeter survey (nonpumping)	Frederick L. Paillet (USGS, written commun., 1992)	12/12/91
Static water levels, atmospheric pressure, and barometric efficiency	Galloway and Rojstaczer (1988)	02/23/86–04/21/86
Borehole history	Fenix and Scisson, Inc. (1986)	08/10/83–02/01/85
	Borehole UE-25c #2	
Caliper logs	Birdwell	02/28/84
	Birdwell	08/23/84
	Atlas Wireline Services	12/11/90
	USGS	12/14/91
Gyroscopic (borehole deviation) survey	Sperry-Sun	02/27/84
Resistivity logs	Birdwell	02/28/84
Temperature logs (nonpumping)	Birdwell	02/28/84
	USGS	12/14/91
Miscellaneous geophysical logs	Nelson and others (1991)	01/27/84–02/29/84
Tracejector survey (pumping)	Gearhart-Owen	03/12/84
Television logs	Westech	02/08/84–04/13/84
	Barbour Well Surveying Corporation	06/02/92
Acoustic televiewer logs	Richard K. Waddell (USGS, written commun., 1984)	02/27/84
	USGS	12/14/91
Lithologic log	Richard E. Spengler (USGS, written commun., 1984)	03/84
Core permeability analyses (3)	Alan L. Flint (USGS, written commun., 1993)	12/92
Pumping test	USGS, assisted by REECo	03/07/84–03/18/84
Constant-flux injection test	USGS, assisted by REECo	10/30/84
Heat-pulse flowmeter survey (nonpumping)	Frederick L. Paillet (USGS, written commun., 1992)	12/16/91
Static water levels, atmospheric pressure and barometric efficiency	Galloway and Rojstaczer (1988)	02/23/86–04/21/86
Borehole history	Fenix and Scisson, Inc. (1986)	01/09/84–06/27/85

Table 1. Information collected at the c-hole complex for determination of rock hydrologic properties[1] --Continued

Information	Source	Dates obtained
	Borehole UE-25c #3	
Caliper logs	Birdwell	04/27/84
	Birdwell	03/21/85
	Atlas Wireline Services	12/11/90
	USGS	12/13/91
Gyroscopic (borehole deviation) survey	Sperry-Sun	04/26/84
Resistivity logs	Birdwell	04/30/84
Temperature logs (nonpumping)	Birdwell	04/30/84
	USGS	12/31/91
Miscellaneous geophysical logs	Nelson and others (1991)	03/28/84–04/30/84
Tracejector survey (pumping)	Gearhart-Owen	05/07/84
Television logs	Westech	04/13/84
	Barbour Well Surveying Corporation	06/02/92
Acoustic televiewer logs	Richard K. Waddell (USGS, written commun., 1984)	04/27/84
	USGS	12/13/91
Lithologic log	Richard E. Spengler (USGS, written commun., 1984)	05/84
Core permeability analyses (8)	Alan L. Flint (USGS, written commun., 1993)	12/92
Pumping tests		
First test	USGS, assisted by REECo	05/14/84–06/12/84
Second test	USGS, assisted by REECo	10/30/84–12/09/84
Heat-pulse flowmeter survey (nonpumping)	Frederick L. Paillet (USGS, written commun., 1992)	12/15/91
Static water levels, atmospheric pressure and barometric efficiency	Galloway and Rojstaczer (1988)	02/23/86–04/21/86
Borehole history	Fenix and Scisson, Inc. (1986)	03/20/84–06/27/85
	Boreholes near the c-holes	
Core permeability analyses		
UE-25b #1 (12)	Lobmeyer and others (1983)	unknown
USW H-1 (15)	Rush and others (1983)	unknown
USW G-3 (22)	Philip Nelson (USGS, written commun., 1992)	unknown
USW G-4 (20)	Philip Nelson (USGS, written commun., 1992)	unknown

[1]Any use of trade names in this report is for descriptive purposes only and does not imply endorsement by the U.S. Geological Survey.

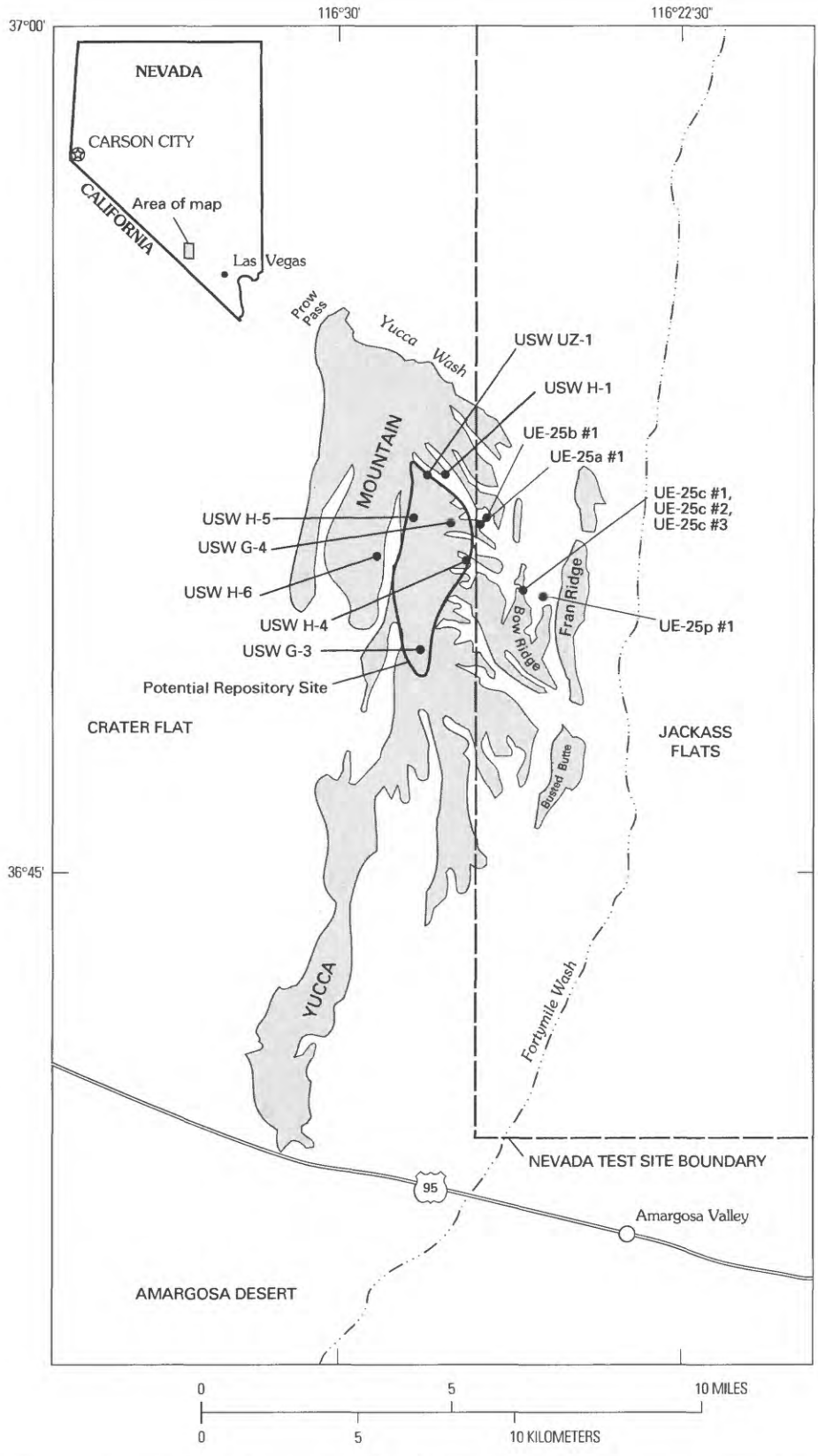

Figure 1. Location of Yucca Mountain, boreholes UE-25c #1, UE-25c #2, and UE-25c #3, and nearby boreholes used for hydrologic investigations.

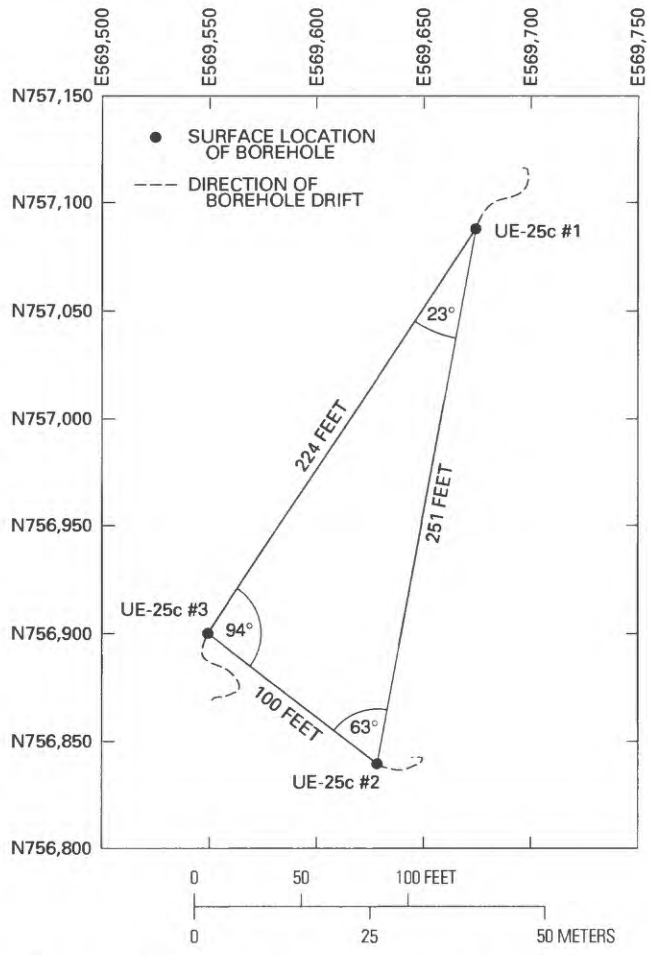

Figure 2. Surface location and drift of boreholes UE-25c #1, UE-25c #2, and UE-25c #3.

Table 2. Distances between pumped wells and monitored intervals in observation wells during some pumping tests conducted in 1984 in boreholes UE-25c #2 and UE-25c #3

Connected points	Monitored interval (feet below land surface)	Thickness-weighted average distance (feet)
Borehole UE-25c #2 test, March 1984		
UE-25c #1 above packers to UE-25c #2	1,371–2,510	270
UE-25c #1 between packers to UE-25c #2	2,520–2,600	277
Borehole UE-25c #3 test, May-June 1984		
UE-25c #1 above packers to UE-25c #3	1,371–1,595	256
UE-25c #1 between packers to UE-25c #3	1,605–1,680	259
Borehole UE-25c #3 test, October-December 1984		
UE-25c #1 above packers to UE-25c #3	1,371–2,514	267
UE-25c #1 between packers to UE-25c #3	2,524–2,594	280
UE-25c #1 below packers to UE-25c #3	2,603–3,000	280
UE-25c #2 between packers to UE-25c #3	2,364–2,475	92

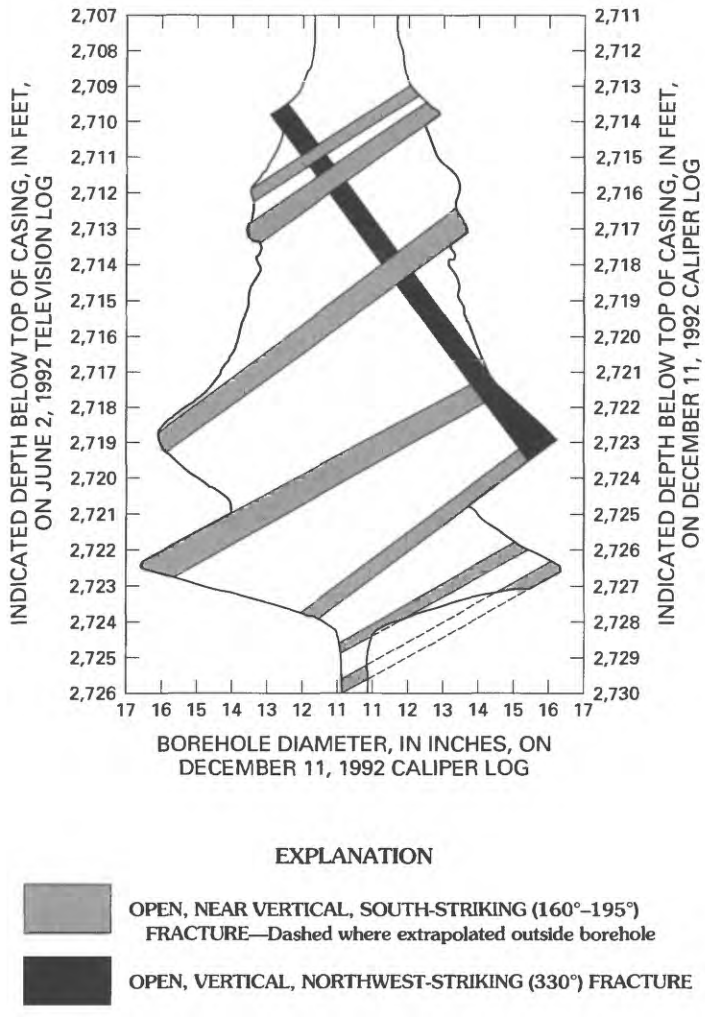

Figure 3. Relation between fractures and borehole diameter in an enlarged, rugose interval of borehole UE-25c #2.

(Grady O'Brien, U.S. Geological Survey, written commun., 1993). As indicated by TV and caliper logs listed in table 1, casing and concrete extend 1,368 ft below the top of the borehole. The open part of the borehole was rotary-drilled with a 14.75-in.-diameter bit through the bottom of the concrete to a depth of 1,514 ft and a 9.875-in.-diameter bit from 1,514 to 3,000 ft. Caliper logs indicate that the borehole walls are very irregular (pl. 3). TV and caliper logs indicate that the bottom of the borehole has collapsed substantially since completion. The bottom of the borehole was at a depth of 3,000 ft in April 1984, 2,976 ft in March 1985, and 2,954 ft in June 1992.

Site Geology

The c-holes are completed in Miocene tuffaceous rocks that are covered by a thin veneer (0–80 ft) of Quaternary alluvium and underlain by dolomite of the Silurian Roberts Mountain Formation and Lone Mountain Dolomite (Carr and others, 1986; Geldon, 1993). Based on information obtained from borehole UE-25p #1, 2,028 ft southeast of borehole UE-25c #1, the Miocene rocks are estimated to be about 5,000 ft thick in the vicinity of the c-holes.

Northerly trending, high-angle faults, such as the Paintbrush Canyon and Bow Ridge Faults, have offset and tilted the Miocene rocks in the vicinity of the

c-holes (Scott and Bonk, 1984). The dip of the Miocene rocks increases in fault blocks from 5° to 10° on the crest of Yucca Mountain to 15° to 20° at the c-hole complex (Frizzell and Shulters, 1990; Geldon, 1993). According to Scott (1990), the high-angle faults merge listrically at depth with a detachment fault that forms the contact between Miocene and Paleozoic rocks in the Yucca Mountain area. However, Carr (1990) considers the contact between the Miocene and Paleozoic rocks to be an unconformity, and the high-angle faults in the Yucca Mountain area to be collapse faults bordering a caldera centered in Crater Flat (location shown in fig. 1).

As indicated in table 3, Miocene rocks penetrated by the c-holes include the Tiva Canyon and Topopah Spring Members of the Paintbrush Tuff, the tuffs and lavas of Calico Hills, and the Prow Pass, Bullfrog, and Tram Members of the Crater Flat Tuff. These geologic units predominantly consist of ash-flow tuff, that is devitrified to vitrophyric and nonwelded to densely welded. Bedded tuff, consisting of ash-fall tuff and volcaniclastic rocks (reworked tuff), is interlayed with the ash-flow tuff at the base of formations and members. Unique to boreholes in the Yucca Mountain area, a tuff breccia occurs in the Tram Member in an interval where moderately welded ash-flow tuff is present in nearby boreholes (Geldon, 1993). Faults that intersect at the c-hole complex apparently have brecciated the upper nonwelded to partially welded part of the Tram Member and cut out the moderately welded part (Geldon, 1993). All of the geologic units at the c-hole complex have been altered partially to zeolite and clay minerals below the water table, which according to information from Robison and other (1988) and USGS files, occurs at depths of between 1,312 and 1,320 ft below the land surface (at altitudes of 2,394 to 2,396 ft above the NGVD of 1929). The water table is slightly above or below the contact between the Paintbrush Tuff and the tuffs and lavas of

Table 3. Stratigraphic column for the c-hole complex

[Summarized from lithologic logs prepared by Richard E. Spengler, USGS, written commun., 1984; dashed line in depth column indicates an unconformity]

Geologic unit	Generalized description	Depth below land surface (feet)		
		UE-25c #1	UE-25c #2	UE-25c #3
Alluvium	Sand and gravel	Absent	0–70	0–80
Paintbrush Tuff				
Tiva Canyon Member	Moderately to densely welded ash-flow tuff with thin basal bedded tuff	0–315	70–290	80–290
Topopah Spring Member	Moderately to densely welded ash-flow tuff with intervals containing lithophysae; thin vitrophyre and nonwelded tuff layers at the top and bottom	315–1,332	290–1,316	290–1,300
Tuffs and lavas of Calico Hills	Nonwelded ash-flow tuff	1,332–1,593	1,316–1,570	1,300–1,560
	Bedded tuff	1,593–1,691	1,570–1,672	1,560–1,629
Crater Flat Tuff				
Prow Pass Member	Nonwelded to partially welded ash-flow tuff	1,692–1,838	1,673–1,810	1,630–1,780
	Moderately welded ash-flow tuff	1,838–1,860	1,810–1,840	1,780–1,830
	Partially welded to nonwelded ash-flow tuff	1,860–2,118	1,840–2,110	1,830–2,085
	Bedded tuff	2,118–2,152	2,110–2,138	2,085–2,112
Bullfrog Member	Nonwelded to partially welded ash-flow tuff	2,153–2,260	2,139–2,240	2,112–2,210
	Moderately to densely welded ash-flow tuff	2,260–2,480	2,240–2,460	2,210–2,430
	Partially welded to nonwelded ash-flow tuff	2,480–2,695	2,460–2,675	2,430–2,650
	Bedded tuff	2,695–2,716	2,675–2,719	2,650–2,670
Tram Member	Nonwelded to partially welded ash-flow tuff	2,716–2,775	2,719–2,775	2,670–2,804
	Indurated tuff breccia	2,775–2,975	2,775–2,935	2,804–3,000
	Partially welded, lithic ash-flow tuff	2,975–3,000	2,935–3,000	Not reached

Calico Hills in individual boreholes (see tables in the Supplementary Data section at the end of this report).

The tuffaceous rocks at the c-hole complex are pervaded by tectonic and cooling fractures. Fracture orientations and frequency in the geologic units penetrated by the c-holes vary from unit to unit and among boreholes, but for the tuffs and lavas of Calico Hills and the Crater Flat Tuff, in general, fractures strike predominantly south-southeast to south-southwest (fig. 4) and dip 50° to 87° to the west-southwest or west-northwest. Largely because of the Tram Member of the Crater Flat Tuff, the second most abundant fractures in the c-holes strike north-northwest to north-northeast and dip east-northeast to east-southeast. Many of the latter fractures are shallow-dipping or mineralized. The least common fractures generally strike to the east (between 70° and 110°) and west (between 250° and 290°), and many of these are shallow-dipping or mineralized. In contrast to boreholes UE-25c #1 and UE-25c #2, southwesterly, westerly, and northwesterly-striking fractures are more common in borehole UE-25c #3 than southeasterly, easterly, and northeasterly striking fractures. Borehole UE-25c #3 differs from the other two c-holes, also, in having a smaller proportion of steep to vertical, nonmineralized fractures to mineralized or shallow, nonmineralized fractures. Because of fault brecciation, fracture frequency is greatest in the Tram Member. The bedded zone of the tuffs and lavas of Calico Hills is also very fractured. On the average, moderately to densely welded zones of the Prow Pass and Bullfrog Members are more fractured than bedded zones, which in turn, are more fractured than nonwelded to partially welded zones (pls. 1–3).

SITE HYDROLOGY

The tuffaceous rocks penetrated by the c-holes are not uniformly permeable. Variations in fracture frequency and openness and matrix permeability confine ground-water movement to relatively thin intervals in the tuffs and lavas of Calico Hills and the Crater Flat Tuff. In combination, laboratory analyses of core permeability, fracture (television and acoustic televiewer) logs, caliper logs, resistivity logs, temperature logs, tracejecter surveys during pumping tests, and heat-pulse flowmeter surveys identify the transmissive intervals.

Matrix Permeability

Permeameter tests were done on 20 samples of core from boreholes UE-25c #1, UE-25c #2, and UE-25c #3 (table 1) to determine horizontal and vertical matrix permeability. These samples were insufficient to characterize the variation in matrix permeability with depth throughout the entire thickness of tuffaceous rocks penetrated by the c-holes. However, with the addition of permeability analyses for 69 samples of core from four boreholes within a three-mile radius of the c-hole complex (table 1), profiles of horizontal matrix permeability as a function of depth within geologic units (sample depth divided by the thickness of the geologic unit from which the sample was obtained) were prepared for the c-holes and nearby boreholes (fig. 5).

To construct the permeability profile shown in figure 5, it was assumed that permeability values would be the same at the same normalized depths within geologic units at different locations. However, it was recognized that this assumption might be incorrect locally because of lateral changes in lithology. Some points shown in figure 5 that deviate substantially from the plotted permeability profile were ignored under the assumption that they represent either locally unusual lithology or a poorly correlated permeability value.

Horizontal matrix permeability as a function of depth for each of the c-holes was calculated from the permeability and percent of thickness values in figure 5 and depths of stratigraphic horizons listed in table 3. As indicated on plates 1–3, horizontal matrix permeability in the tuffaceous rocks at the c-hole complex is estimated to range from 0.001 to 20 mD. With respect to matrix permeability, the tuffaceous rocks at the c-hole complex are slightly anisotropic (fig. 6). Matrix permeability is slightly larger in the horizontal direction than in the vertical direction. Expressed as a function of horizontal matrix permeability (k_r), vertical matrix permeability (k_z) can be found from the following empirically derived equation ($R^2 = 0.71$):

$$\log k_z = 0.88 \log k_r - 0.36 \qquad (1)$$

Vertical matrix permeability in the tuffaceous rocks at the c-hole complex is estimated to range from 0.001 to 6 mD.

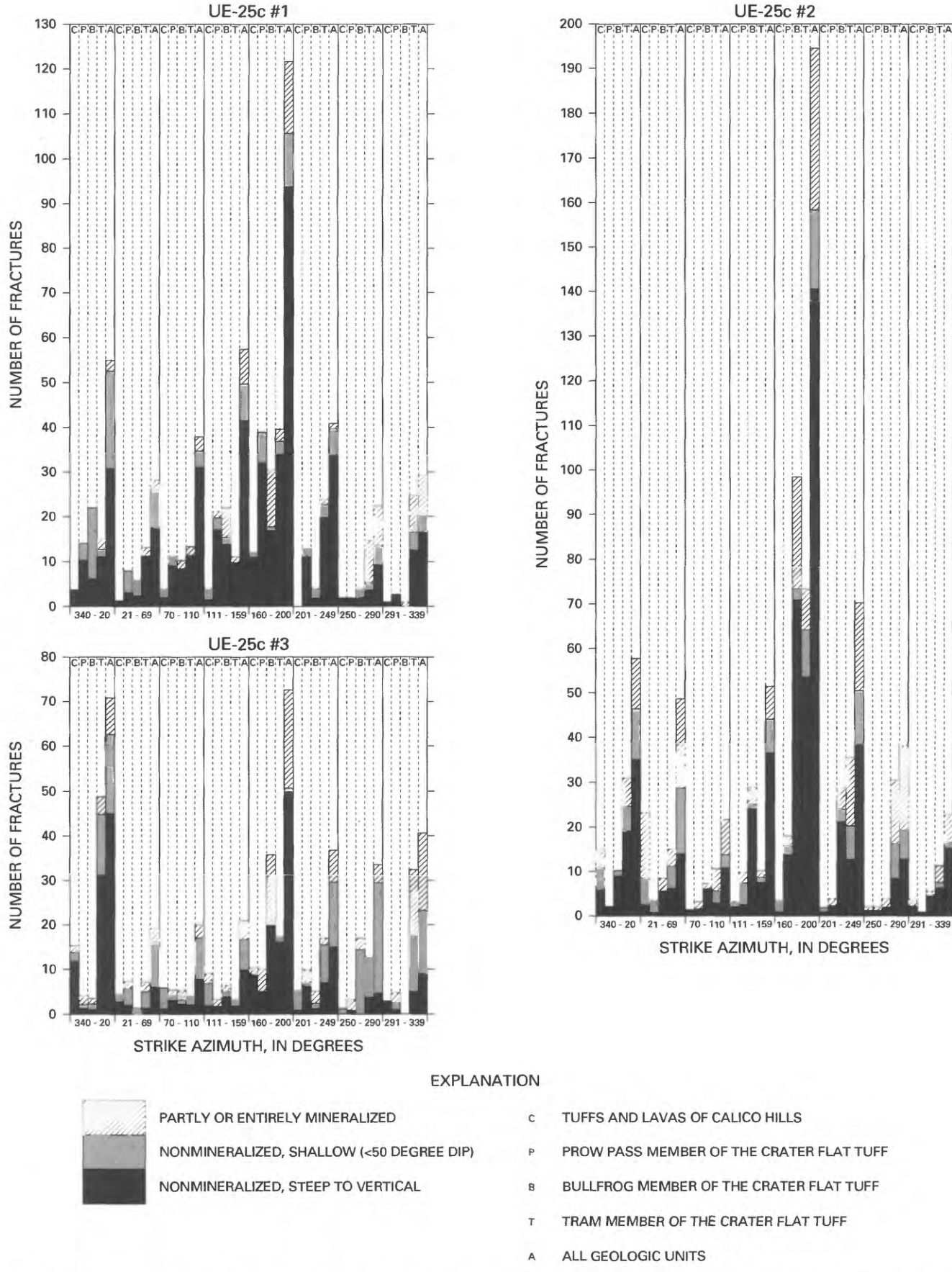

Figure 4. Frequency distribution of fracture orientations in boreholes UE-25c #1, UE-25c #2, and UE-25c #3. (Based on TV and acoustic televiewer logs. Fractures identified in the c-holes are listed in the Supplementary Data section at the end of this report.)

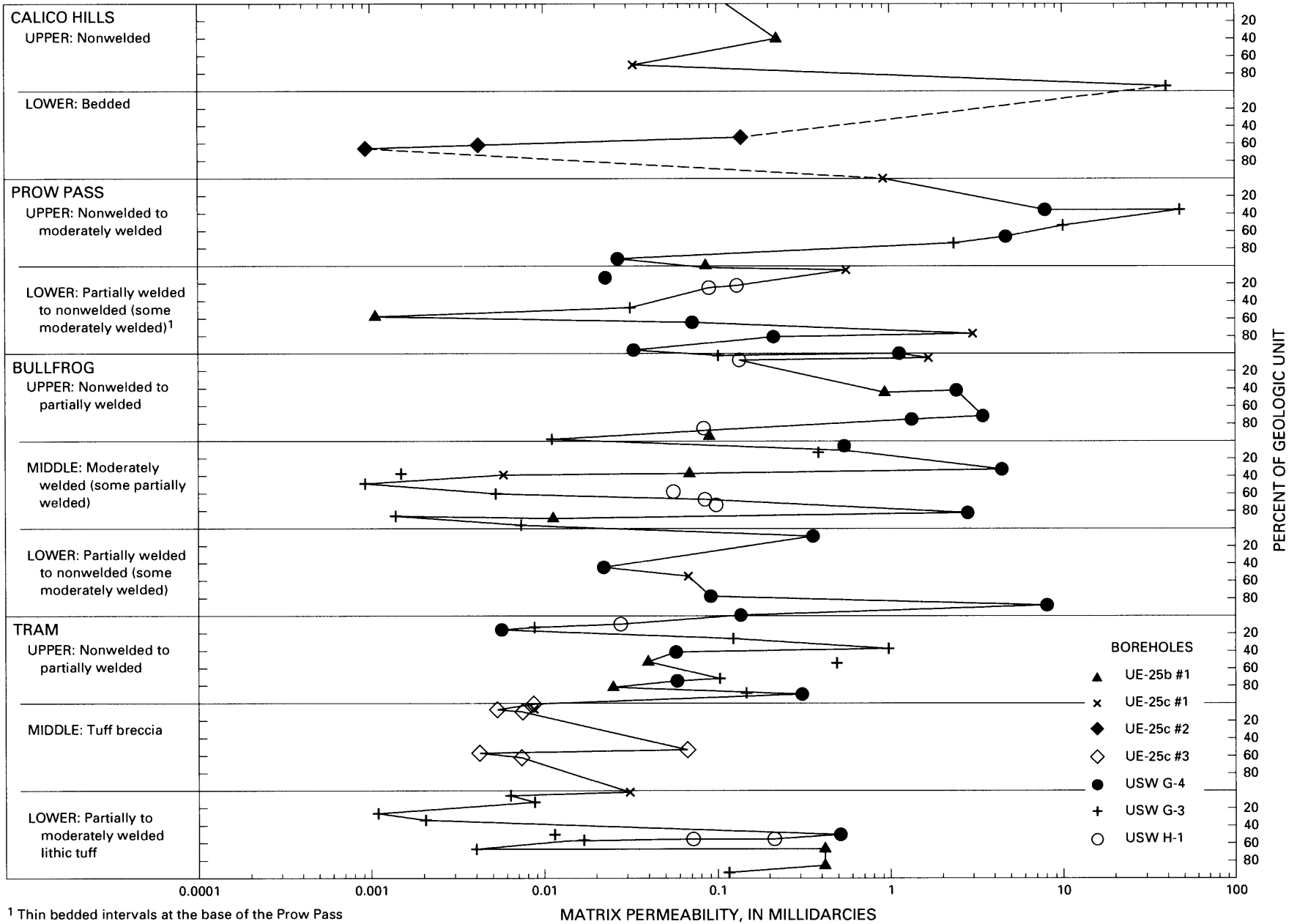

[1] Thin bedded intervals at the base of the Prow Pass and Bullfrog Members are omitted. One sample of bedded tuff had a permeability of 0.26 millidarcies

Figure 5. Horizontal matrix permeability in the tuffs and lavas of Calico Hills and Crater Flat Tuff, east-central Yucca Mountain area, as a function of depth within geologic units (based on core analyses listed in table 1).

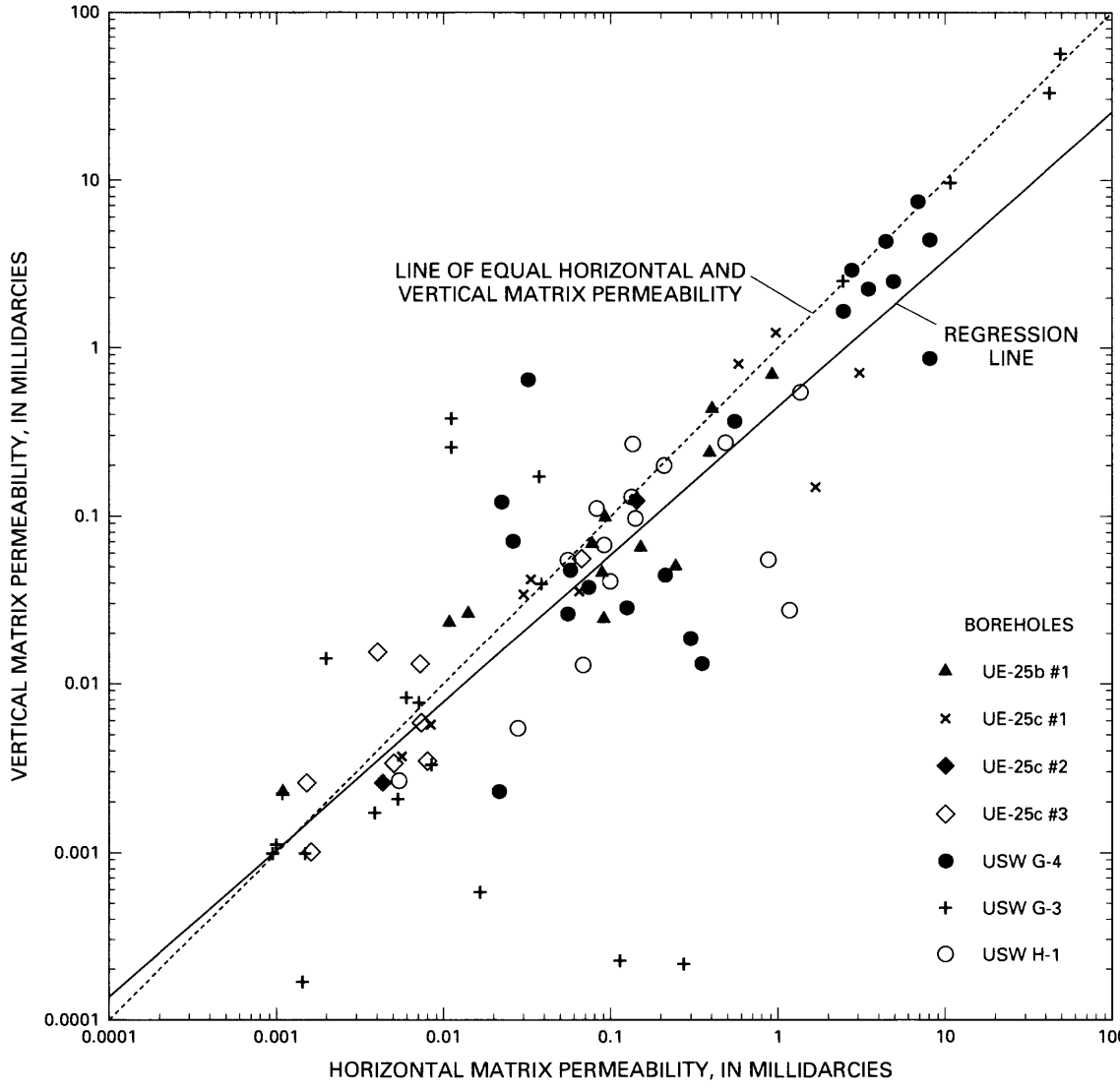

Figure 6. Relation of vertical to horizontal matrix permeability in core samples from the tuffs and lavas of Calico Hills and Crater Flat Tuff in the c-holes and nearby boreholes.

Heat-Pulse Flowmeter Surveys

Heat-pulse flowmeter surveys were conducted in each of the c-holes in December 1991 by Alfred E. Hess and Frederick L. Paillet of the USGS Borehole Geophysics Research Project to identify zones of intraborehole flow under natural hydraulic gradients (undisturbed by pumping or drilling). As described by Hess (1990), the method used involves lowering the flowmeter probe by cable to intervals of a borehole previously identified by fracture (television and acoustic televiewer) logs, caliper logs, and temperature logs as possibly transmissive intervals. Measurements are made with the probe above and below an interval of interest. A packer is inflated above the probe to restrict the measurement to the depth of interest. The flow measurement is made by releasing a heat pulse from an open grid of resistance wire and timing the movement of the heat pulse to sensors located at equal distances above and below the heat source. A positive deflection on a strip-chart recording of heat-pulse transit time indicates movement of the heat pulse to the upper sensor and, hence, upward intraborehole flow. A negative deflection on a strip-chart recorder indicates movement of the heat pulse to the lower sensor and, hence, downward intraborehole flow. Heat-pulse transit time is converted to flow rate by an empirically derived calibration equation for the probe.

Heat-pulse flowmeter surveys indicated distinctly different patterns of intraborehole flow in each of the c-holes (pls. 1–3). In borehole UE-25c #1, the flow fluctuated slightly but remained less than 0.09 gal/min and downward from 1,505 to about 2,520 ft. Below about 2,520 ft, the intraborehole flow became upward. The upward flow increased from 0 to 1.18 gal/min between about 2,520 and 2,735 ft, decreased to 0.91 gal/min between 2,735 and 2,765 ft, and became too small to measure reliably between 2,765 and 2,830 ft.

Similar to the pattern in borehole UE-25c #1, flow in borehole UE-25c #2 was downward in the top of the borehole and upward in the bottom of the borehole. However, downward and upward flow in borehole UE-25c #2 remained small (less than 0.15 gal/min) throughout the entire surveyed part of the borehole, and the change from downward to upward flow was 230 ft lower than in borehole UE-25c #1.

In contrast to the situation in boreholes UE-25c #1 and UE-25c #2, the flow in borehole UE-25c #3 was upward throughout the entire surveyed part of the borehole, although it is possible that small downward flow might be occurring above the uppermost measuring depth. The flow in borehole UE-25c #3 decreased from 0.10 to 0.05 gal/min between 1,505 and 1,650 ft, increased gradually to 0.08 gal/min between 1,650 and 2,275 ft, increased sharply to 4.0 gal/min between 2,275 and 2,550 ft, and decreased from 4.0 to 1.7 gal/min between 2,800 ft and the bottom of the borehole.

As described in the next section, changes in flow in the c-holes generally coincide with zones of moderately to very fractured rock. Faults, partings, and intervals with relatively large matrix permeability, also influence intraborehole flow.

Transmissive Intervals

The best indicators of transmissivity are aquifer tests and numerical modeling. However, both techniques require some knowledge of hydrogeologic conditions in advance of use for the most reliable calculation of hydrologic properties. Diverse laboratory and geophysical data obtained at the c-hole complex from 1983–1992 were used to determine transmissive intervals in and between the c-holes in order to improve the analysis and interpretation of preliminary aquifer tests conducted at the c-hole complex. For example, knowing that ground-water flow was occurring in only 50 ft of a packed-off interval 500-ft thick instead of the entire interval, substantially would change the calculation of hydraulic conductivity from a transmissivity value determined by a pumping test. The analytical solution used to calculate transmissivity from drawdown, residual drawdown, or recovery data, and hence the numerical value obtained, would be expected to differ substantially if pre-test analysis showed that the source of ground water in a borehole was a fracture zone, an unfractured interval with large matrix permeability, a fault, or gravity drainage from the water table. In this study, the following criteria were used to identify transmissive intervals:

1. Gains and losses in intraborehole flow detected during heat-pulse flowmeter surveys;
2. Gains in discharge detected by tracejector surveys during pumping tests;
3. Inflections in nonpumping temperature gradients (caused by inflow, outflow, upflow, or downflow);
4. Relatively low resistivity associated with moderate to intense fracturing, relatively large matrix permeability, or partings (indicating that the resistivity is related to water and not weathering, mineralization, or other factors); and
5. Borehole enlargement associated with fracture zones, an indicator of the openness of individual fractures, or the presence of cavities created by fracture intersections.

Transmissive intervals in each of the c-holes and their characteristics are listed in tables 4–6. Figure 7, a hydrogeologic section of the c-holes, drawn along lines shown in figure 2, extrapolates transmissive intervals between the c-holes. For purposes of discussion in this report, the c-hole transmissive intervals informally were grouped into four aquifers that are separated by three confining units. The aquifers cannot be considered as formal hydrogeologic units because (1) the aquifers are defined largely by the extent of fracturing within them; (2) fractures are spatially related to faults at the c-hole complex; and (3) in different areas, faults and related fractures can be expected to penetrate geologic units differently than at the c-hole complex.

Calico Hills Aquifer

The Calico Hills aquifer extends from the water table, at depths between 1,312 and 1,320 ft to about 1,700 ft below land surface and is unconfined. It consists of three relatively thin zones of moderately to very fractured rock separated by unfractured to sparsely fractured rock, much of which contains large matrix permeability (fig. 7). Fractures, some of which are

Table 4. Transmissive intervals in borehole UE-25c #1

[Features discussed briefly in this table are shown in detail on plate 1]

Depth below land surface (feet)	Characteristics	Intraborehole flow (gallons per minute)	Pumping discharge (percent)	Supporting information
1,406–1,516	Poor visibility but believed to be sparsely to moderately fractured. Known fractures shallow-near vertical, north, south, southeast, and west-striking	≥0.09 down	0	Low resistivity
1,521–1,593	Very fractured to 1,544 ft, large matrix permeability below; fractures are steep-vertical, north, east, southeast, south, and west-striking	0.02 out	0	Low resistivity, concave temperature gradient inflection
1,623–1,639	Very fractured; fractures are near vertical-vertical, south-striking	0.01 out	0	Low resistivity
1,691–1,692	Open parting at Calico Hills-Crater Flat contact	0.02 in and down	0	Low resistivity, convex temperature gradient inflection
1,803–1,846	Very fractured, large matrix permeability; fractures are steep-vertical, mostly north, south, southeast, and southwest-striking	0.02 out	0	Borehole enlargement
1,860–1,861	Open parting between moderately welded and partially welded to nonwelded zones of Prow Pass Member		0	Abrupt resistivity decrease
1,919–1,925	Very fractured; fractures are open, shallow-steep, north, east, and south-striking	0.02 in and down	0	Low resistivity, borehole enlargement
1,963–1,975	Moderately fractured; fractures are open, shallow, north-striking	0.01 out	0	Very low resistivity
2,050–2,156	Poor visibility but believed to be sparsely to very fractured; known fractures are shallow-vertical, mostly south and northeast-striking. Intervals with large matrix permeability and an open parting at the Prow Pass-Bullfrog contact	0.01 in and down	0	Low resistivity, borehole enlargement
2,215–2,260	Very fractured to 2,243 ft, large matrix permeability below; fractures, some of which are open, are shallow-vertical, north, southeast, and south-striking	0.01 out	0	Low resistivity, borehole enlargement
2,392–2,457	Sparsely to very fractured, with large matrix permeability below 2,415 ft; fractures are near vertical-vertical, south and east-striking	0.03 in and down	0	
2,463–2,560	Very fractured rock separated by thin intervals of unfractured rock; fractures, many of which are open are steep-vertical, south, east, and southeast-striking	0.12 out (changing from down to up at 2,520 ft)	0	Low resistivity, borehole enlargement, pronounced concave temperature gradient inflection
2,560–2,604	Moderately to very fractured; fractures are open, shallow-steep, north and northeast-striking and near vertical or vertical, east-striking	0.76 out	64	Very low resistivity, convex temperature gradient inflection, borehole enlargement
2,656–2,715	Moderately fractured, large matrix permeability; fractures are shallow-steep, north-striking	0.38 out	0	Low resistivity, borehole enlargement
2,729–2,752	Very fractured; fractures, some of which are open, are shallow-vertical and diversely oriented	0.29 in to maximum upward flow of 1.18	0	Very low resistivity, concave temperature gradient inflection, borehole enlargement
2,759–2,790	Very fractured; fractures, some of which are open, are shallow-steep, mostly south and southwest-striking. Two of the fractures comprise the Paintbrush Canyon Fault zone	<0.91 in and up	25	Convex temperature gradient inflection, extensive borehole enlargement
2,790–2,840	Very fractured; fractures, some of which are open, are steep-vertical and diversely oriented	Small up	0	Borehole enlargement
2,890–2,915	Very fractured; fractures are near vertical-vertical, diversely oriented	Small up(?)	11	Concave temperature gradient inflection, borehole enlargement
2,921–2,941	Very fractured; fractures are shallow-vertical, diversely oriented	Small up(?)	0	Convex temperature gradient inflection
2,960–2,980	Moderately fractured(?): uncertain because interval concealed by borehole collapse	Small up(?)	0	Low resistivity, borehole enlargement

Table 5. Transmissive intervals in borehole UE-25c #2

[Features discussed briefly in this table are shown in detail on plate 2]

Depth below land surface (feet)	Characteristics	Intraborehole flow (gallons per minute)	Pumping discharge (percent)	Supporting information
1,441–1,570	Poor visibility to 1,514 ft, but believed to be sparsely to moderately fractured to 1,552 ft. Large matrix permeability below 1,539 ft. Known fractures are vertical, northwest, north, and northeast-striking; two are open	≥0.04 down	0	Low resistivity; convex temperature gradient inflection at about 1,465 ft, and concave temperature gradient inflection at about 1,520 ft; borehole enlargement and rugosity
1,624–1,634	Very fractured; fractures are shallow, north and northeast-striking	0.01 in and down	0	Very low resistivity, borehole enlargement
1,644–1,653	Very fractured; fractures are shallow-vertical, diversely oriented, open at intersections		0	Very low resistivity, convex temperature gradient inflection, borehole enlargement
1,672–1,673	Open parting at Calico Hills-Crater Flat contact		0	Low resistivity, borehole enlargement
1,812–1,870	Very fractured, with large matrix permeability; fractures are near vertical-vertical, south and southeast-striking	0.10 in and down to maximum downward-flow of 0.15	0	Decrease to low resistivity concave temperature gradient inflection
1,948–1,968	Moderately fractured(?). No known fractures because of poor visibility	0.01 out	0	Low resistivity, borehole enlargement
2,045–2,093	Poor visibility; could be sparsely to moderately fractured, although no fractures were detected. Interval known to have large matrix permeability		0	Generally low resistivity, convex temperature gradient inflection, substantial borehole enlargement
2,107–2,122	Poor visibility, but believed to be moderately fractured. Known to have large matrix permeability	0.01 out	0	Generally low resistivity, borehole enlargement and rugosity
2,138–2,139	Open parting at Prow Pass-Bullfrog contact		7	Low resistivity, borehole enlargement
2,252–2,267	Very fractured; fractures, one of which is open, are near vertical-vertical, south-striking	0.01 out	0	Low resistivity
2,380–2,416	Very fractured, with large matrix permeability; fractures, about a third of which are open, are steep-vertical, mostly north and south-striking (also northeast, east, southeast, and southwest-striking)	0.04 out	79	Resistivity trough, major convex temperature gradient inflection, borehole enlargement
2,437–2,499	Very fractured rock with thin intervals of unfractured rock; fractures mostly are open, steep-vertical, south, southeast, southwest, and northwest-striking	0.02 out	14	Decrease to low resistivity, concave temperature gradient inflection; minor borehole enlargement
2,691–2,694	Very fractured; interval contains a single partly mineralized, vertical, south-striking fracture, indicated on lithologic log to be a fault	Small loss(?)	0	Low resistivity
2,707–2,726	Very fractured; fractures mostly are open, steep-vertical, southeast, south, and southwest-striking	≥0.03 out	0	Low resistivity, major concave temperature gradient inflection, major borehole enlargement
2,749–2,789	Very fractured; fractures, three of which are open, are steep-vertical, north and south-striking	0.08 out (changing from downward to upward at 2,750 ft)	0	Low resistivity, convex temperature gradient inflection, borehole enlargement and rugosity
2,789–2,797	Very fractured; fractures mostly are shallow-steep, south-striking; three open fractures at 2,793–2,795 ft comprise the Paintbrush Canyon Fault zone	≥0.05 in to maximum upward flow	0	Low resistivity
2,891–2,942	Very fractured; fractures, four of which are open, are steep-vertical, diversely oriented	Small up(?)	0	Low resistivity, concave temperature gradient inflection
2,942–2,961	Sparsely fractured; interval known to contain two shallow, south-striking fractures, one of which is open	Small up(?)	0	Low resistivity

Table 6. Transmissive intervals in borehole UE-25c #3

[Features discussed briefly in this section are shown in detail on plate 3]

Depth below land surface (feet)	Characteristics	Intraborehole flow (gallons per minute)	Pumping discharge (percent)	Supporting information
1,414–1,483	Sparsely to moderately fractured. Known fractures are steep-near vertical, north and northwest-striking. Unfractured rock apparently transmits water	Small down(?)	0	Low resistivity; borehole enlargement
1,483–1,522	Moderately to very fractured; large matrix permeability; fractures, mostly open to 1,510 ft, are shallow-vertical, north, south, and southwest-striking. Water apparently is transmitted by fractures and matrix	≥0.10 out (any downward flow and all remaining upward flow lost)	0	Low resistivity, concave temperature gradient inflection, borehole enlargement
1,522–1,586	Sparsely to moderately fractured, large matrix permeability; fractures are shallow-vertical, northeast, east, and south-striking. Water apparently transmitted by fractures and matrix	0.04 in and up	0	Low resistivity, convex temperature gradient reflection
1,615–1,640	Very fractured, large matrix permeability below 1,629 ft, open parting at Calico Hills-Crater Flat contact; fractures, mostly open 1,622–1,625 ft, are shallow-near vertical, diversely oriented. Most flow probably is through open fractures and parting	0.01 in and up	0	Very low resistivity, borehole enlargement to about 32 inches
1,640–1,674	Sparsely fractured to 1,666 ft, moderately fractured below; large matrix permeability; fractures are near vertical, east, south, and southwest-striking. Water apparently transmitted by fractures and matrix	Small gain(?)	0	Low resistivity, borehole enlargement
1,846–1,865	Moderately fractured, large matrix permeability; fractures are near vertical-vertical east, southeast, and south-striking. Water apparently transmitted by fractures and matrix	Small loss(?)	0	Low resistivity, minor borehole enlargement
1,865–1,950	Sparsely to moderately fractured(?): No fractures detected, but matrix permeability is too small for unfractured rock to be transmissive	Small loss(?)	0	Low resistivity, concave temperature gradient inflection
2,050–2,132	Sparsely fractured to 2,116 ft, very fractured below; large matrix permeability throughout. Fractures are shallow-near vertical, west and south-striking. Water apparently transmitted by matrix above 2,116 ft, fractures and matrix below	≤0.01 out	0	Low resistivity, borehole enlargement
2,200–2,215	Moderately fractured(?), large matrix permeability; although no fractures detected, sharp peak on caliper log implies presence of one or more. Water probably transmitted by fractures and matrix	0.02 out	0	Low resistivity, concave temperature gradient inflection, borehole enlargement
2,374–2,381	Very fractured, large matrix permeability; fractures, one of which is open, are mostly near vertical-vertical, southeast-striking	1.72 out	17	Convex temperature gradient inflection, borehole enlargement
2,421–2,478	Very fractured; fractures are open, near vertical-vertical, south-striking	1.7 out	55	Low resistivity, borehole enlargement to 2,450 ft
2,503–2,527	Very fractured; fractures, two of which are open, are vertical, south-striking	0.5 out	3	Low resistivity, borehole enlargement
2,535–2,665	Sparsely to moderately fractured(?), with large matrix permeability below 2,610 ft.Interval known to contain an open, shallow, north-striking fracture and a near vertical south-striking fracture; other fractures implied by sharp caliper peaks. Water probably transmitted through open fractures and matrix	Small loss(?)	0	Low resistivity, borehole enlargement

Table 6. Transmissive intervals in borehole UE-25c #3 --Continued

Depth below land surface (feet)	Characteristics	Intraborehole flow (gallons per minute)	Pumping discharge (percent)	Supporting information
2,685–2,755	Moderately to very fractured; fractures, two of which are open, are shallow-steep, northeast, southwest, west, northwest, and north-striking	Estimated small gain to maximum upward flow of >4.0	0	Low resistivity, borehole enlargement around open fractures at 2,685 and 2,703 ft
2,758–2,851	Very fractured rock, including the Paintbrush Canyon Fault zone at 2,820–2,825 ft, separated by thin intervals of unfractured rock; fractures four of which are open, are shallow-vertical, mostly north, south, and southwest-striking	2.0 in and up	25	Low resistivity, convex temperature gradient inflection, borehole enlargement to about 22 inches below 2,830 ft
2,884–2,887	Very fractured; fractures are shallow-steep, north and northwest-striking	0.1 in and up	0	Low resistivity, borehole enlargement
2,899–2,910	Very fractured; fractures are shallow-steep, mostly west, northwest, and north-striking	0.1 in and up	0	Concave temperature gradient inflection
2,923–2,945	Moderately fractured; fractures are shallow-vertical, mostly north and west-striking	0.1 in and up	0	Low resistivity, convex temperature gradient inflection
2,950–3,000	Moderately fractured(?); extent of fracturing uncertain because interval is concealed by cable and borehole collapse	1.7 in and up	0	Low resistivity

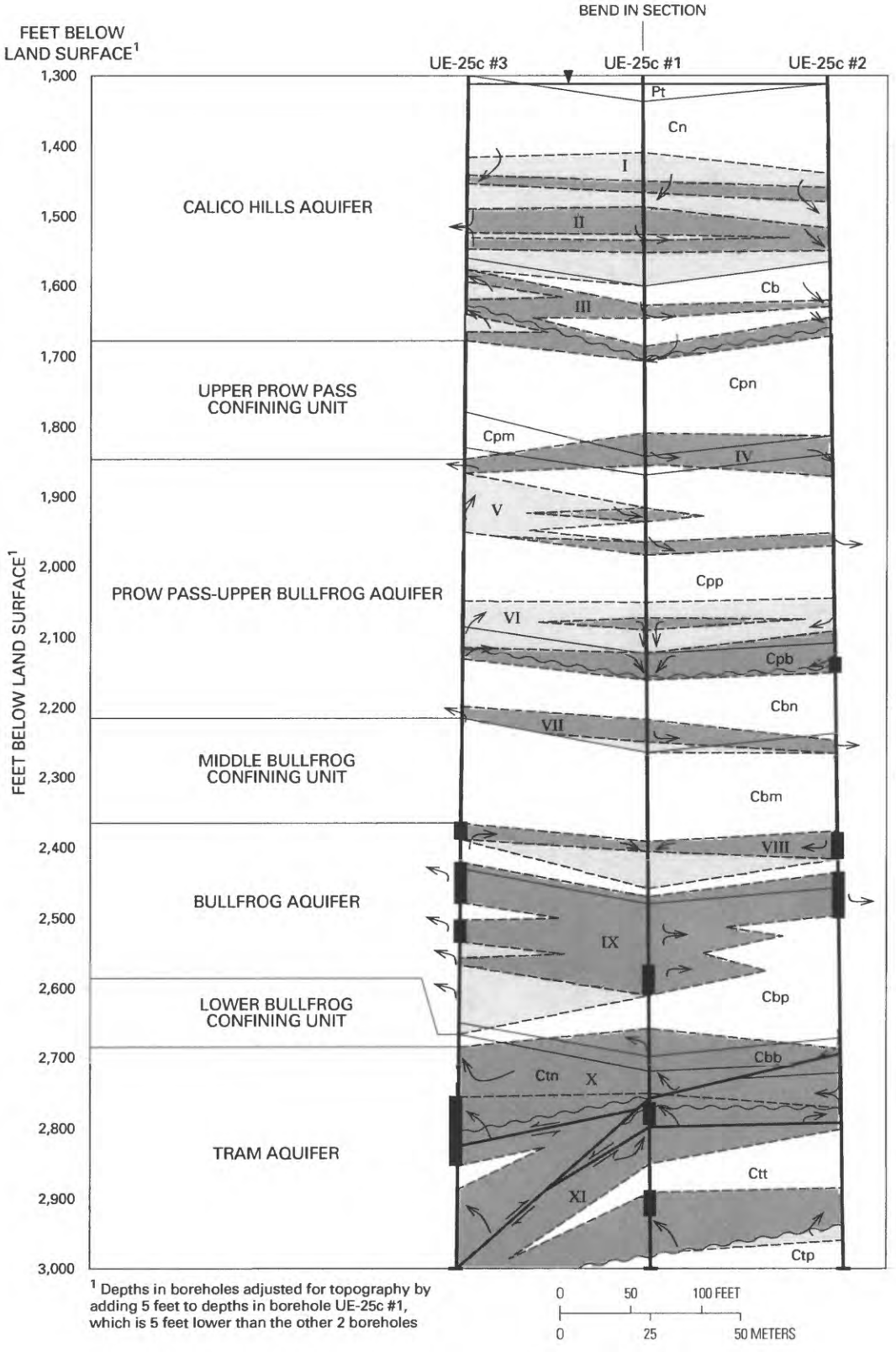

Figure 7A. Hydrogeologic section of the c-hole complex.

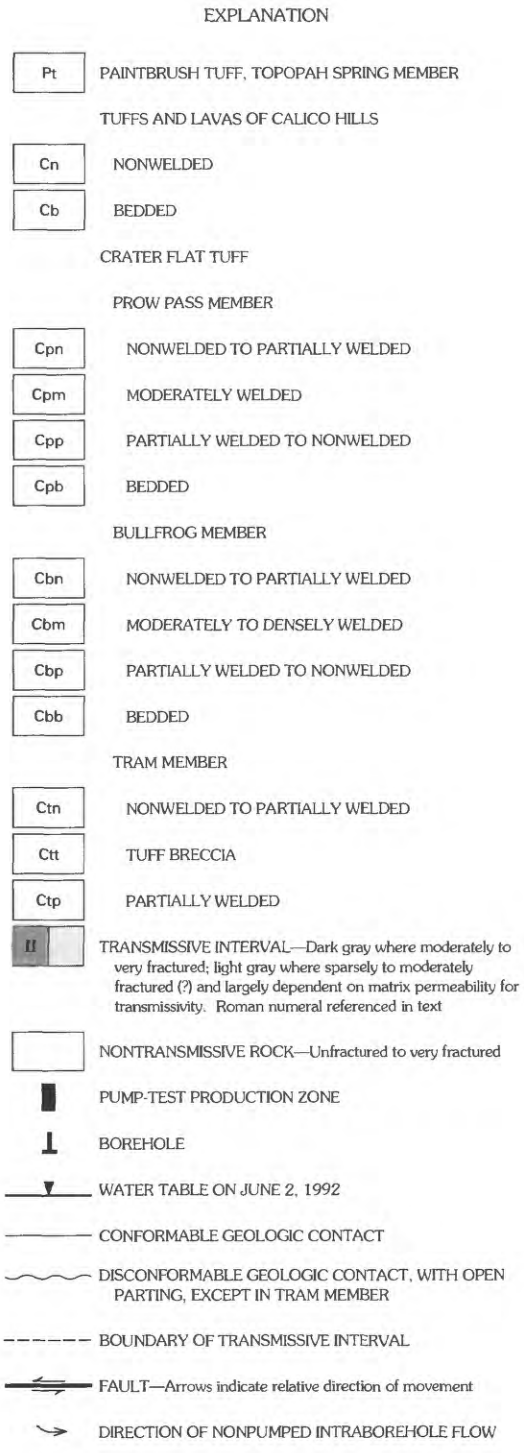

Figure 7B. Hydrogeologic section of the c-hole complex.

open, are shallow to vertical and diversely oriented. The upper part of the aquifer (transmissive interval I) is characterized by small to moderate downflows from the water table. In the middle part of the aquifer (transmissive intervals II and III), all downward flow in borehole UE-25c #3, all remaining upward flow from lower in borehole UE-25c #3, and about a third of the downwardflow in borehole UE-25c #1 are lost through fractures and the rock matrix; some of this water flows into borehole UE-25c #2. At the bottom of the aquifer, small upflows and downflows enter the c-holes through a parting at the contact between the tuffs and lavas of Calico Hills and the Crater Flat Tuff.

Prow Pass - Upper Bullfrog Aquifer

The Prow Pass - upper Bullfrog aquifer extends from about 1,800 ft to about 2,270 ft below land surface and probably either is unconfined or is a fissure-block aquifer. It consists of four relatively thin zones of moderately (?) to very fractured rock separated by thin to thick intervals of unfractured to sparsely fractured rock, some of which contain large matrix permeability (fig. 7). Fractures, some of which are open, are shallow to vertical and diversely oriented, although many are north- or south-striking. A parting at the contact between the Prow Pass and Bullfrog Members of the Crater Flat Tuff occurs near the bottom of the aquifer. In the upper part of the aquifer (transmissive intervals IV and V), a small outflow from borehole UE-25c #3 is transmitted toward borehole UE-25c #1, and a small outflow from borehole UE-25c #1 is transmitted toward borehole UE-25c #2. Lower in this part of the aquifer, these inflows leave boreholes UE-25c #1 and UE-25c #2 through fractures. In the middle part of the aquifer (transmissive interval VI), small outflows from boreholes UE-25c #2 and UE-25c #3 are transmitted by fractures, the rock matrix, and the parting at the Prow Pass - Bullfrog contact toward borehole UE-25c #1. At the bottom of the aquifer (transmissive interval VII), small outflows to fractures occur in all of the c-holes. Seven percent of the discharge from borehole UE-25c #2 during a pumping test in March 1984 came from this aquifer.

Bullfrog Aquifer

The Bullfrog aquifer extends from about 2,370 to 2,660 ft below land surface and is confined by more than 100 ft of overlying unfractured to sparsely fractured, moderately to densely welded tuff (fig. 7). The aquifer consists mostly of moderately to very fractured rock with thin intervals of unfractured to sparsely fractured rock, but the lower 50 ft of the aquifer in borehole UE-25c #3 is sparsely to moderately fractured. The upper part of the aquifer (transmissive interval VIII) contains large matrix permeability. Fractures, most of which are open, are shallow to vertical, and diversely oriented. In the upper part of the aquifer, small to large outflows from boreholes UE-25c #2 and UE-25c #3 are transmitted toward borehole UE-25c #1. In the lower part of the aquifer (transmissive interval IX), all downward flow and all remaining upward flow from lower in borehole UE-25c #1 are lost through fractures; small to large outflows from boreholes UE-25c #2 and UE-25c #3 occur, as well. Sixty-four percent of the discharge from a pumping test in borehole UE-25c #1 in September 1983, 93 percent of the discharge from a pumping test in borehole UE-25c #2 in March 1984, and 75 percent of the discharge from a pumping test in borehole UE-25c #3 in May-June 1984 came from this aquifer.

Tram Aquifer

The Tram aquifer extends from about 2,660 ft below land surface to the bottom of the c-holes and is confined. However, leakage occurs from two faults that transect this aquifer. The aquifer consists almost entirely of moderately to very fractured rock (fig. 7). Fractures, many of which are open, are shallow to vertical and diversely oriented. At the top of the aquifer (transmissive interval X), all downward flow and all remaining upward flow from lower in the borehole are lost from borehole UE-25c #2 and are transmitted toward boreholes UE-25c #1 and UE-25c #3. In the lower part of the aquifer (transmissive interval XI), small to large upward flows enter the c-holes. Thirty-six percent of the discharge from a pumping test in borehole UE-25c #1 in September 1983 and 25 percent of the discharge from a pumping test in borehole UE-25c #3 in May-June 1984 came from this aquifer.

FLUID-INJECTION TESTS

Twenty-six fluid-injection tests were conducted in the c-holes in 1983 and 1984. In October 1983, 16 falling-head (slug) tests and nine pressure-injection tests were conducted in borehole UE-25c #1. In October 1984, a constant-head injection test was conducted in borehole UE-25c #2 using boreholes UE-25c #1 and UE-25c #3 as observation wells. The constant-head test, soon after it began, developed into a constant-flux test and is discussed later in this report with pumping tests conducted in the c-holes.

Falling-Head Tests

Falling-head tests conducted in borehole UE-25c #1 are listed in table 7, which indicates that test intervals were successively reduced from 160 to 40 to 22 ft, except near the top and bottom of the borehole, where test interval thicknesses were determined partly by the bottom of the concrete and the bottom of the borehole. As shown in figure 8, tests intervals were isolated by TAM International inflatable packers, monitored primarily by contractor-supplied Kuster and Sperry-Sun pressure and temperature gauges above, between, and below the packers, and monitored secondarily by a USGS-supplied Bell and Howell pressure-transducer suspended inside the 2.26-in.-inside diameter plastic riser pipe above the packer string. For all tests except test 1, the transducer was set at 1,370 ft below the top of the riser pipe; for test 1, it was set at 1,330 ft below the top of the pipe.

According to Devin L. Galloway (USGS, oral commun., 1993), the contractor-supplied gauges, with pressure ranges of 0 to 2,150 lb/in.^{2} and 0 to 5,000 lb/in.^{2} (Tam International, written commun., 1983), were insensitive to small changes in head that are common to aquifer tests. Moreover, because of a recording interval of 2 min, these gauges missed the initial head in some tests, and in very permeable intervals, the gauges missed most or all of the head recovery. The USGS-supplied pressure transducer, with a pressure range of 0 to 500 lb/in.^{2} and a minimum recording interval of eight seconds, was considered more reliable for data collection and analysis than the contractor-supplied gauges. Consequently, only the pressure-transducer data for the falling-head tests were analyzed.

An additional problem with the design of the falling-head tests was the large column of water injected into borehole UE-25c #1 during the tests. As indicated in table 7, initial injected heads in these tests ranged from 592 to 1,022 ft above the static water level, averaging about 700 ft. Galloway (USGS, written commun., 1986) reported that calculations for a representative test conducted in a permeable zone indicate that a head loss of 35 to 40 percent probably occurred during the falling-head tests as a result of friction between the injected water as it descended and the riser pipe. Although early-time recovery data could have been affected by any initial head loss to friction, later recovery data probably would not have been affected. Consequently, the later-time recovery data were emphasized in analyzing these tests.

The commonly used method for analyzing falling-head tests, in a confined aquifer, is that of Cooper and others (1967), which assumes radial flow to a fully penetrating well in a homogeneous, isotropic, compressible aquifer. Reed (1980) presents type curves of the well function for the analytical solution of Cooper and others (1967). As pointed out by Cooper and others (1967), matching data curves with the type curves can provide a good determination of transmissivity, whereas the determination of storativity is not reliable because of the similar shape of the type curves. Barker and Black (1983) indicate that the solution of Cooper and others (1967) can be applied successfully to formations with very low storativity and to fractured rock, provided that there is no exchange of water between fractures and the rock matrix and that fracture apertures are not changed by the pressure of the injected water column. However, Barker and Black (1983) state that even where water is derived from fractures and the rock matrix, a situation commonly termed a "dual-porosity" aquifer, transmissivity determined by the method of Cooper and others (1967) will be underestimated by a factor of no more than 2–3. This potential error generally would be considered insignificant in a complicated hydrogeologic environment, such as the c-hole complex, where one might expect transmissivity calculations to be within an order of magnitude of actual values. Barker and Black (1983) cautioned against using the method of Cooper and others (1967) to determine storativity in a dual-porosity aquifer, because the method can underestimate storativity by a factor of as large as 0.000001. Because of large potential error, storativity was not determined from the falling-head tests in borehole UE-25c #1.

In the solution of Cooper and others (1967), values of the ratio of injected head at time t to initial injected head (H/H_o) are plotted against time elapsed since the injection of fluid occurred. A match between the data curve and a type curve plot of H/H_o as a function of $\beta = Tt/r_c^2$ gives a value of $\alpha = r_s^2/r_c^2 \times S$, β, and time, where,

T = transmissivity (L^2/T);
r_c = radius of casing (plastic riser pipe in UE-25c #1) in which water level fluctuates (L);
r_s = radius of open hole (L);
t = time (T); and
S = storativity (dimensionless).

Transmissivity is found by picking a match point where $\beta = 1$ and solving the equation:

$$T = r_c^2/t \qquad (2)$$

On the basis of the solution of Cooper and others (1967), falling-head tests in borehole UE-25c #1 indicated transmissivity values for tested intervals that

Table 7. Results of falling-head tests conducted in borehole UE-25c #1, October 6–12, 1983

Test number	Test interval depth (feet)	Geologic description of test interval	Static water level (feet below land surface)	Initial head above static water level (feet)	Duration of recovery (minutes)	Transmissivity (feet square per day)	Hydraulic conductivity (feet per day)
1	1,371–1,515	Unfractured to sparsely fractured, nonwelded and bedded tuff with thin intervals that are moderately fractured	1,314	649	41	20	0.1
2	1,685–1,845	Unfractured to very fractured, nonwelded to moderately welded tuff	1,313	638	84	10	0.07
3	1,865–2,025	Unfractured to very fractured, nonwelded to partially welded tuff	1,313	699	243	0.8	0.005
4	2,050–2,210	Unfractured to very fractured, bedded and nonwelded to partially welded tuff	1,313	728	422	10	0.08
6	2,610–2,770	Unfractured to very fractured, nonwelded to partially welded tuff	1,314	656	100	8	0.05
7	2,780–2,995	Very fractured tuff breccia and tuff within unfractured intervals	1,312	750	13	40	0.2
10	1,805–1,845	Very fractured, nonwelded to moderately welded tuff	1,314	705	111	4	0.1
12	1,900–1,940	Unfractured and very fractured, nonwelded to partially welded tuff	1,312	666	281	0.3	0.008
15	2,555–2,595	Moderately to very fractured, nonwelded to partially welded tuff	1,314	784	2.75	80	2
16	2,746–2,786	Very fractured, nonwelded to partially welded tuff and tuff breccia	1,313	592	12	20	0.5
17	2,818–2,858	Unfractured and very fractured tuff breccia	1,314	792	70	10	0.3
18	2,880–2,920	Very fractured tuff breccia	1,313	822	41	20	0.5
19	2,930–2,995	Unfractured and very fractured tuff breccia and partially welded tuff	1,314	1,022	116	5	0.08
20	2,445–2,467	Moderately to very fractured, moderately to densely welded tuff	1,313	683	87	9	0.4
21	2,476–2,498	Very fractured, partially to densely welded tuff	1,314	666	35	10	0.6
26	2,607–2,995	Mostly moderately to very fractured, nonwelded to partially welded tuff and tuff breccia	1,314	869	12.5	50	0.1

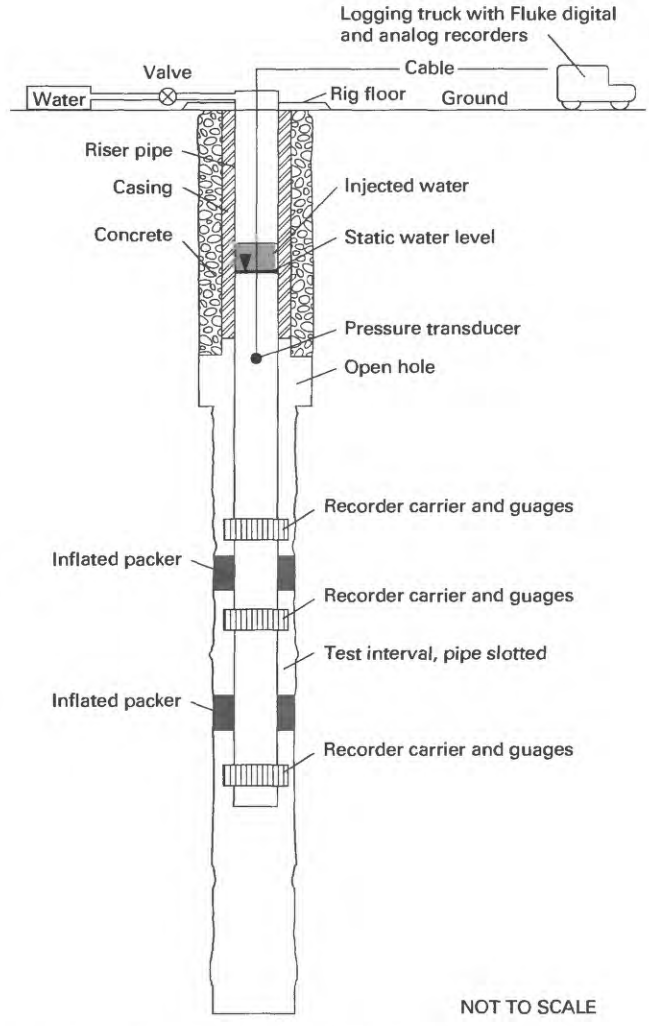

Figure 8. Design configuration of falling-head tests in borehole UE-25c #1, October 1983.

ranged from 0.3 to 80 ft^2/d (table 7). Assuming that head is dissipated uniformly throughout tested intervals, and not through preferred pathways, such as fractures and partings, then dividing transmissivity by test interval thickness provides estimates of hydraulic conductivity for the tested intervals. Estimated values of hydraulic conductivity from the falling-head tests, range from 0.005 to 2 ft/d (table 7 and fig. 9).

Values of transmissivity and hydraulic conductivity calculated using the method of Cooper and others (1967) are considered reasonable because:

1. In all tests, there was fair to good agreement between data curves and type curves. There was no systematic improvement in curve matching for intervals with less fracturing and, presumably, more dependence on matrix flow (fig. 10). Therefore, one can conclude that the presence of fractures in a test interval generally did not invalidate the fundamental assumption of radial flow through a homogeneous, isotropic aquifer.

2. In the three sections of the borehole where multiple tests were conducted, 1,685 to 1,845 ft, 1,865 to 2,025 ft, and 2,607 to 2,995 ft, tests of successively smaller intervals produced successively smaller values of transmissivity, the sum of which did not exceed the transmissivity of the larger test interval (fig. 10). Transmissivity is additive and should increase with increasing test-interval thickness.

One problem common to all of the falling-head tests conducted in borehole UE-25c #1 is the small to large divergence between the late-time recovery data and the tail of the type curve to which the data curve was matched (fig. 9). Analytical solutions invoking different conceptual flow models than that of Cooper and others (1967) were tried to provide more precise determinations of transmissivity (Devin L. Galloway, USGS, written commun., 1986). A linear flow model, which simulates flow in and perpendicular to fracture planes, produced a poorer solution because type curves are much flatter than those of Cooper and others (1967). Imposing a linear or radial constant-head boundary at some variable distance from borehole UE-25c #1, simulating radial flow through a borehole skin (although not justified by the drilling technique), or considering spherical flow through the test interval, all produced type curves and tails steeper than those of Cooper and others (1967), but less steep than the data curves. None of the alternative analytical solutions were considered substantially more accurate or conceptually more realistic than the method of Cooper and others (1967). Consequently, calculations using only the method of Cooper and others (1967) are presented in this report.

Pressure-Injection Tests

Pressure-injection tests conducted in borehole UE-25c #1 are listed in table 8, which indicates that test intervals were 22, 40, or 160 ft. Some of the tests were planned for intervals thought to have small permeability (Devin L. Galloway, USGS, oral commun., 1993), but most of the tests were changed from falling-head tests after a few minutes of extremely slow gravity drainage (USGS, unpublished log book for borehole UE-25c #1). Four of the tests could not be analyzed because of apparent mechanical problems and insufficient or unreliable data.

The pressure-injection tests were designed similarly to the falling-head tests (fig. 8), except that a valve in the water line was closed during the pressure-injection tests to isolate the test interval from atmospheric pressure. With the system pressurized (shut in), the pressure transducer used in the falling-head tests would have no hydraulic connection to the test interval and, therefore, could not be used (see fig. 8). The Sperry-Sun gauge, which provided digital output at two-minute intervals, produced the primary record for the pressure-injection tests. The procedure for the pressure-injection tests (Neuzil, 1982) consisted of the following steps:

1. The valve in the water line was opened, and a slug of water was released into the borehole;

2. The test interval was shut in by closing the valve in the water line;

3. Pressure decay in the test interval was monitored until pressure was constant or nearly constant;

4. The control valve was opened briefly, and another slug of water was released into the borehole;

5. The control valve was closed, again shutting in the test interval;

6. Pressure in the test interval again was allowed to decay to a constant or nearly constant level; and

7. The control valve was opened, and pressure on the system was released.

The pressure-injection tests were analyzed by the method of Bredehoeft and Papadopulos (1980), as

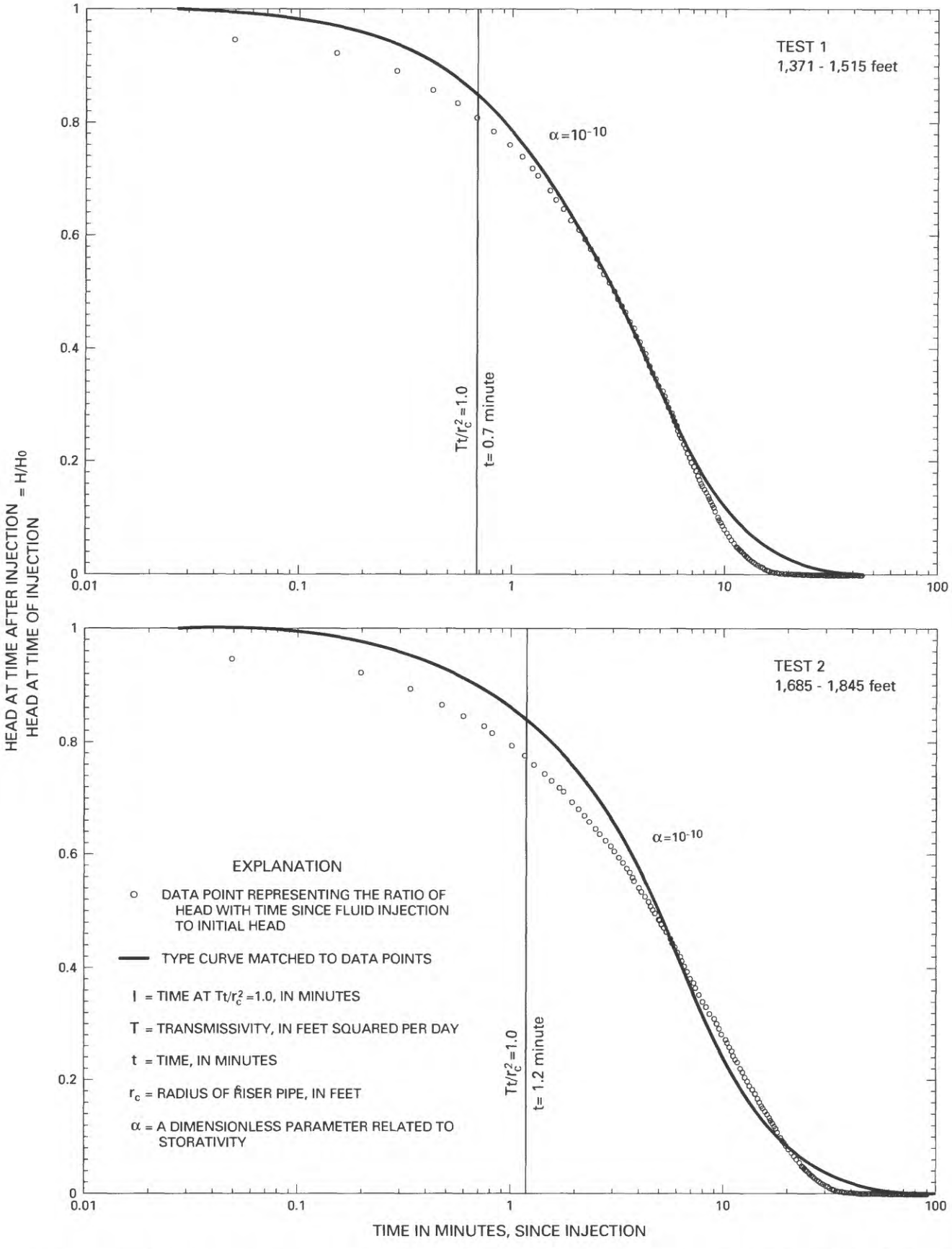

Figure 9A. Analyses of falling-head tests in borehole UE-25c #1, October 1983, assuming an infinite, homogeneous, isotropic, confined aquifer (symbols on plots explained in text).

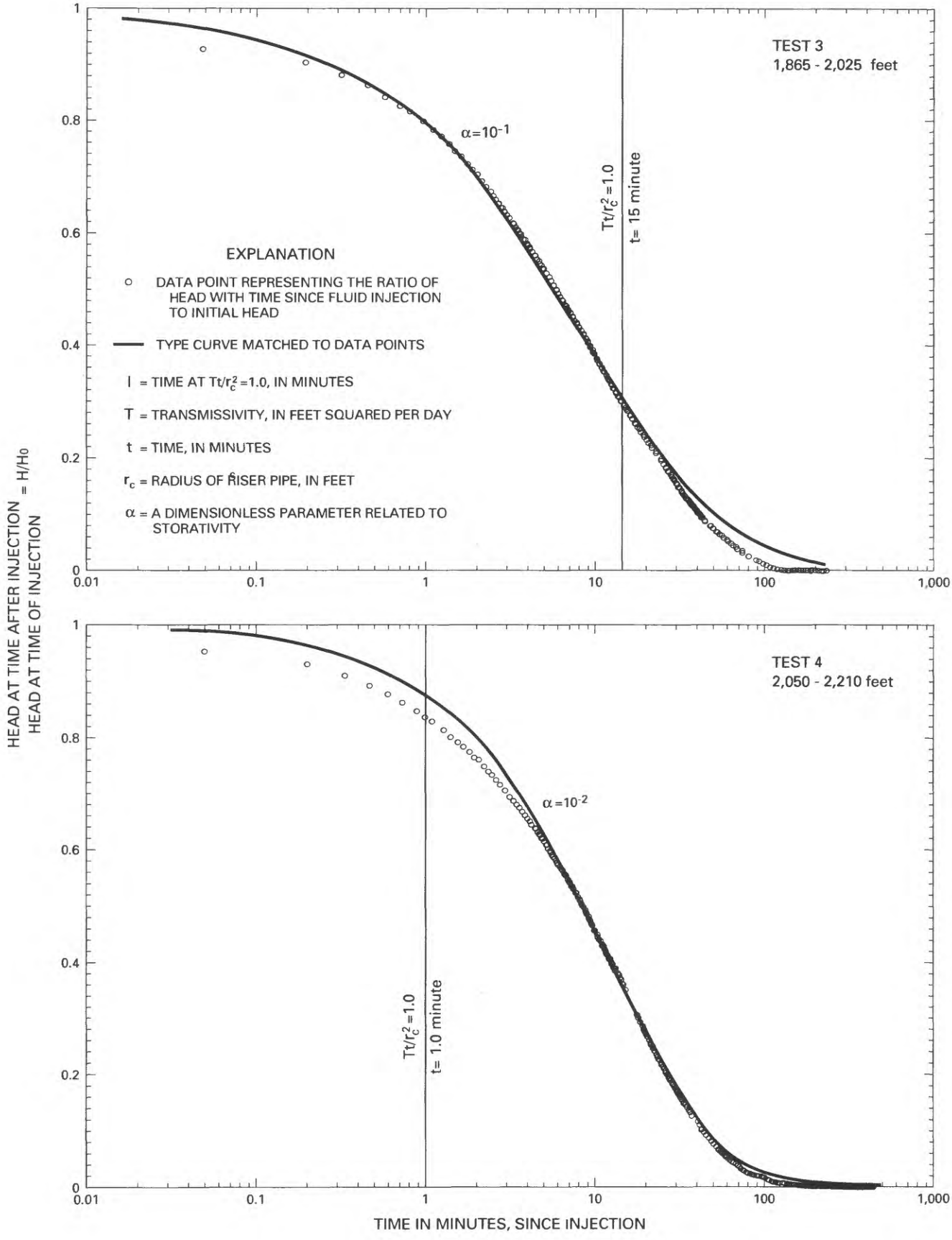

Figure 9B. Analyses of falling-head tests in borehole UE-25c #1, October 1983, assuming an infinite, homogeneous, isotropic, confined aquifer (symbols on plots explained in text).

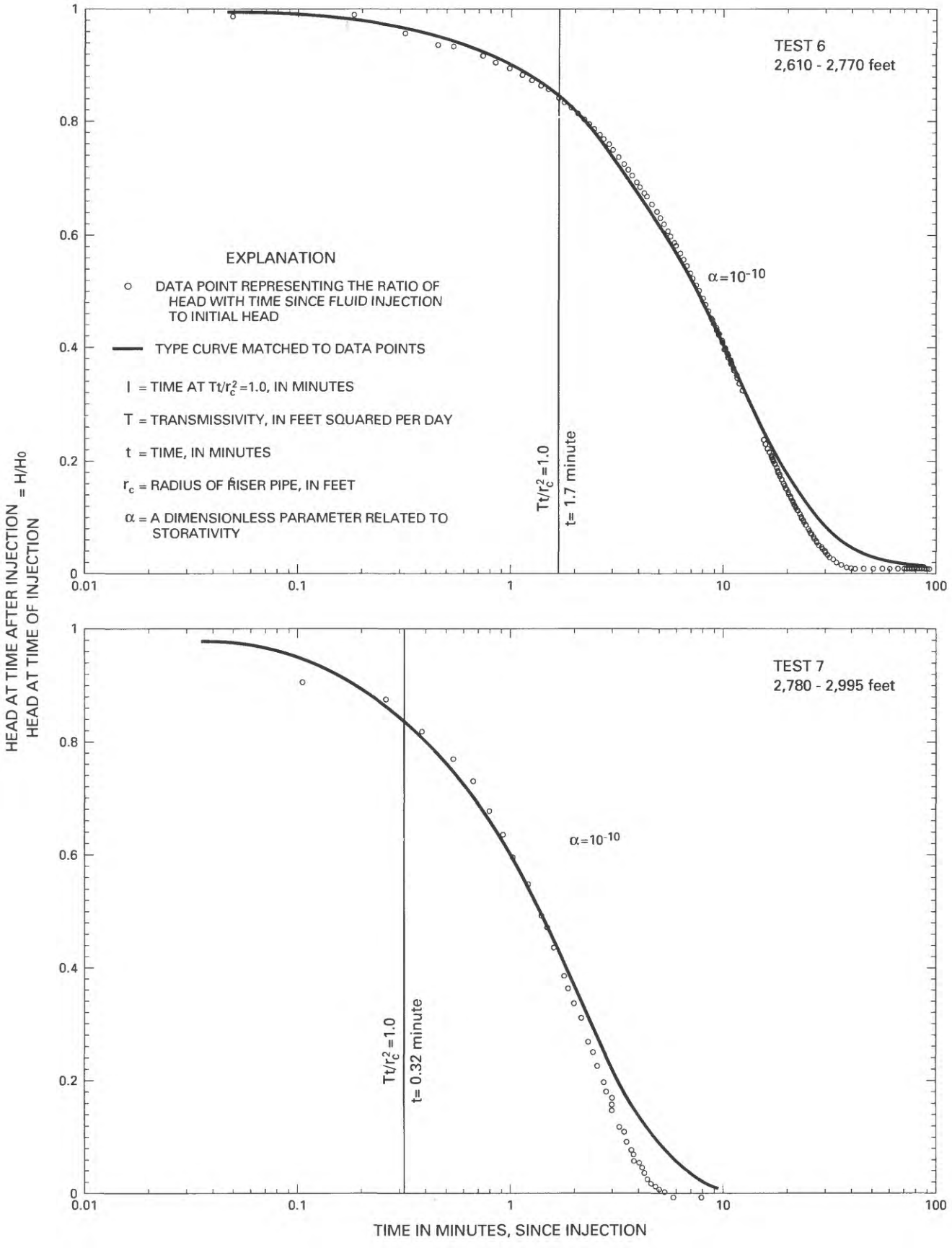

Figure 9C. Analyses of falling-head tests in borehole UE-25c #1, October 1983, assuming an infinite, homogeneous, isotropic, confined aquifer (symbols on plots explained in text).

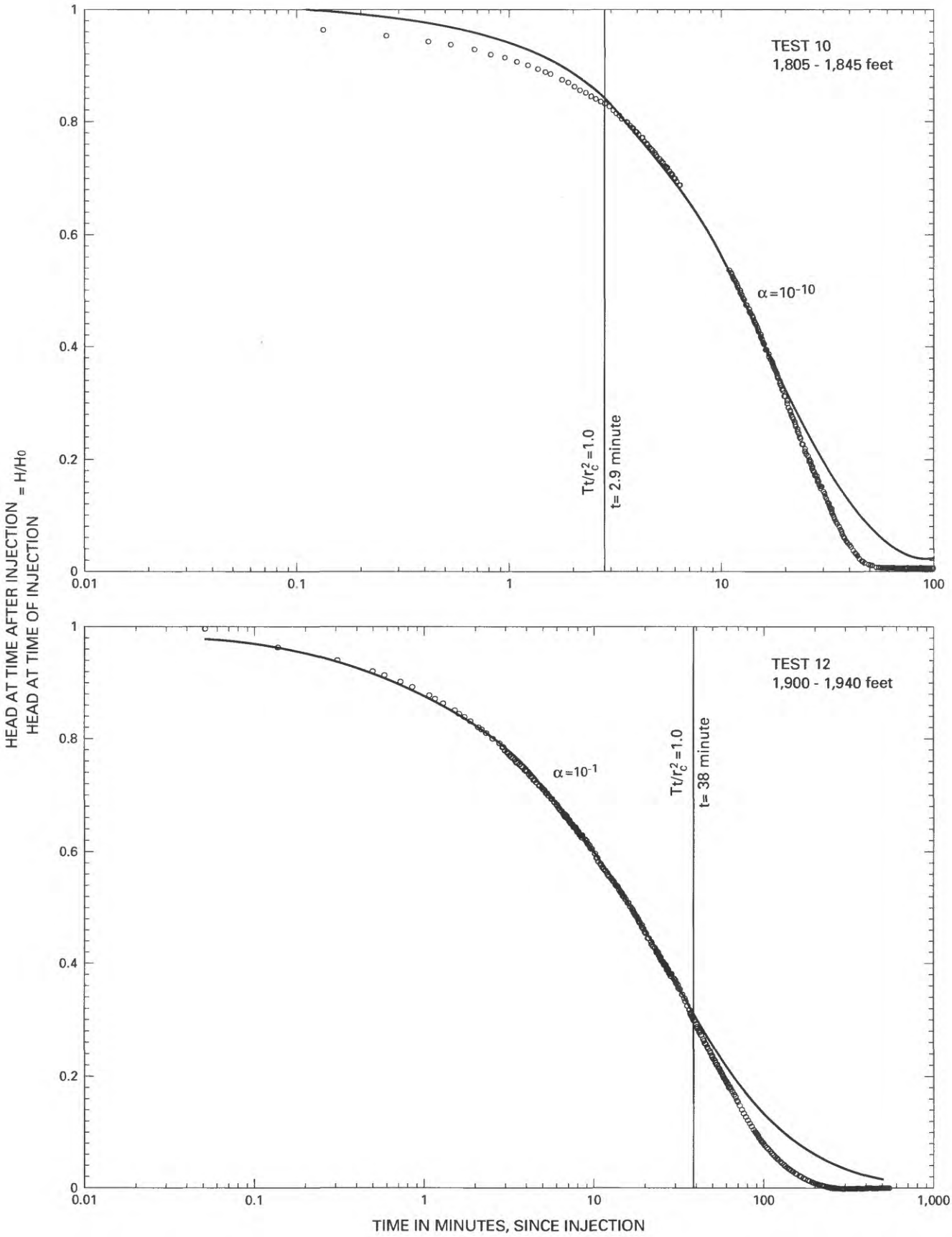

Figure 9D. Analyses of falling-head tests in borehole UE-25c #1, October 1983, assuming an infinite, homogeneous, isotropic, confined aquifer (symbols on plots explained in text).

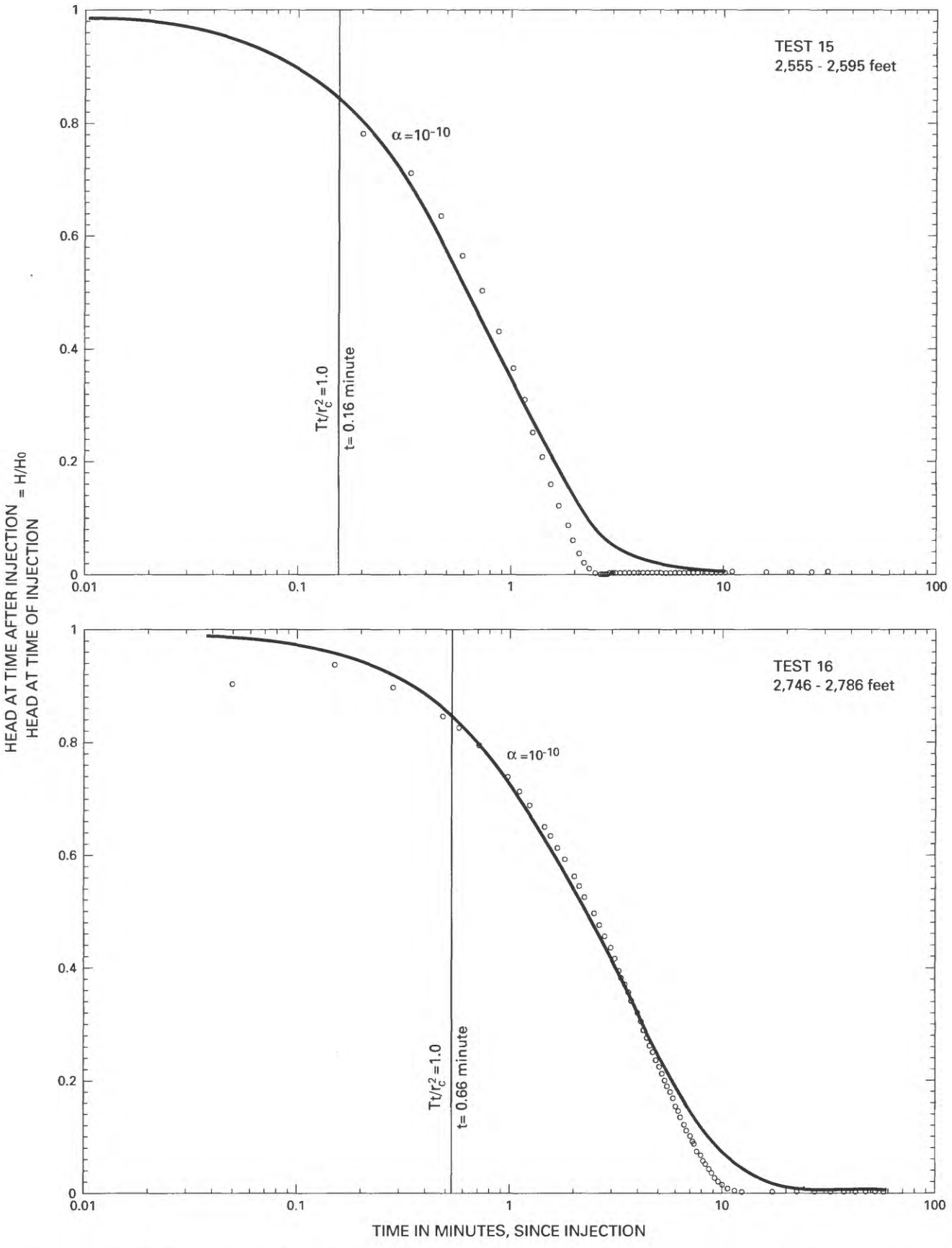

Figure 9E. Analyses of falling-head tests in borehole UE-25c #1, October 1983, assuming an infinite, homogeneous, isotropic, confined aquifer (symbols on plots explained in text).

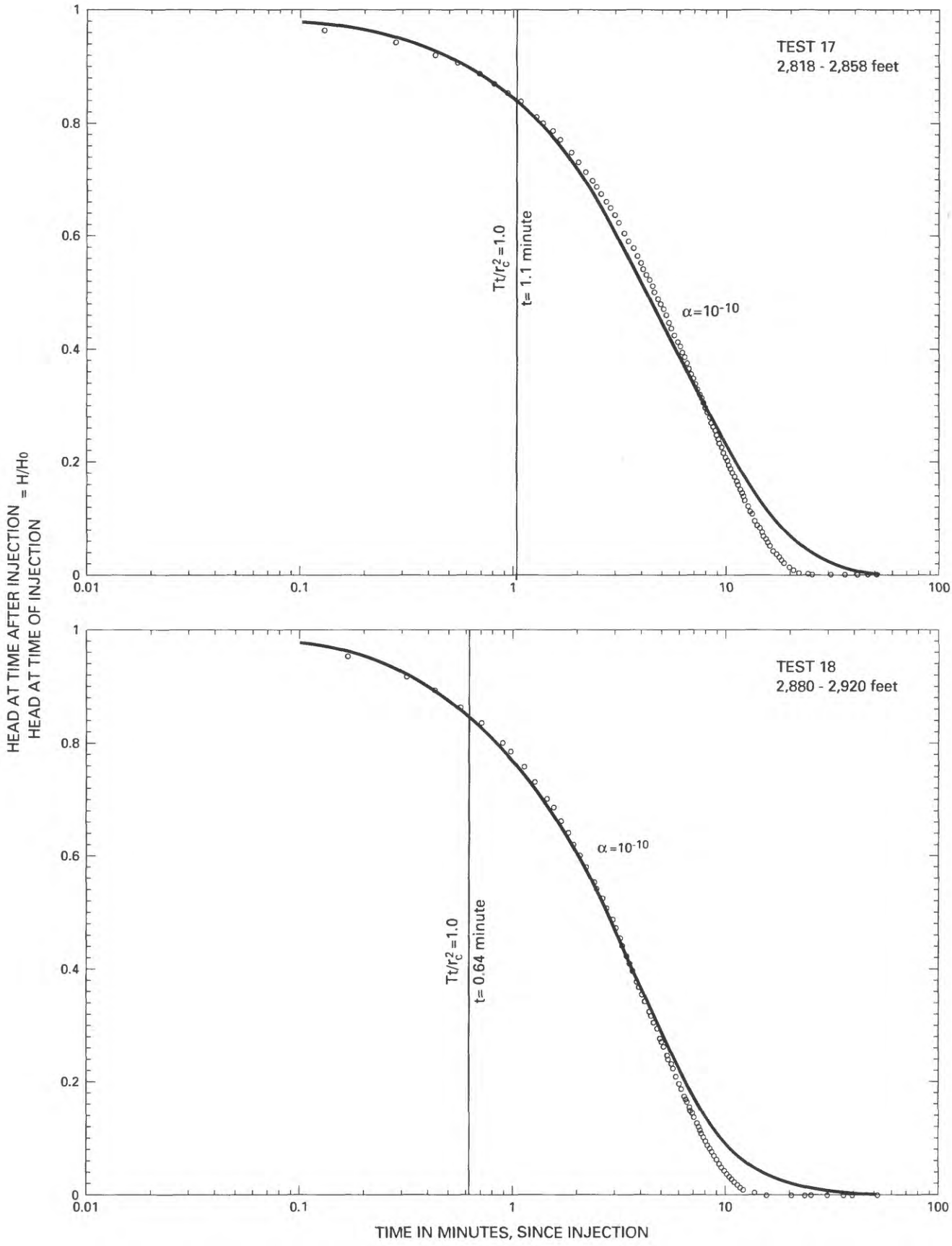

Figure 9F. Analyses of falling-head tests in borehole UE-25c #1, October 1983, assuming an infinite, homogeneous, isotropic, confined aquifer (symbols on plots explained in text).

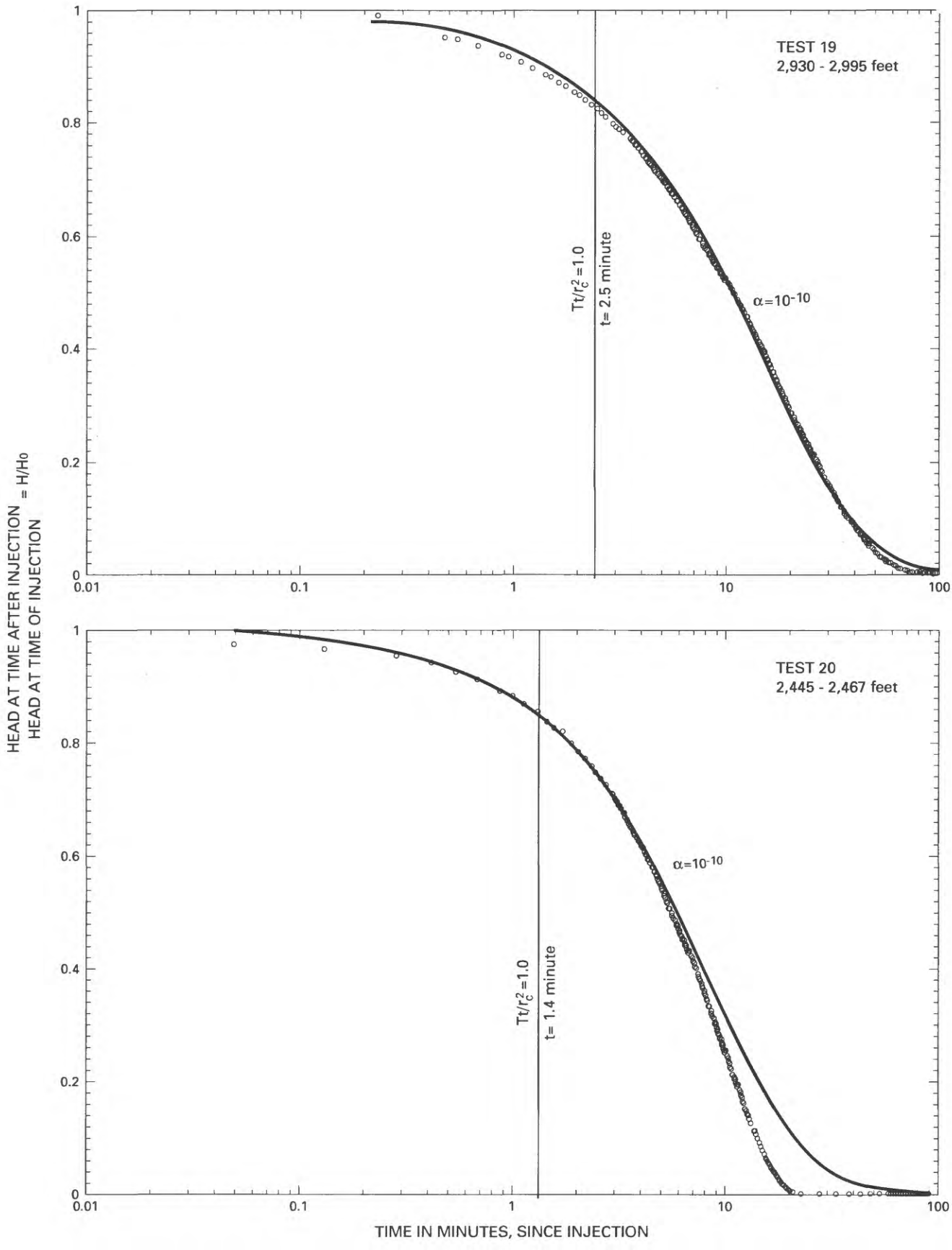

Figure 9G. Analyses of falling-head tests in borehole UE-25c #1, October 1983, assuming an infinite, homogeneous, isotropic, confined aquifer (symbols on plots explained in text).

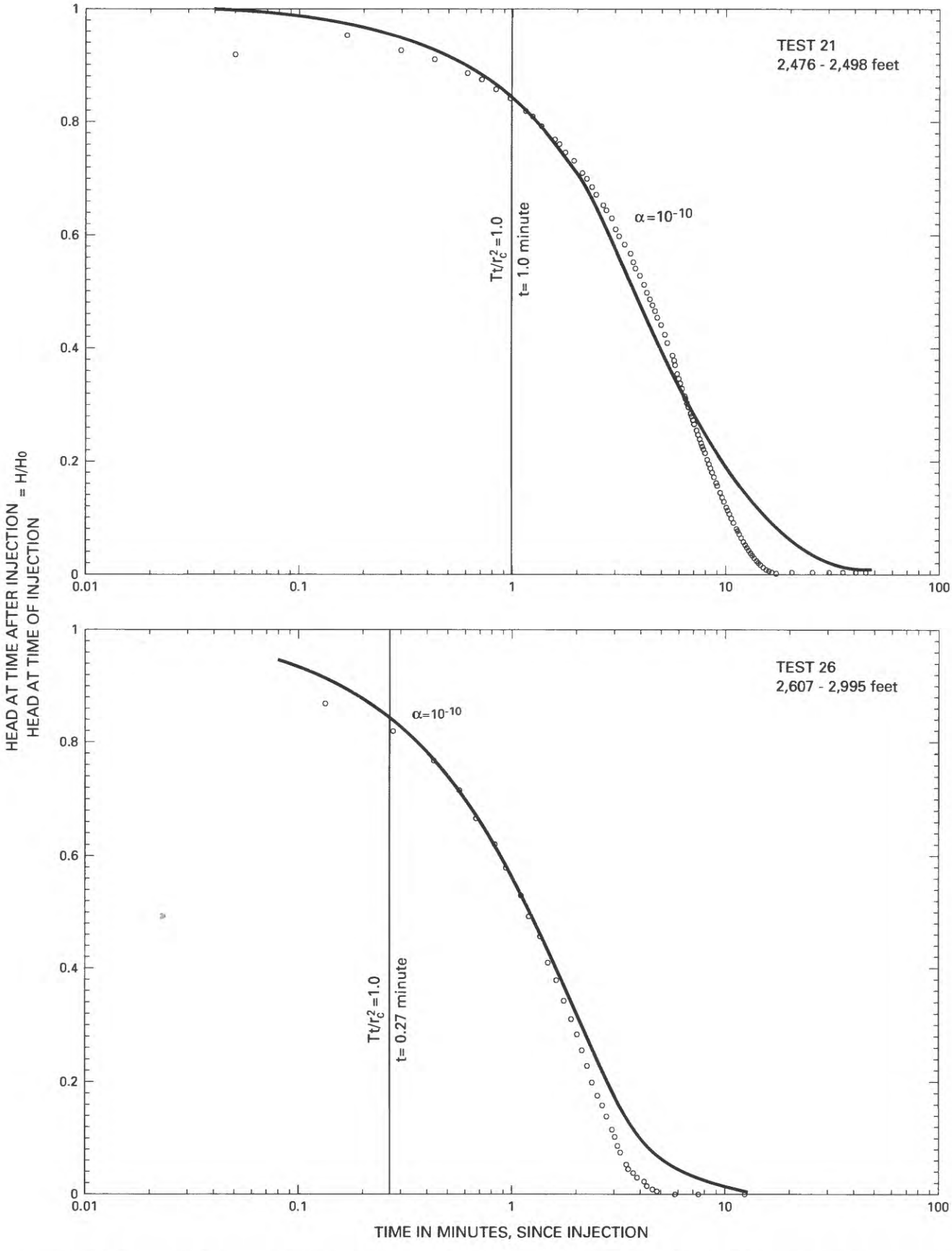

Figure 9H. Analyses of falling-head tests in borehole UE-25c #1, October 1983, assuming an infinite, homogeneous, isotropic, confined aquifer (symbols on plots explained in text).

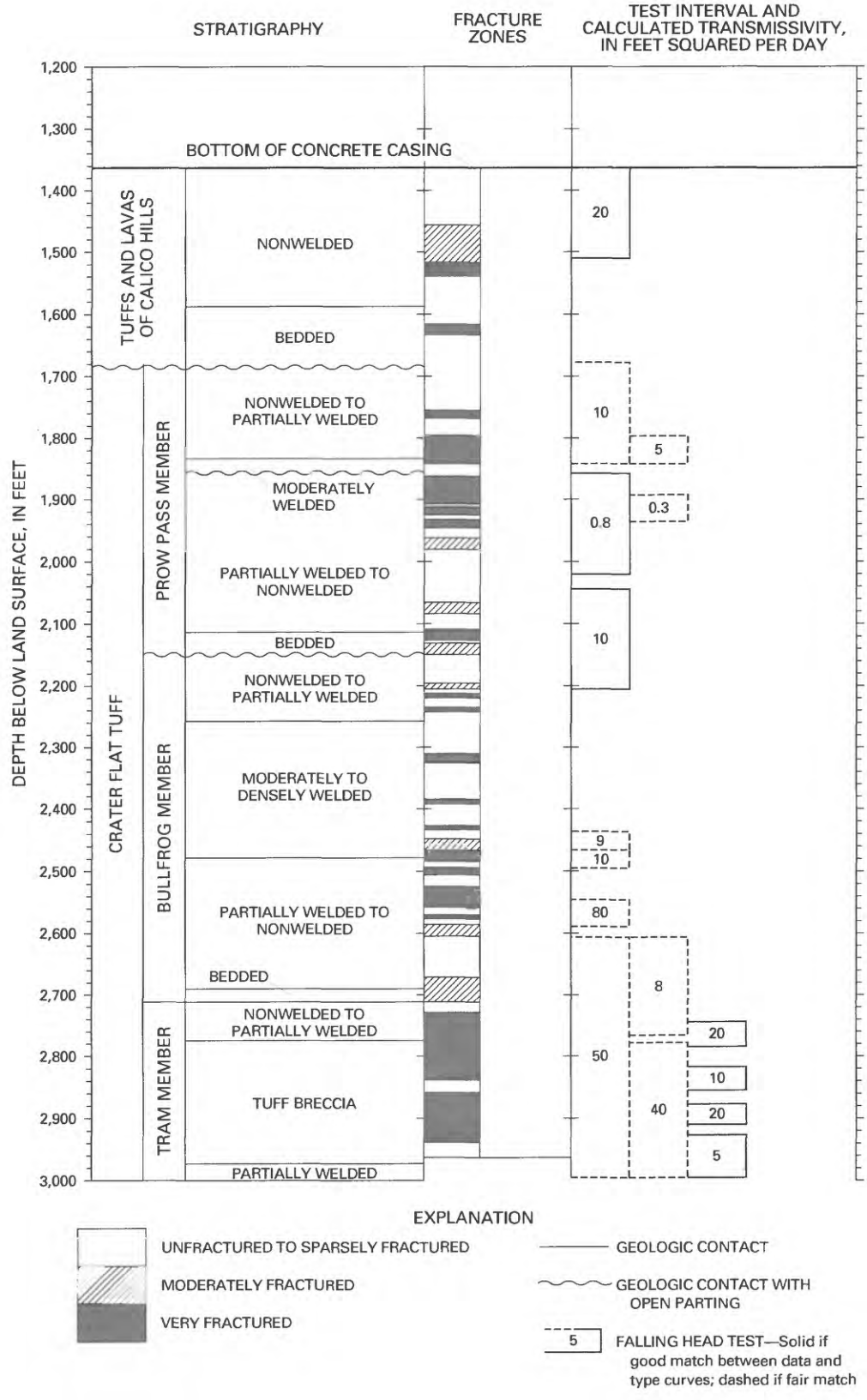

Figure 10. Falling-head tests and transmissivity values obtained in relation to geology, borehole UE-25c #1.

Table 8. Results of pressure-injection tests conducted in borehole UE-25c #1, October 6–12, 1983

[n.a., test not analyzed because of insufficient or unreliable data; n.s., no solution determined]

Test number	Test interval depth (feet)	Geologic description of test interval	Recorded head (pounds per square inch)	Antecedent head (pounds per square inch)	Residual head (pounds per square inch)	Duration of pressure decay (minutes)	Transmissitivity (feet squared per day)	Hydraulic conductivity (feet per day)
5	2,270–2,430	Unfractured, moderately to densely, welded tuff with thin fractured intervals	n.a.	n.a.	n.a.	n.a.	n.a.	n.a.
8	1,525–1,565	Unfractured and very fractured, nonwelded tuff	388.65	142.28	246.37	96	n.s.	n.s.
9	1,634–1,674	Sparsely fractured, bedded tuff	552.97	397.35	155.62	98	1	0.03
11	1,870–1,910	Very fractured, nonwelded to partially welded tuff	n.a.	n.a.	n.a.	n.a.	n.a.	n.a.
13	1,940–1,980	Unfractured to very fractured, nonwelded to partially welded tuff	567.31	315.09	252.22	78	6	0.2
14	2,215–2,255	Unfractured and very fractured, nonwelded to partially welded tuff	550.17	389.36	160.81	34	10	0.3
22	2,498–2,520	Unfractured and very fractured, nonwelded to partially welded tuff	n.a.	n.a.	n.a.	n.a.	n.a.	n.a.
23	2,575–2,597	Unfractured to very fractured, nonwelded to partially welded tuff	922.52	544.63	377.89	96	10	0.4
25	2,508–2,530	Sparsely to moderately fractured, nonwelded to partially welded tuff	n.a.	n.a.	n.a.	n.a.	n.a.	n.a.

modified by Neuzil (1982). Assumptions of this method are the same as those discussed previously for the falling-head tests. In this method, pressure decay at the end of the first shut-in period is extrapolated to establish unambiguously an antecedent pressure trend before the second shut-in period. Antecedent pressure is subtracted from pressures recorded during the second shut-in period, and the residual pressure decay is analyzed. If α, as defined previously, is less than or equal to 0.1, then transmissivity is calculated from equation 2 (Cooper and others, 1967). If α is between 0.1 and 10, the product of transmissivity and storativity, TS, can be calculated from the following equations (Bredehoeft and Papadopulos, 1980; Neuzil, 1982):

$$\alpha\beta = \frac{\pi r_s^2 TSt}{\left(V_w C_{obs} \rho_w g\right)^2} \qquad (3)$$

and

$$C_{obs} = \frac{\Delta V / V_w}{\Delta P} \qquad (4)$$

where,

ρ_w = density of water (M/L^3);
g = gravitational acceleration (L/T^2);
V_w = volume of water in pressurized interval (L^3);
ΔV = injected volume of water (L^3); and
ΔP = pressure pulse resulting from injected volume of water (M/L^2).

At values of α greater than 0.1, transmissivity can be calculated if the storativity can be determined independently.

The five pressure-injection tests that could be analyzed, all had in common a downward bulge in the middle-time data on a semi-log plot of head recovery as a function of time. This bulge made it impossible to match the data curve for test 8 to any type curve. For test 9, a questionable match was made between the data and type curves. For tests 13, 14, and 23, the bulge was small enough that a fairly reliable match could be made between data curves and type curves (fig. 11).

The reason for the downward bulge in the data curves is unknown. It could be an artifact of the coarse recording interval of the Sperry-Sun gauge (two minutes), or it could indicate a problem in the mechanical set-up. A transmissivity value obtained from test 13 that is substantially larger than would be expected from a falling-head test conducted in an interval that includes the one in which test 13 was run seems to indicate that pressures applied could have opened fracture apertures in some pressure-injection tests. This would violate one of the fundamental assumptions of the test method, that fracture apertures are independent of pressure, and would invalidate the results of any tests thus affected. The transmissivity value obtained from test 13 was considered invalid because of possible "hydrofracturing".

Only tests 9, 14, and 23 were considered to have produced reasonable values of transmissivity and hydraulic conductivity. Transmissivity values in tests 9, 14, and 23 ranged from 1 to 10 ft^2/d, and hydraulic conductivity values in these tests ranged from 0.03 to 0.4 ft/d (table 8).

The results of the falling head and pressure injection tests were combined to extrapolate the hydraulic conductivity distribution within a small radius of borehole UE-25c #1. As shown in figure 12, hydraulic conductivity in the vicinity of borehole UE-25c #1 was estimated to range from 0.005 to 0.6 ft/d. The average hydraulic conductivity in the horizontal direction was estimated to be 0.2 ft/d, whereas the average hydraulic conductivity in the vertical direction was estimated to be 0.02 ft/d.

On the basis of the hydraulic conductivity distribution, the transmissivity distribution within a small radius of borehole UE-25c #1 was estimated for aquifers and the entire thickness of rocks in the open part of the borehole (fig. 12). The Calico Hills aquifer was estimated to have a transmissivity of 22 ft^2/d; the Prow Pass-upper Bullfrog aquifer was estimated to have a transmissivity of 34 ft^2/d; the Bullfrog aquifer was estimated to have a transmissivity of 152 ft^2/d; and the Tram aquifer was estimated to have a transmissivity of 44 ft^2. The composite transmissivity of rocks below casing and concrete in borehole UE-25c #1 was estimated to be 261 ft^2. As discussed later in the report, the composite transmissivity value obtained from fluid-injection tests in borehole UE-25c #1 virtually is identical to the composite transmissivity value obtained by pumping borehole UE-25c #3.

CONSTANT-FLUX TESTS

Five pumping tests and a constant-flux injection test were conducted in the c-holes between September 1983 and December 1984. With the completion of each additional borehole at the c-hole complex, the monitoring network for these constant-flux tests was expanded, the conceptual model of ground-water flow at the c-hole complex was refined, and test components, such as the rate of flux, the duration of fluid injection or withdrawal, and the length of time that recovery was monitored, were changed in accordance with information learned from previous tests. The design of these tests, problems encountered, possible

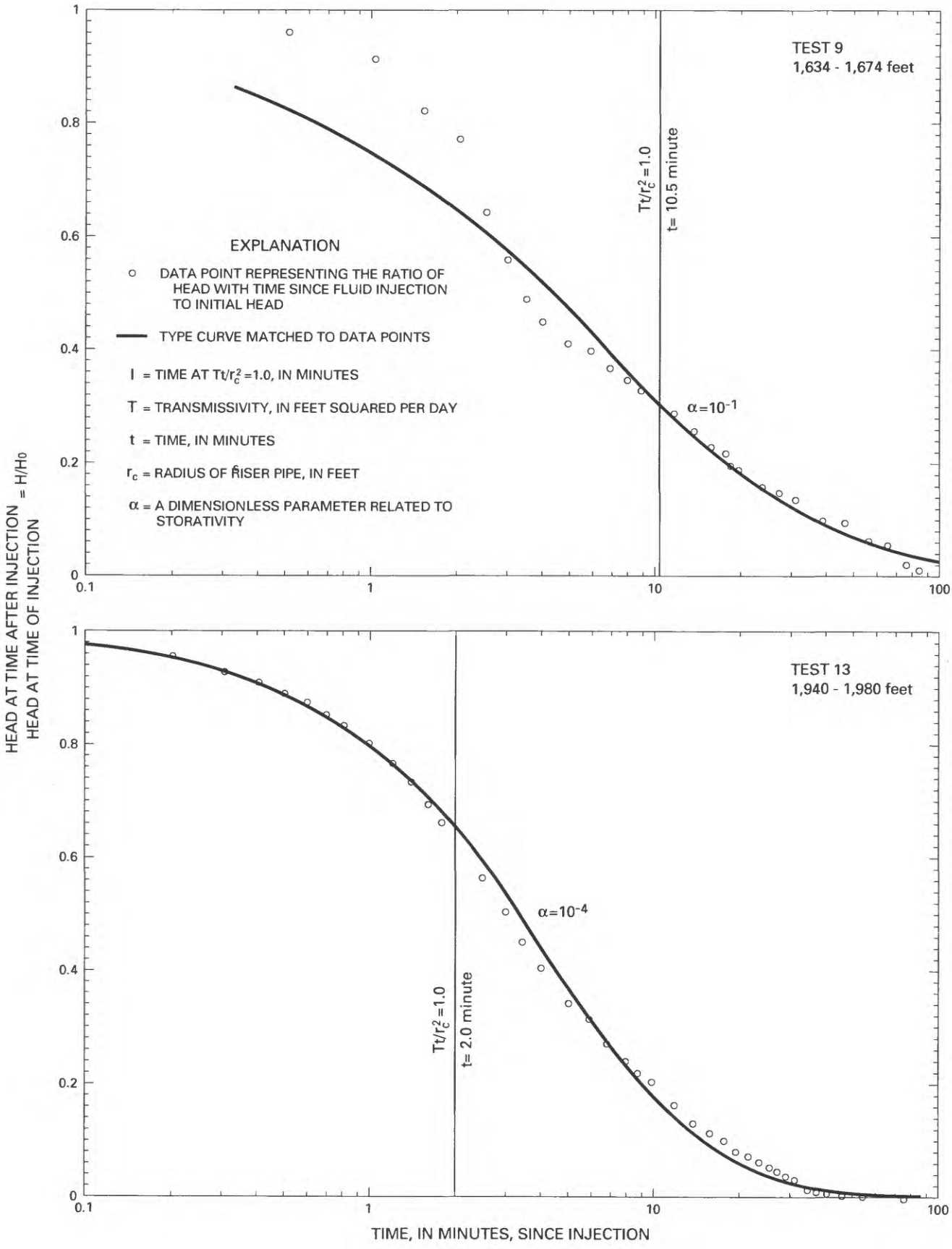

Figure 11A. Analyses of pressure-injection tests conducted in borehole UE-25c #1, October 1983, assuming an infinite, homogeneous, isotropic, confined aquifer (symbols on plots are explained in the text).

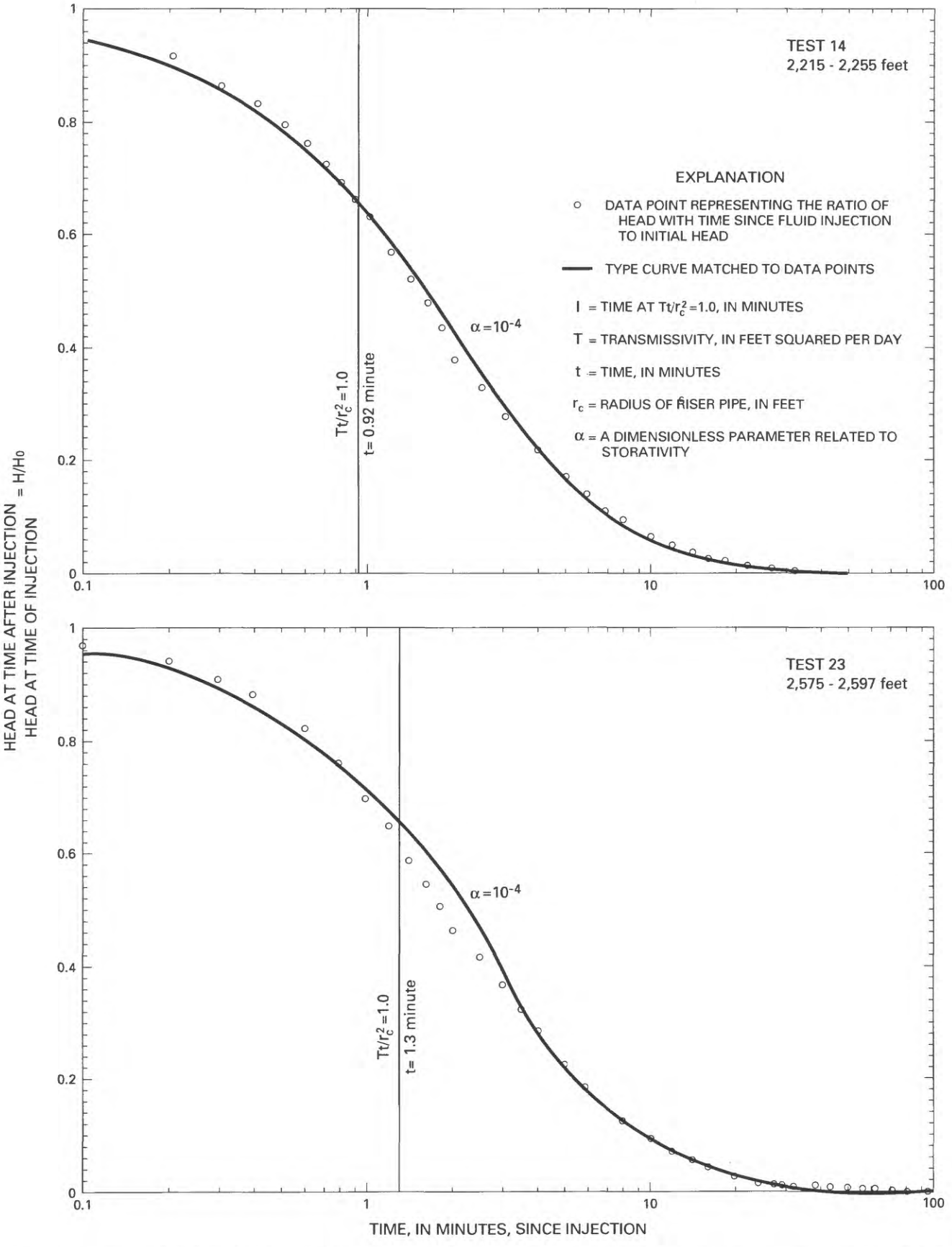

Figure 11B. Analyses of pressure-injection tests conducted in borehole UE-25c #1, October 1983, assuming an infinite, homogeneous, isotropic, confined aquifer (symbols on plots are explained in the text).

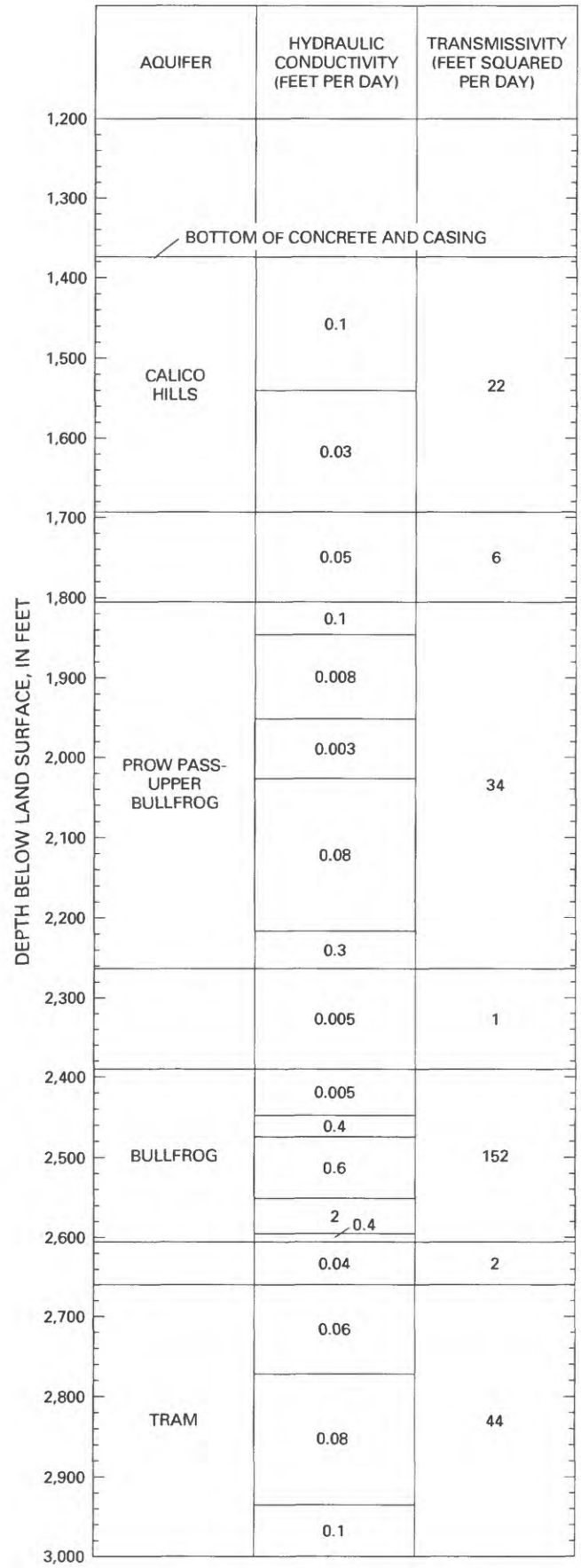

Figure 12. Transmissivity and hydraulic conductivity distributions within a small radius of borehole UE-25c #1, estimated from falling-head and pressure-injection tests.

ground-water flow models that explain hydraulic head changes with time during the tests, and ranges in hydrologic properties calculated on the basis of analytical solutions for different possible ground-water flow models are presented in this section of the report. For a general discussion of the principles of aquifer tests, the reader is referred to Lohman (1979) and Driscoll (1986).

Analytical Methods

Constant-flux tests conducted at Yucca Mountain, including tests conducted in the c-holes discussed later in this section, rarely produce a transient response characteristic of an infinite, homogeneous, isotropic, confined aquifer—the exponential-integral curve of Theis (1935). As indicated by Robison and Craig (1991), plots of the log of water-level change as a function of the log of time typically result in a two-humped curve or a curve that flattens out. Additionally, the early-time data are characterized by borehole storage effects (Gringarten, 1982), and the late-time data commonly contain oscillations that Galloway and Rojstaczer (1988) attributed to Earth tides and changes in atmospheric pressure. In this report, constant-flux tests in the c-holes are interpreted with respect to four analytical ground-water models: (1) An infinite, homogeneous, isotropic, confined aquifer (Theis, 1935; Cooper and Jacob, 1946); (2) a leaky, homogeneous, isotropic, confined aquifer (Cooper, 1963); (3) a fissure-block (dual-porosity) aquifer (Streltsova-Adams, 1978); and (4) an infinite, homogeneous, anisotropic, unconfined aquifer (Neuman, 1975). The four analytical models used were selected because of their applicability to hydrogeologic characteristics of the c-hole complex discussed previously in this report.

Under the assumption of an infinite, homogeneous, isotropic, confined aquifer, water-level changes in observation wells are plotted as a function of time on log-log paper and matched to the exponential-integral type curve of Theis (1935). The following equations are used to calculate hydrologic properties:

$$T = \frac{Q \times W(\mu)}{4\pi s} \tag{5}$$

$$K_r = T/b \tag{6}$$

and

$$S = \frac{4Tt\mu}{r^2} \tag{7}$$

where,

T = transmissivity (L^2/T);
Q = rate of injection or withdrawal (L^3/T);
$W(\mu)$ = well function for an infinite, homogeneous, isotropic, confined aquifer (also called the exponential integral);
μ = a dimensionless parameter defined by equation 7;
K_r = horizontal hydraulic conductivity (L/T);
b = thickness of transmissive intervals (L);
S = storativity (dimensionless);
t = time since injection or withdrawal started or stopped (T) corresponding to μ;
s = water-level change (L) corresponding to $W(\mu)$; and
r = distance from the pumped well to an observation well (L).

Under the same assumptions applicable to equations 5, 6, and 7, the transmissivity of rocks in the pumped well can be analyzed by plotting residual drawdown as a function of the log of the ratio of time since injection or withdrawal started to time since injection or withdrawal stopped and solving the following equation (Theis, 1935):

$$T = \frac{2.3Q}{4\pi\Delta s_d'} \tag{8}$$

where:

$\Delta s_d'$ = the residual water-level change (L) over one log cycle of the ratio of time since injection or withdrawal started to time since injection or withdrawal stopped; and all other variables are defined as in equation 5.

Flattening of a plot of the log of drawdown in the pumped well or an observation well as a function of the log of time can be interpreted to indicate induced recharge from an aquifer boundary, as a hydraulic gradient develops between the boundary and the aquifer in response to pumping. This situation is analogous to leakage from a confining unit without storage during pumping. Analysis of drawdown in an aquifer with leakage from a confining unit without storage, according to Cooper (1963), is done by plotting the log of drawdown as a function of the log of the ratio of time since pumping started to the distance squared from the pumped well, matching the data curve to one of a family of type curves, and solving the following equations:

$$T = \frac{Q \times L(\mu, \nu)}{4\pi s} \tag{9}$$

$$S = \frac{4Tt/r^2}{1/\mu} \quad (10)$$

and

$$v = \frac{r}{2} \times \sqrt{\frac{K'}{Tb'}} \quad (11)$$

where,

$L(\mu,v)$= well function of an infinite, homogeneous, isotropic, confined aquifer with leakage from a confining unit without storage;
K' = vertical hydraulic conductivity of the confining unit (L/T);
b' = thickness of the confining unit (L); and
v = a dimensionless parameter defined by equation 11; and all other variables are as defined previously.

The fissure-block model of ground-water flow can be analyzed either by straight-line techniques (Robison and Craig, 1991) or by curve-matching (Streltsova-Adams, 1978). If a pumping test proceeds long enough, a plot of drawdown in an observation well as a function of the log of time since pumping started is characterized by three segments. The first and third segments have twice the slope of the second segment, which is relatively flat. The third segment is analyzed using the following equations (Cooper and Jacob, 1946):

$$T = \frac{2.3Q}{4\pi\Delta s_d} \quad (12)$$

and

$$S = \frac{2.25Tt_o}{r^2} \quad (13)$$

where,

Δs_d = drawdown (L) over one log cycle of time;
t_o = time at point of zero drawdown (T); and
r = distance from pumped well to observation well (L); and all other variables are as defined previously.

If the test is terminated before the third segment is obtained, the second segment is analyzed with the denominator of equation 12 multiplied by 2.

In the curve-matching technique of Streltsova-Adams (1978), the log of drawdown in an observation well as a function of the log of time is plotted and matched to a type curve with a shape determined by the ratio of total storativity to fracture storativity (η), and by the ratio of the distance from the pumped well to the parameter B, which is defined by the following equation:

$$B = \sqrt{\frac{TH}{K_b}} \quad (14)$$

where,

T = transmissivity (L^2/T);
H = the distance from the center of a block to a bounding fracture, equivalent to half the average distance between fractures (L); and
K_b = hydraulic conductivity of the blocks (L/T).

Matching the data curve to the type curve gives the transmissivity of the aquifer; matching the data curve to the early-time part of the type curve gives the fracture storativity; substituting the fracture storativity and η into equation 17 below, gives the block storativity; rearranging equation 14 and solving for K_b gives the block hydraulic conductivity; and dividing transmissivity by the thickness of transmissive intervals in the test interval gives the average fracture hydraulic conductivity. The analytical equations are:

$$T = \frac{Q \times W(\theta)}{4\pi s} \quad (15)$$

$$S_f = \frac{4Tt}{r^2\theta} \quad (16)$$

$$S_b = S_f \times (\eta - 1) \quad (17)$$

$$K_b = \frac{TH}{B^2} \quad (18)$$

and

$$K_f = \frac{T}{b} \quad (19)$$

where,

$W(\theta)$ = well function of a fissure-block aquifer;
s = drawdown in fractures (L) corresponding to $W(\theta)$;
S_f = fracture storativity (dimensionless);
θ = a dimensionless parameter defined by equation 16;
t = time since pumping started (T) corresponding to θ;
K_f = hydraulic conductivity of the fractures (L/T);
S_b = block storativity (dimensionless); and all other variables are as defined previously.

Because the type curves are very similar, estimating r/B in advance of curve-matching is recommended. In analyzing the c-hole pumping tests, values of r/B were estimated using the fracture data in the Supplementary Data section of this report, values of matrix permeability shown on pls. 1–3, and values of transmissivity estimated from plots of drawdown or recovery during aquifer tests as a function of the log of time. Hydraulic conductivity (K), in feet per day, was estimated from matrix permeability (k), in millidarcies by the following equation:

$$K = \frac{k\rho_w g}{\mu} \tag{20}$$

where,

μ = the dynamic viscosity of water (in centipoise); and

ρ_w and g are defined as in equation 3.

The final analytical model considered in this report is an infinite, homogeneous, anisotropic, unconfined aquifer (Neuman, 1975). The method of analysis requires plotting the log of drawdown or recovery in either the pumped well or an observation well as a function of the log of the ratio of time since pumping started or stopped to distance squared from the pumped well and matching the data curve to a type curve that consists of two relatively steep segments (Type A and Type B curves) separated by a relatively flat transitional segment. The shape of the transitional curve is related to the anisotropy of the aquifer. Matching the data curve to either the early-time or late-time part of a type curve gives the transmissivity; matching the data curve to the early-time part of a type curve gives the storativity; and matching the data curve to the late-time part of a type curve gives the specific yield. Hydrologic properties are calculated using the following equations:

$$T = \frac{Q \times W\left(\mu_A, \mu_B, \beta\right)}{4\pi s} \tag{21}$$

$$S = \frac{4Tt\mu_A}{r^2} \tag{22}$$

$$S_y = \frac{4Tt\mu_B}{r^2} \tag{23}$$

and

$$\beta = \frac{K_z r^2}{K_r b^2} \tag{24}$$

where,

$W(\mu_A, \mu_B, \beta)$ = well function for an unconfined aquifer;

s = drawdown (L) corresponding to $W(\mu_A, \mu_B, \beta)$;

μ_A = a dimensionless parameter defined by equation 22;

μ_B = a dimensionless parameter defined by equation 23;

t = time since pumping started (T) corresponding to μ_A or μ_B;

β = a dimensionless parameter defined by equation 24;

S_y = specific yield (dimensionless);

K_z = vertical hydraulic conductivity (L/T); and all other variables are as defined previously.

To calculate hydrologic properties using the unconfined aquifer solution of Neuman (1975) first requires estimating the parameter ß, which, in turn, requires estimates of vertical hydraulic conductivity (K_z) and horizontal hydraulic conductivity (K_r). Initial estimates of K_z and K_r were obtained from values of interval hydraulic conductivity determined from the previously discussed fluid-injection tests in borehole UE-25c #1. The values of hydraulic conductivity determined from the fluid injection tests were inserted into equations given by Freeze and Cherry (1979) for determining average values of vertical and horizontal hydraulic conductivity in rocks with layered hydraulic conductivity. The equations used were:

$$K_z = \frac{b}{\sum_{i=1}^{n} \frac{b_i}{K_i}} \tag{25}$$

and

$$K_r = \sum_{i=1}^{n} \frac{K_i b_i}{b} \tag{26}$$

where:

K_i = hydraulic conductivity of a layer (L/T);

b_i = thickness of a layer (L);

b = total thickness of layers (L); and

n = the number of layers.

In observation wells with packers emplaced to isolate selected intervals, the proportion of discharge contributed from above, between, and below the packers in an observation well had to be estimated to solve equations 5, 9, 15, and 21. The results of heat-pulse flowmeter surveys conducted in the c-holes, that are

shown on plates 1–3, were used to proportionalize discharge.

Pumping tests with residual head changes from preceding tests or significant recovery (more than about 10 percent of drawdown) caused by a pump failure during the test were analyzed applying the principle that the effects of superimposed cycles of fluid injection or withdrawal and recovery are additive. The following equations were used during analysis of a pumping test to separate total recorded drawdown into component parts:

$$s = s_T - s_A \tag{27}$$

$$r_1 = s_1 - s_T \tag{28}$$

$$s_2 = s_T - s_1 + r_1 \tag{29}$$

and

$$r_2 = s_1 - r_1 + s_2 - s_T \tag{30}$$

where

s_T = total recorded drawdown (L);
s = drawdown caused by continuous pumping (L);
s_A = residual drawdown from a previous aquifer test (L);
s_1 = drawdown caused by continuous pumping or pumping prior to a pump failure (L);
s_2 = drawdown caused by pumping following a period during which a pump failure occurred (L);
r_1 = water-level recovery after shutting off a pump following continuous pumping or during a pump failure (L); and
r_2 = water-level recovery following pumping interrupted by a pump failure (L).

Values of s_A, s_1, s_2, and r_1 were estimated beyond the time each was recorded by extrapolation of the slope of the recorded data on a plot of water-level change as a function of the log of time.

Where depths to water were recorded in piezometers open to the surface, and a recording barometer was operated during an aquifer test, recorded drawdown data were corrected for atmospheric pressure changes based on values of barometric efficiency obtained by Galloway and Rojstaczer (1988) from simultaneous records of water levels in the c-holes and borehole UE-25p #1 and atmospheric pressure during 1986. Above packers emplaced between depths of about 2,400 to 2,600 ft, and in open boreholes, a barometric efficiency of 0.8 was used for the c-holes. Between packers emplaced between 2,400 and 2,600 ft and below the packers, a barometric efficiency of 0.85 was used for the c-holes. In borehole UE-25p #1 below a packer emplaced 4,255 ft below the land surface to isolate the Miocene tuffaceous rocks from the Paleozoic carbonate rocks, a barometric efficiency of 0.75 was used. Oscillations in recorded drawdown caused by Earth tides were handled by a visual best-fit match of type curves to curves of drawdown or recovery through the oscillations.

Pumping Tests in Borehole UE-25c #1

Two unsuccessful pumping tests were conducted in borehole UE-25c #1 in September and October 1983, immediately after completion of the borehole. During each test, borehole UE-25p #1, 2,028 ft southeast of the pumped well, was monitored to determine whether the Miocene tuffaceous rocks, and the Paleozoic carbonate rocks are connected hydraulically in the vicinity of the c-holes. Atmospheric pressure at borehole UE-25c #1 was recorded on a Validyne digital barometer.

Borehole UE-25c #1 was open during the pumping tests in the tuffs and lavas of Calico Hills and the Crater Flat Tuff, from the bottom of concrete at a depth of 1,371 ft, to the bottom of the borehole at a depth of 2,995 ft (USGS logbook for borehole UE-25c #1, unpublished). A Centrilift submersible pump was emplaced in the borehole from 1,399 to 1,477 ft below land surface, with the pump intake at 1,416 ft below land surface (Fenix and Scisson, Inc., written commun., 1983). A 5.5-in.-outside-diameter riser pipe extended from the pump to the wellhead, where it was coupled to a 6-in.-diameter, steel discharge pipe with an in-line flowmeter and end-line orifice plate and manometer (USGS logbook for borehole UE-25c #1, unpublished). Depth to water in the borehole was monitored with a Bell and Howell pressure transducer with a recording range of 0 to 50 lb/in.^{2}, that was connected at the surface to a Fluke data logger (USGS logbook for borehole UE-25c #1, unpublished). The calibrated depth of the transducer was 1,423 ft below land surface (110 ft below the static water level in the borehole).

Borehole UE-25p #1 is part of a water-level monitoring network at Yucca Mountain and is permanently configured to record hydraulic head in the Paleozoic rocks near the c-hole complex (Robison and others, 1988). Borehole UE-25p #1 is cased and grouted through the tuffaceous rocks to a depth of 4,256 ft below land surface (175 ft below the contact between the Miocene and Paleozoic rocks in the borehole). Hydraulic head in the Paleozoic rocks is recorded with a pressure transducer suspended inside a

1.9-in.-outside-diameter plastic piezometer tube. During the pumping tests in borehole UE-25c #1, a Bell and Howell pressure transducer with a recording range of 0 to 10 lb/in.^{2}, that was connected at the surface to a Fluke data logger, was used in the borehole (USGS logbook for borehole UE-25c #1, unpublished). The calibrated depth of the transducer was 1,198 ft below land surface, and 7.5 ft below the static water level in the piezometer tube (USGS records, unpublished).

Following several periods of pumping lasting from 10 minutes to 11.5 hours, during which the discharge rate was varied between 242 and 500 gal/min, equipment to be used in the pumping tests was evaluated, borehole UE-25c #1 was flushed of drilling debris, and a pumping test was started in borehole UE-25c #1 on September 27, 1983. The pump was off for 22 hours prior to the test, and the water level was static when the test began. At an average discharge rate of 234 gal/min, a volume of 1,192,969 gal of water was withdrawn from the pumped well during the test (USGS records, unpublished). Pumping lowered the water level in borehole UE-25c #1 about 100 ft to the pump intake in about 12 minutes, where it remained until pumping ceased on September 30, 1983, 3.5 days after the test began (USGS records, unpublished). After the pump was shut off, the water level in borehole UE-25c #1 rose abruptly, and residual drawdown was negligible 10.3 minutes after pumping ended (USGS records, unpublished).

A second pumping test in borehole UE-25c #1 took place 11 hours after the first pumping test on October 1, 1983 (USGS logbook for borehole UE-25c #1, unpublished). During the first 12 minutes of the test, pumping at an average rate of 216 gal/min again lowered the water level in the pumped well to the pump intake (USGS records, unpublished). After 11.8 hours, the pump failed for about 10 minutes, and the water level in the pumped well recovered 83 percent (USGS records, unpublished). After the pump was restarted, the water level again decreased rapidly to the pump intake. Pumping continued at an average rate of 213 gal/min for another 19.6 hours until on October 2, the pump was shut off, and the water level in the pumped well again recovered rapidly (USGS records, unpublished).

The pumping tests conducted in borehole UE-25c #1 generally were a failure. Drawdown and recovery in borehole UE-25c #1 could not be analyzed quantitatively, because the depth to water during most of each pumping test was controlled by the depth of the pump intake and not the hydrologic properties of the rocks being tested. Clearly, a smaller capacity pump should have been used for these tests. Both pumping tests in borehole UE-25c #1 were too short to produce any discernible effect on the water level in borehole UE-25p #1. Thus, neither test could be used to determine whether the Miocene and Paleozoic rocks are connected hydraulically in the vicinity of the c-holes.

Pumping Test in Borehole UE-25c #2

A pumping test was conducted in borehole UE-25c #2 in March 1984, several days after completion of the borehole. During the test, water levels in the pumped well, in borehole UE-25c #1, 251 ft north-northeast of the pumped well, and in borehole UE-25p #1, 1,971 ft east-southeast of the pumped well, were monitored. Atmospheric pressure during the test was recorded on a Validyne digital barometer located at borehole USW H-4, 7,466 ft northwest of borehole UE-25c #2.

Procedures and Problems

Borehole UE-25c #2 was open during the pumping test in the tuffs and lavas of Calico Hills and the Crater Flat Tuff, from the bottom of concrete, at a depth of 1,365 ft, to the bottom of the borehole, at a depth of 2,999 ft (USGS logbook for borehole UE-25c #2, unpublished). A Centrilift submersible pump was emplaced in the borehole from 1,420 to 1,485 ft below land surface, with the pump intake at 1,447 ft below land surface (Fenix and Scisson, Inc., written commun., 1984). A 5.5-in.-outside-diameter riser pipe extended from the pump to the wellhead, where it was coupled to a 6-in.-diameter, steel discharge pipe with an in-line flowmeter and end-line orifice plate and manometer (USGS logbook for borehole UE-25c #2, unpublished). Depth to water in the borehole was monitored with a Bell and Howell pressure transducer with a recording range of 0 to 25 lb/in.^{2}, that was suspended inside a 2.4-in.-diameter access tube and connected at the surface to a Fluke data logger (USGS logbook for borehole UE-25c #2, unpublished). The calibrated depth of the transducer was 1,369 ft below the top of the access tube, 50 ft below the static water level inside the tube (USGS records, unpublished).

Borehole UE-25c #1 was monitored above and between straddle packers suspended on a 2.9-in.-outside-diameter plastic tube between depths of 2,510 and 2,610 ft (Fenix and Scisson, Inc., written commun., 1984). From the bottom of concrete to the top of the packers, borehole UE-25c #1 was open from the Calico Hills aquifer to the top of the Bullfrog aquifer (fig. 7). Between the packers, at depths of 2,520 to 2,600 ft, borehole UE-25c #1 was open in the lower part of the Bullfrog aquifer. Depth to water above the packers was

monitored with a Bell and Howell pressure transducer with a recording range of 0 to 10 lb/in.^{2}, that was connected at the surface to a Fluke data logger (USGS logbook for borehole UE-25c #2, unpublished). The calibrated depth of the transducer to monitor the interval above the packers was 1,355 ft below the top of casing, 20 ft below the static water level in the borehole. Depth to water between the packers was monitored with a Bell and Howell pressure transducer with a recording range of 0 to 25 lb/in.^{2}, that was suspended inside the tube on which the packers were hung and connected at the surface to a Fluke data logger (USGS logbook for borehole UE-25c #2, unpublished). The calibrated depth of the transducer to monitor the interval between the packers was 1,369 ft below the top of tubing, 50 ft below the static water level inside the tube.

In borehole UE-25p #1, depth to water inside the piezometer tube that was open to the Paleozoic rocks was monitored with a Bell and Howell vented pressure transducer with a recording range of 0 to 15 lb/in.^{2}, that was connected at the surface to a Fluke data logger (USGS logbook for borehole UE-25c #2, unpublished). The calibrated depth of the transducer was 1,205 ft below the top of the piezometer tube, 15 ft below the static water level inside the tube.

Five days prior to the pumping test in borehole UE-25c #2, the borehole was cleaned of debris by repeated cycles of pumping and recovery over a period of five hours. Discharges during this procedure ranged from 321 to 335 gal/min (USGS logbook for borehole UE-25c #2, unpublished). On March 7, 1984, from 0350 to 0423, several attempts were made to begin a pumping test in borehole UE-25c #2, but the longest the pump remained operative during this time was 23 minutes (USGS logbook for borehole UE-25c #2, unpublished).

After complete water-level recovery (USGS records, unpublished) and several modifications to the equipment, a pumping test in borehole UE-25c #2 was started successfully at 1742 on March 7, 1984 (USGS logbook for borehole UE-25c #2, unpublished). Pumping continued until 1029 on March 14, 1984 (a period of about 6.7 days). Discharge during the pumping test stabilized within minutes of the pump being started at an average rate of 245 gal/min, and a volume of 2,361,386 gal of water was withdrawn during the test (USGS records, unpublished).

The pumping in borehole UE-25c #2 caused the water level in the pumped well to decrease 8 ft during the first minute of the test; shutting off the pump at the end of the test caused an equally abrupt increase in the water level (fig. 13). Complete recovery to the pre-test static water level in the pumped well occurred 1,165 minutes after pumping ceased. The pumping in borehole UE-25c #2 drew down water levels in borehole UE-25c #1 about 1.2 ft above the packers and about 1.4 ft between the packers (fig. 14). Considering the changes in atmospheric pressure during the test (fig. 15), water-level recovery in borehole UE-25c #1, about 3.7 days after pumping ceased, was about 79 percent complete above the packers and 100 percent complete between the packers. The pumping in borehole UE-25c #2 apparently caused the water level in borehole UE-25p #1 to decrease after about 1,000 minutes (fig. 14), indicating that the Miocene tuffaceous rocks and Paleozoic carbonate rocks at the c-hole complex are connected hydraulically. Corrected for changes in atmospheric pressure, the water level in borehole UE-25p #1 decreased 1.4 ft while the pump was on and another 0.5 ft in the 3.7 days that water levels were monitored after the pump was shut off.

Test Analyses

Despite oscillations, drawdown and recovery data from borehole UE-25c #1 above the packers could be interpreted to conform to the analytical solution of either Streltsova-Adams (1978) for a fissure-block aquifer or Neuman (1975) for an unconfined, anisotropic aquifer. For both solutions, tuffaceous rocks above the packers were estimated from a heat-pulse flowmeter survey done in December 1991 to contribute 12.5 percent of the discharge from the entire thickness of rocks below casing and concrete in borehole UE-25c #1.

Aquifer-test analysis using the fissure-block solution of Streltsova-Adams (1978) was guided by an estimate of r/B = 0.09 that was obtained from the following: (1) Half the average distance between fractures in the interval above the packers = 2.6 ft; (2) log mean matrix hydraulic conductivity in the interval above the packers = 0.0009 ft/d; and (3) a first approximation-estimate of transmissivity from the slope of the late-time data on a plot of drawdown as a function of the log of time during the pumping test = 3,200 ft^2/d. The parameter r/B was calculated as follows:

$$\frac{r}{B} = \frac{r}{\sqrt{\frac{T \times H}{K_b}}} = \frac{270ft}{\sqrt{\frac{3,200ft^2/d \times 2.6ft}{0.0009ft/d}}} = 0.09$$

Fit to the type curve for $\eta = 10$ and r/B = 0.3, the drawdown data from borehole UE-25c #1 above the packers (fig. 16) indicated the following values of transmissivity (T), fracture storativity (S_f), block storativity (S_b), fracture hydraulic conductivity (K_f), and block hydraulic conductivity (K_b):

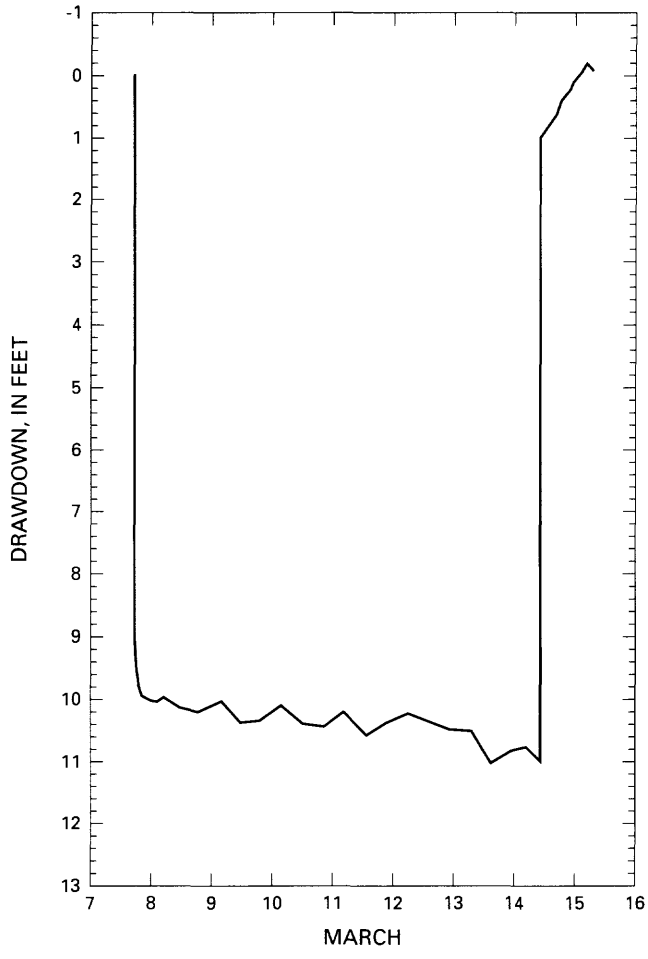

Figure 13. Drawdown as a function of time in borehole UE-25c #2 during the pumping test in borehole UE-25c #2, March 1984.

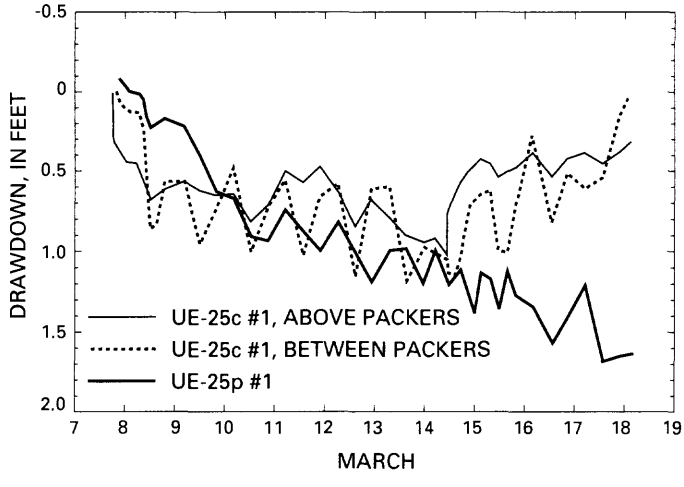

Figure 14. Drawdown as a function of time in boreholes UE-25c #1 and UE-25p #1 during the pumping test in borehole UE-25c #2, March 1984.

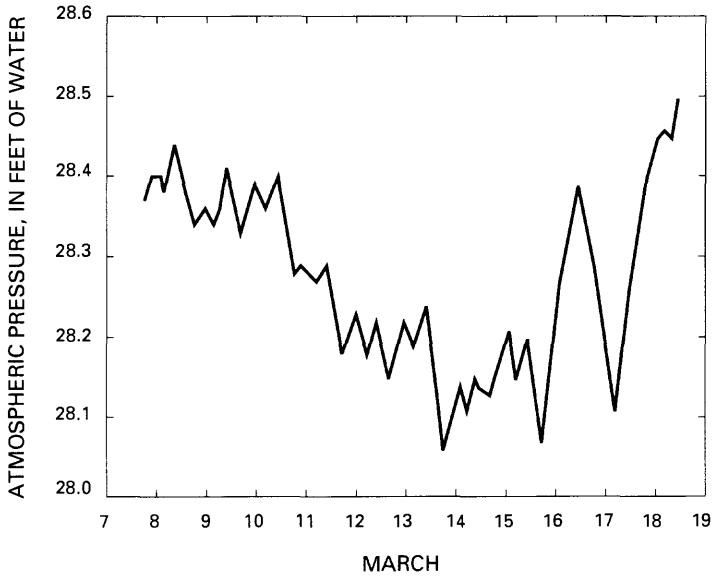

Figure 15. Atmospheric pressure at borehole USW H-4 during the pumping test in borehole UE-25c #2, March 1984.

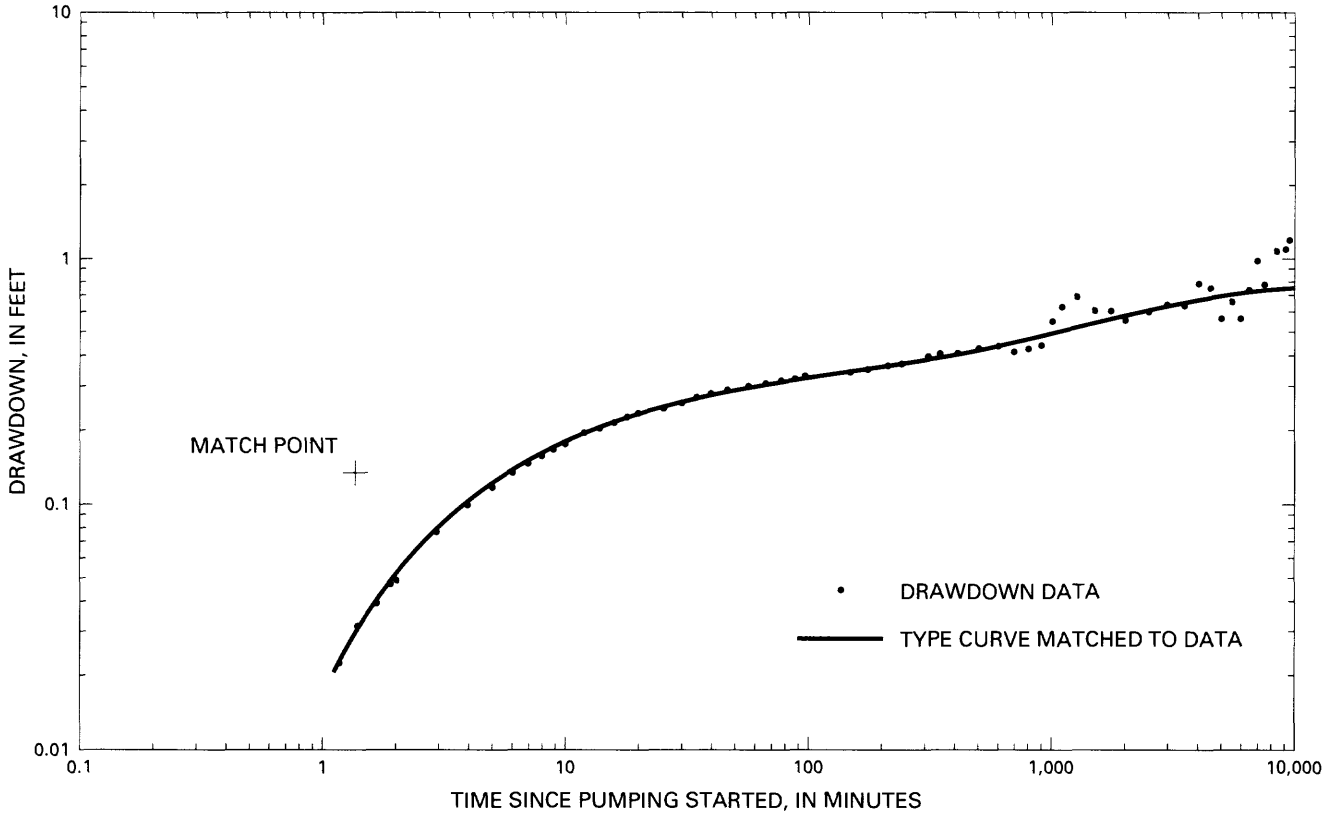

Figure 16. Analytical solution for drawdown data from borehole UE-25c #1 above the packers assuming a fissure-block aquifer, pumping test in borehole UE-25c #2, March 1984.

$$T = \frac{Q \times W(\theta)}{4\pi s} = \frac{\left(0.125 \times 245 gal/min \times 192.5 ft^3/d\right) \times 1}{(4\pi \times 0.135 ft) \times 1 gal/min} = 3,500 ft^2/d$$

$$K_f = \frac{T}{b} = \frac{3,500 ft^2/d}{524 ft} = 7 ft/d$$

$$S_f = \frac{4Tt}{r^2\theta} = \frac{4 \times 3,500 ft^2/d \times 1.35 min}{(270 ft)^2 \times 1 \times 1,440 min/d} = 0.0002$$

$$S_b = S_f \times (\eta - 1) = 0.0002 \times (10 - 1) = 0.002$$

$$r/B = 0.3$$

$$B = \frac{r}{0.3} = \frac{270 ft}{0.3} = 900 ft$$

$$K_b = \frac{T \times H}{B^2} = \frac{3,500 ft^2/d \times 2.6 ft}{(900 ft)^2} = 0.01 ft/d$$

Aquifer-test analysis using the unconfined aquifer solution of Neuman (1975) was guided by an estimate of the parameter ß, as follows:

$$K_z = \frac{b}{\sum_{i=1}^{i} \frac{b_i}{K_i}}$$

$$K_z = \frac{1,139}{(40/0.6 + 25/0.4 + 40/0.3 + 209/0.1 + 190/0.08 + 120/0.05 + 145/0.03 + 105/0.008 + 190/0.005 + 75/0.003)}$$

$$K_z = 0.013 ft/d$$

$$K_r = \sum_{i=1}^{i} \frac{K_i b_i}{b}$$

$$K_r = \frac{(40 \times 0.6 + 25 \times 0.4 + 40 \times 0.3 + 209 \times 0.1 + 190 \times 0.08 + 120 \times 0.05 + 145 \times 0.03 + 105 \times 0.008 + 190 \times 0.005 + 75 \times 0.003)}{1,139}$$

$$K_r = 0.083 ft/d$$

Assuming b is the thickness of transmissive intervals above the packers:

$$\beta = \frac{K_z r^2}{K_r b^2} = \frac{0.013 ft/d \times (270 ft)^2}{0.083 ft/d \times (524 ft)^2} = 0.04$$

Fit to the type curve for ß = 0.06, the drawdown and recovery data from borehole UE-25c #1 above the packers (fig. 17) indicated the following values of transmissivity (T), storativity (S), specific yield (S_y), horizontal hydraulic conductivity, vertical hydraulic conductivity, and anisotropy (K_z/K_r).

Drawdown

$$T = \frac{Q}{4\pi s} \times W\left(\mu_A, \mu_B, \beta\right)$$

$$T = \frac{\left(0.125 \times 245 gal/min \times 192.5 ft^3/d\right) \times 1}{4\pi \times 0.16 ft \times 1 gal/min}$$

$$T = 2,900 ft^2/d$$

$$S = \frac{4Tt\mu_A}{r^2}$$

$$S = \frac{4 \times 2,900 ft^2/d \times 1.5 min \times 1}{(270 ft)^2 \times 1,440 min/d}$$

$$S = 0.0002$$

$$S_y = \frac{4Tt\mu_B}{r^2}$$

$$S_y = \frac{4 \times 2,900 ft^2/d \times 35 min \times 1}{(270 ft)^2 \times 1,440 min/d}$$

$$S_y = 0.004$$

Recovery

$$T = \frac{Q}{4\pi s} \times W\left(\mu_A, \mu_B, \beta\right)$$

$$T = \frac{\left(0.125 \times 245 gal/min \times 192.5 ft^3/d\right) \times 1}{4\pi \times 0.16 ft \times 1 gal/min}$$

$$T = 2,900 ft^2/d$$

$$S = \frac{4Tt\mu_A}{r^2}$$

$$S = \frac{4 \times 2,900 ft^2/d \times 2 min \times 1}{(270 ft)^2 \times 1,440 min/d}$$

$$S = 0.0002$$

$$S_y = \frac{4Tt\mu_B}{r^2}$$

$$S = \frac{4 \times 2,900 ft^2/d \times 25 min \times 1}{(270 ft)^2 \times 1,440 min/d}$$

$$S_y = 0.003$$

Assuming b is the thickness of transmissive intervals:

$$K_r = T/b = \frac{2,900ft^2/d}{524ft} = 6ft/d$$

$$K_z = \frac{K_r b^2 \beta}{r^2} = \frac{6ft/d \times (524ft)^2 \times 0.06}{(270ft)^2} = 1ft/d$$

$$K_z/K_r = 1/6 = 0.2$$

First Pumping Test in Borehole UE-25c #3

A pumping test was conducted in borehole UE-25c #3 from May to June 1984, primarily to determine the composite transmissivity of the tuffaceous rocks penetrated by borehole UE-25c #3 and the transmissivity of the tuffs and lavas of Calico Hills at the c-hole complex. During the test, water levels were monitored in the pumped well, in borehole UE-25c #2 (100 ft southeast of the pumped well) in borehole UE-25c #1 (224 ft northeast of the pumped well) and in borehole UE-25p #1 (2,067 ft southeast of the pumped well). No barometric record during this pumping test was found in USGS files.

Procedures and Problems

The pumped well, borehole UE-25c #3, was open in the tuffs and lavas of Calico Hills and the Crater Flat Tuff, from the bottom of concrete, at a depth of 1,368 ft, to the bottom of the borehole, at a depth of 3,000 ft (Fenix and Scisson, Inc., written commun., 1984). A Centrilift submersible pump was emplaced in the borehole from 1,439 to 1,484 ft below land surface, with the pump intake at 1,454 ft below land surface (Fenix and Scisson, written commun., 1984). A 5.5-in.-outside-diameter riser pipe extended from the pump to the wellhead, where it was coupled to a 6-in.-diameter, steel discharge pipe with an in-line flowmeter and an end-line orifice plate and manometer (USGS logbook for borehole UE-25c #3, unpublished). Depth to water in the pumped well was monitored with a Bell and Howell pressure transducer with a recording range of 0 to 50 lb/in.^{2}, that was suspended inside a

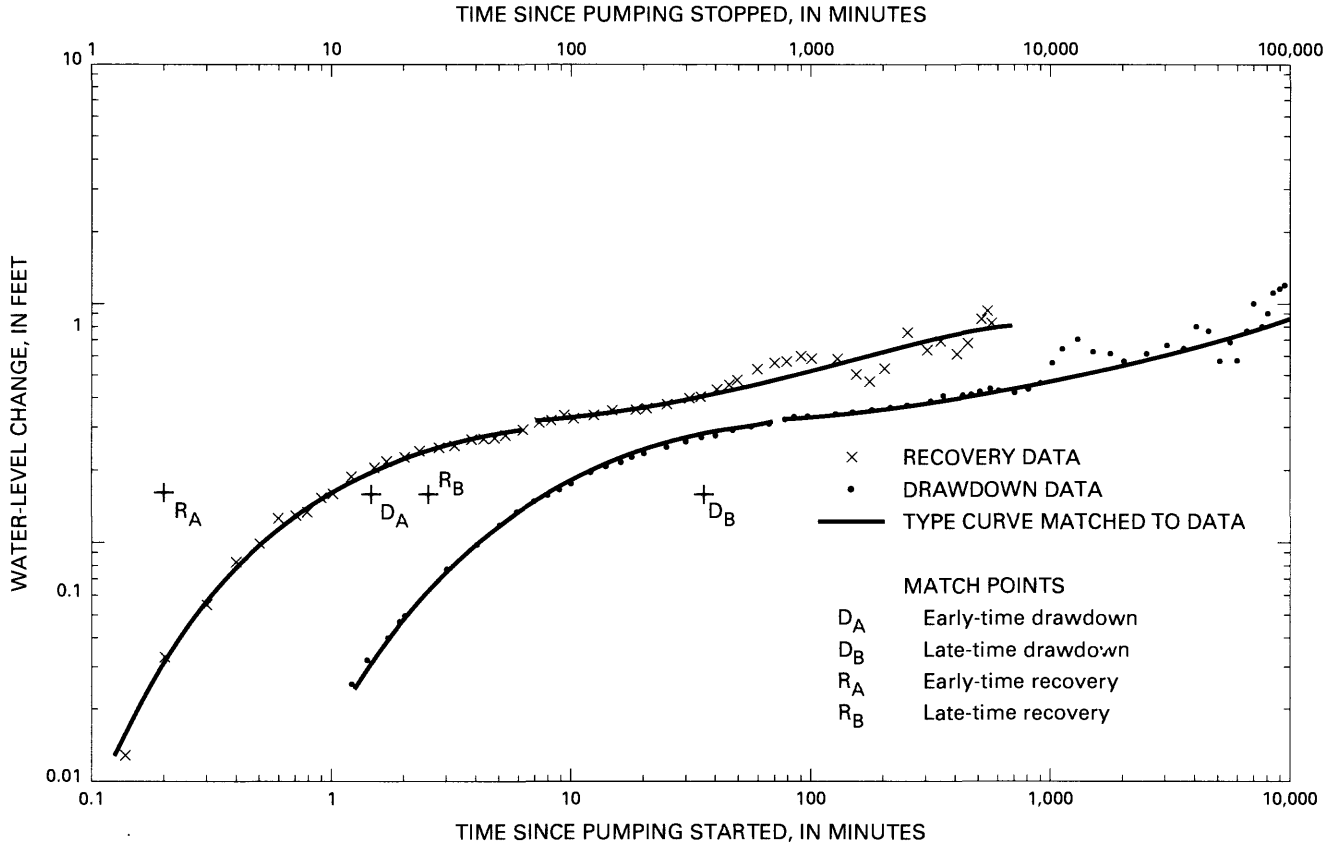

Figure 17. Analytical solutions for drawdown and recovery data from borehole UE-25c #1 above the packers assuming an infinite, homogeneous, anisotropic, unconfined aquifer, pumping test in borehole UE-25c #1, March 1984.

2.4-in.-diameter access tube and connected at the surface to a Fluke data logger (USGS logbook for borehole UE-25c #3, unpublished). The calibrated depth of the transducer was 1,420 ft below the top of the access tube, 100 ft below the static water level inside the tube (USGS records, unpublished).

Borehole UE-25c #2 was open in the tuffs and lavas of Calico Hills and the Crater Flat Tuff, from the bottom of concrete, at a depth of 1,365 ft, to the bottom of the borehole, at a depth of about 2,990 ft (USGS logbook for borehole UE-25c #3, unpublished). Depth to water in the borehole was monitored with a Bell and Howell pressure transducer with a recording range of 0 to 25 lb/in.^{2}, that was connected at the surface to a Fluke data logger. The calibrated depth of the transducer was 1,340 ft below the top of the casing, 20 ft below the static water level in the borehole (USGS records, unpublished).

Borehole UE-25c #1 was monitored above, between, and below straddle packers (Fenix and Scisson, Inc., written commun., 1984). Above the packers, between depths of 1,371 and 1,595 ft, the borehole was open in the nonwelded, upper part of the tuffs and lavas of Calico Hills. Between the packers, from 1,605 to 1,680 ft, the borehole was open in the bedded, lower part of the tuffs and lavas of Calico Hills. Below the packers, between depths of 1,690 and 2,962 ft, the borehole was open in the Crater Flat Tuff. Hydraulic heads above, between, and below the packers were monitored with GRC temperature-compensated pressure transducers with a recording range of 0 to 2,500 lb/in.^{2} (USGS records, unpublished). The packers and instrumentation were suspended on 2.9-in.-outside-diameter plastic tubing. The transducers were connected at the surface by waterproofed cable to a Hewlett-Packard (HP-85) data logger (USGS logbook for borehole UE-25c #3, unpublished). After installation of equipment and prior to testing, borehole UE-25c #1 was shut in to minimize barometric effects on water-level changes (USGS logbook for borehole UE-25c #3, unpublished).

Borehole UE-25p #1, as in previous tests, was monitored to record hydraulic head in the Paleozoic rocks in the vicinity of the c-holes. Depth to water inside a piezometer tube was monitored with a pressure transducer with a recording range of 0 to 15 lb/in.^{2}, that was connected at the surface to a Fluke data logger. The calibrated depth of the transducer was 1,190 ft below the top of the piezometer tube, 9 ft below the static water level inside the tube (USGS records, unpublished).

Without prior development, pumping began in borehole UE-25c #3 at 2257 on May 4, 1984, and continued until 1002 on May 14, 1984, a period of about 9.5 days (USGS logbook for borehole UE-25c #3, unpublished). The test was interrupted by a pump failure on May 9, 1984 (6,520 min into the test), that lasted 163 minutes. Prior to the pump failure, the discharge averaged 420 gal/min, but it took 25 hours for the discharge to stabilize. After the pump was restarted, the discharge quickly stabilized at an average rate of 414 gal/min. For the entire pumping period, the average discharge rate was 418 gal/min, and a volume of 5,623,928 gallons of water was withdrawn (USGS logbook for borehole UE-25c #3, unpublished).

In addition to the pump failure, the first pumping test in borehole UE-25c #3 was hampered by several other mechanical problems. Diurnal fluctuations of 1 to 4 mv in the system power supply, coupled with Earth tides, caused daily fluctuations of water levels in some of the boreholes. On the average, the water level in borehole UE-25c #2 was 0.35 ft higher at 0600 than at 1700 during and after the period in which the pump was operating; the water level in borehole UE-25c #3 fluctuated 1.5 ft between 0600 and 1700 after the pump was shut off. The transducer in borehole UE-25c #1 below the packers was inoperative during the entire pumping test. Finally, intermittent failure of data logging equipment resulted in gaps of as much as seven days in recorded drawdown and recovery in each of the c-holes.

As in the pumping test in borehole UE-25c #2, turning the pump on and off during the pumping test in borehole UE-25c #3 caused rapid, large changes in the water level in the pumped well (fig. 18A). Ten minutes after pumping began, the water level in borehole UE-25c #3 had decreased 61 ft; during the pumping failure, the water level in this borehole recovered to within three percent of the static level; when the pump was shut off on May 14, 1984, the water level in the pumped well rose 67 ft in ten minutes. Maximum drawdown in the pumped well during this test was about 72 ft (USGS records, unpublished).

The drawdown in boreholes UE-25c #2 and UE-25c #1 caused by pumping borehole UE-25c #3 was much slower and smaller than in the pumped well. The maximum drawdown in borehole UE-25c #2 was about 1.7 ft (fig. 18B), the maximum drawdown in borehole UE-25c #1 above the packers was about 18 ft (fig. 19A), and the maximum drawdown in borehole UE-25c #1 between the packers was about 11 ft (fig. 19B). The pumping did not cause a change in the water level in borehole UE-25 p#1 that could be distinguished from water-level fluctuations related to Earth tides, atmospheric pressure changes, variations in the discharge rate, and mechanical problems (USGS records, unpublished). The pump failure caused an 86 percent water-level recovery in borehole

UE-25c #2, about one percent recovery in borehole UE-25c #1 between the packers, and no discernible recovery in borehole UE-25c #1 above the packers (figs. 18 and 19). On June 12, 28.9 days after the pump was shut off, recovery in borehole UE-25c #2 was 100 percent complete, recovery in borehole UE-25c #1 between the packers was 20 percent complete, and no recovery had occurred in borehole UE-25c #1 above the packers.

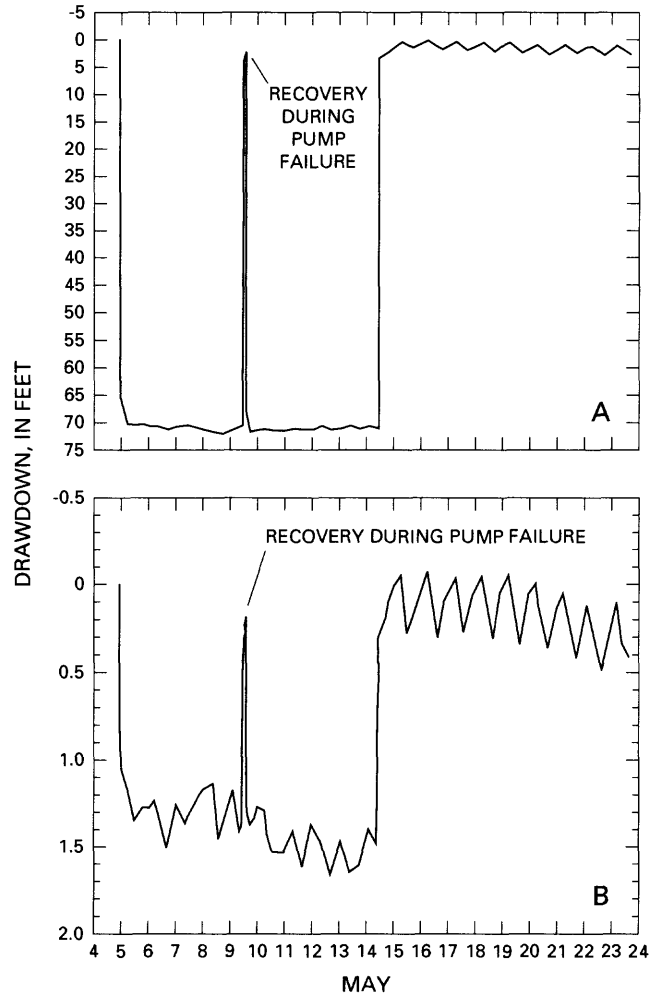

Figure 18. Drawdown as a function of time during the pumping test in borehole UE-25c #3, May to June 1984: (A), Borehole UE-25c #3; (B), Borehole UE-25c #2 (data from unpublished USGS records).

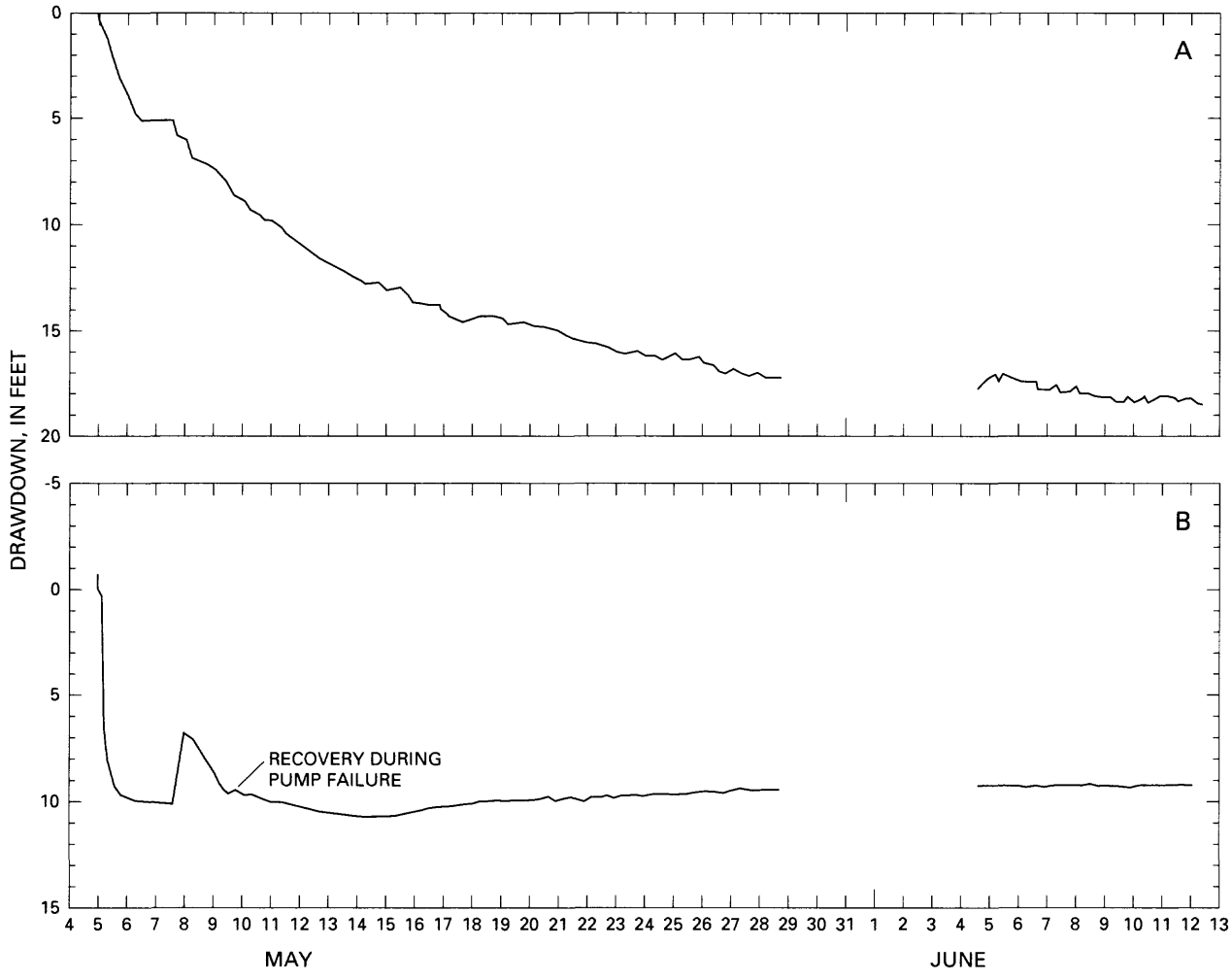

Figure 19. Drawdown as a function of time in borehole UE-25c #1 during the pumping test in borehole UE-25c #3, May to June 1984: (A), above the packers; (B), between the packers (data from unpublished USGS records).

Test Analyses

The first pumping test in borehole UE-25c #3 provided analyzable data sets from boreholes UE-25c #3, UE-25c #2, UE-25c #1 above the packers, and UE-25c #1 between the packers. Because of the variable discharge rate during the first 25 hours of the test, more weight was given in analyses to data obtained later in the pumping phase and during the recovery phase of the test. Based on atmospheric corrections of less than 0.25 ft that were applied during the pumping test in borehole UE-25c #2, it is believed that failure to obtain a barometric record during the first pumping test in borehole UE-25c #3 potentially would have affected only analyses of data from monitored intervals where drawdown or recovery did not exceed two feet. Thus, only analyses of data from borehole UE-25c #2 and recovery data from borehole UE-25c #1 between the packers might have been improved by correcting for atmospheric pressure change.

Analyses of the data from the pumped well, borehole UE-25c #3, by two methods indicated nearly identical values of transmissivity and hydraulic conductivity. Under the assumption of an infinite, homogeneous, isotropic, confined aquifer (Theis, 1935), a plot of residual drawdown as a function of the log of the ratio of time since the pump was restarted to time since pumping stopped (fig. 20) indicated the following:

$$T = \frac{2.3Q}{4\pi\Delta s_d} = \frac{2.3 \times 414 gal/min \times 192.5 ft^3/d}{4\pi \times (60.0 - 5.6 ft) \times 1 gal/min} = 270 ft^2/d$$

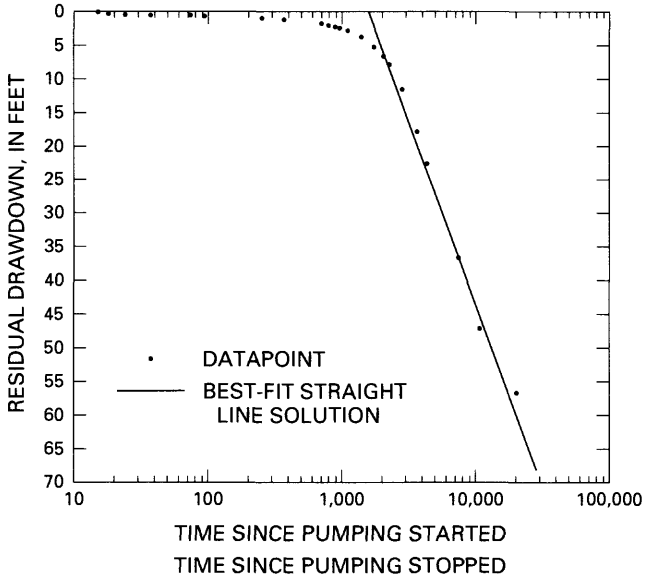

Figure 20. Analytical solution for residual drawdown data from borehole UE-25c #3 assuming an infinite, homogeneous, isotropic, confined aquifer, pumping test in borehole UE-25c #3, May to June 1984.

Assuming b = the thickness of transmissive intervals (table 6):

$$K_r = T/b = \frac{270 ft^2/d}{899 ft} = 0.3 ft/d$$

Flattening of a log-log plot of drawdown as a function of time since pumping started implies that a recharge boundary exists very close to borehole UE-25c #3. Hence, the solution of Cooper (1963) was applied to the drawdown data. Fit to the type curve for $v = 0.1$, the drawdown data from borehole UE-25c #3 after the pump was restarted (fig. 21) indicated the following values of transmissivity and horizontal hydraulic conductivity:

$$T = \frac{Q \times L(\mu, v)}{4\pi s} = \frac{414 gal/min \times 192.5 ft^3/d \times 1}{4\pi \times 21 ft \times 1 gal/min} = 300 ft^2/d$$

If b is assumed to equal the total thickness of transmissive intervals in the borehole,

$$K_r = T/b = \frac{300 ft^2/d}{899 ft} = 0.3 ft/d$$

The drawdown and recovery data obtained from borehole UE-25c #2 could be interpreted to conform to the analytical solution of either Streltsova-Adams (1978) for a fissure-block aquifer or Neuman (1975) for an unconfined, anisotropic aquifer. For both analyses, the distance between boreholes UE-25c #2 and UE-25c #3 (r) was considered to be the average distance between the open sections of the boreholes. Taking into account the drift of both boreholes, the average interborehole distance was determined from gyroscopic surveys to be 95 ft.

For the analytical solution of Streltsova-Adams (1978), the parameter r/B was estimated as follows:

1. Half the average distance between fractures in transmissive intervals (from Supplementary Data section) = 1.7 ft
2. Log-mean matrix hydraulic conductivity (from pl. 2) = 0.0004 ft/d
3. Transmissivity (from the slope of late-time data on a plot of recovery as a function of time during this pumping test) = 25,000 ft²/d

$$\frac{r}{B} = \frac{r}{\sqrt{\frac{T \times H}{K_b}}} = \frac{95 ft}{\sqrt{\left(\frac{25,000 ft^2/d \times 1.7 ft}{0.0004 ft/d}\right)}} = 0.009$$

Fit to the type curve for $\eta = 10$ and r/B = 0.05, the drawdown data from borehole UE-25c #2 after the pump was restarted (fig. 22) indicated the following values of transmissivity (T), fracture storativity (S_f), block storativity (S_b), fracture hydraulic conductivity (K_f), and block hydraulic conductivity (K_b):

$$T = \frac{Q \times W(\theta)}{4\pi s} = \frac{414 gal/min \times 192.5 ft^3/d \times 1}{4\pi \times 0.22 ft \times 1 gal/min} = 29,000 ft^2/d$$

$$K_f = \frac{T}{b} = \frac{29,000 ft^2/d}{544 ft} = 50 ft/d$$

$$S_f = \frac{4Tt}{r^2\theta} = \frac{4 \times 29,000 ft^2/d \times 0.49 min}{(95 ft)^2 \times 1 \times 1,440 min/d} = 0.004$$

$$S_b = S_f \times (\eta - 1) = 0.004 \times (10 - 1) = 0.04$$

$$\frac{r}{B} = 0.05$$

$$B = \frac{r}{0.05} = \frac{95 ft}{0.05} = 1,900 ft$$

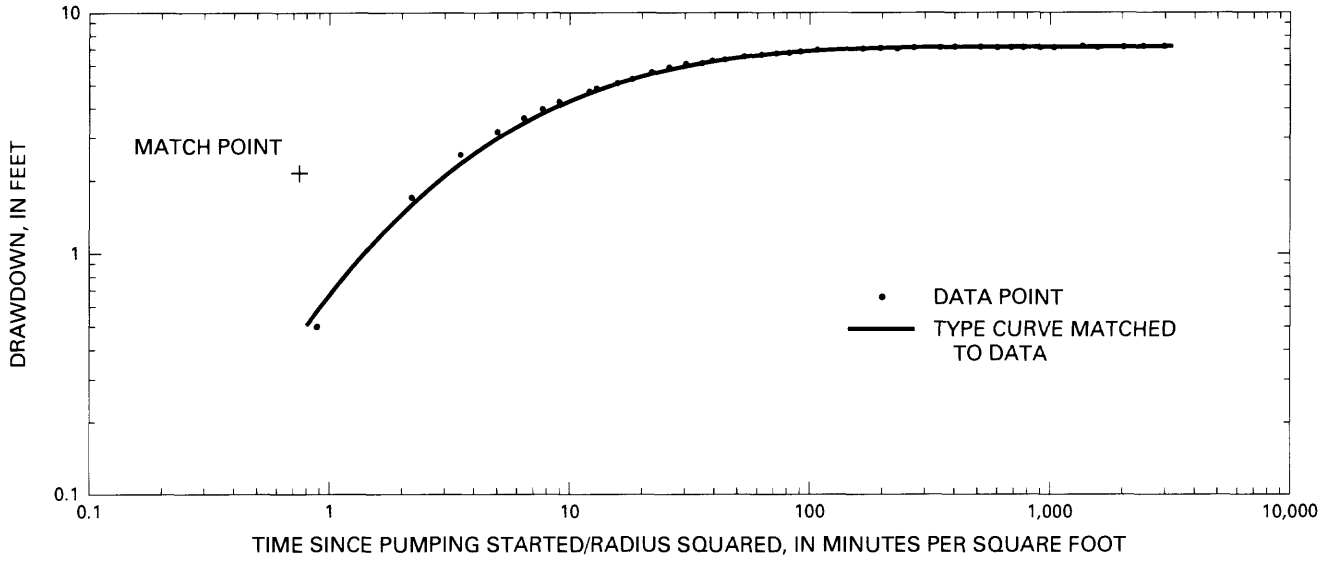

Figure 21. Analytical solution for drawdown data from borehole UE-25c #3 assuming an infinite, homogeneous, isotropic, confined aquifer with leakage from a confining unit without storage, pumping test in borehole UE-25c #3, May to June 1984.

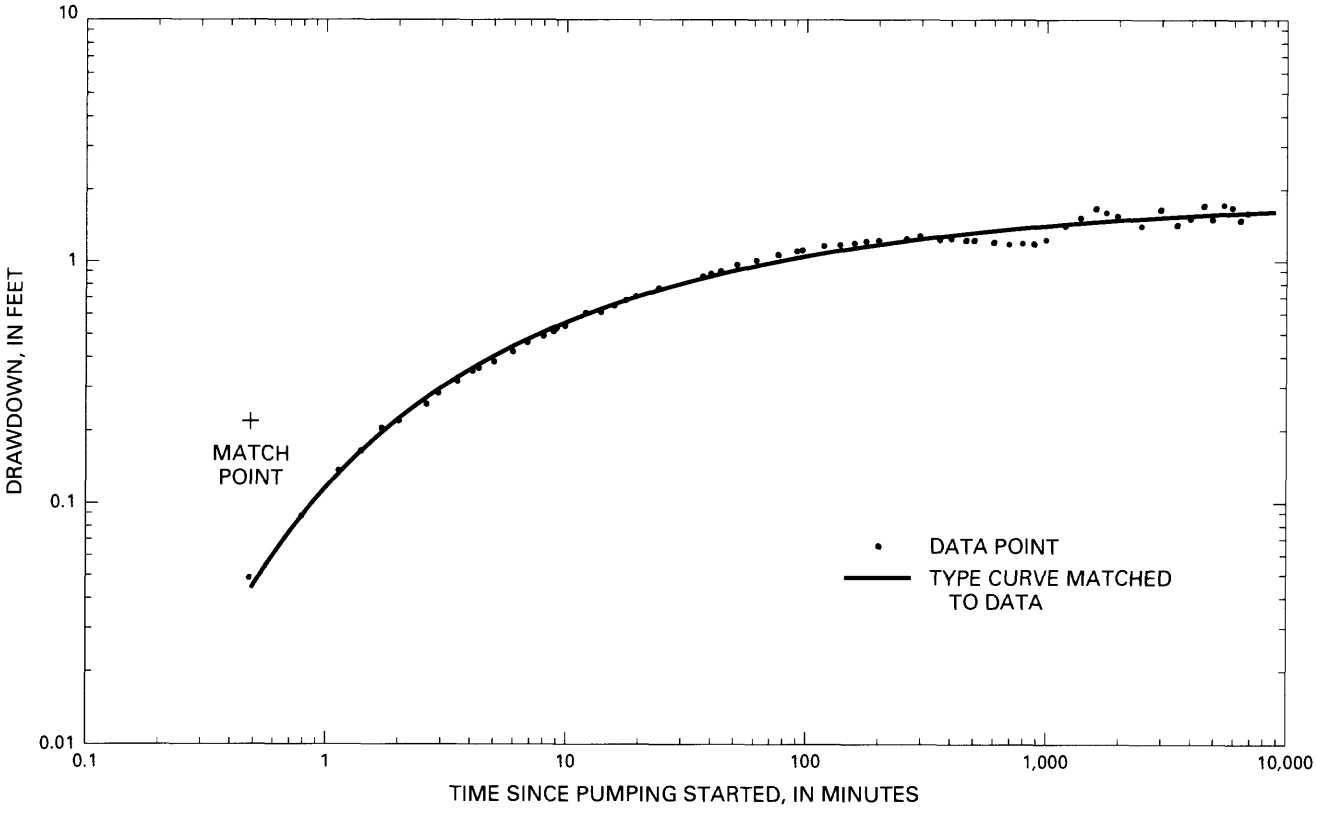

Figure 22. Analytical solution for drawdown data from borehole UE-25c #2 assuming a fissure-block aquifer, pumping test in borehole UE-25c #3, May to June 1984.

$$K_b = \frac{T \times H}{B^2} = \frac{29,000 ft^2/d \times 1.7 ft}{(1,900 ft)^2} = 0.01 ft/d$$

For the analytical solution of Neuman (1975), it was assumed that the vertical hydraulic-conductivity profile determined by injection tests in borehole UE-25c #1 applied, also, in UE-25c #2. Consequently, values of vertical hydraulic conductivity (K_z), horizontal hydraulic conductivity (K_r), and the parameter ß in the first pumping test in UE-25c #3 were estimated for borehole UE-25c #2 as follows:

$$K_z = \frac{b}{\sum_{i=1}^{i} \frac{b_i}{K_i}}$$

$$K_z = \frac{1,625}{(70/2 + 55/0.6 + 135/0.4 + 80/0.2 + 250/0.08 + 345/0.05 + 145/0.03 + 175/0.01 + 105/0.008 + 190/0.005 + 75/0.003)}$$

$$K_z = 0.015 ft/d$$

$$K_r = \frac{\sum_{i=1}^{i} K_i b_i}{b}$$

$$K_r = \frac{(70 \times 2 + 55 \times 0.6 + 135 \times 0.4 + 80 \times 0.2 + 250 \times 0.08 + 345 \times 0.05 + 145 \times 0.03 + 175 \times 0.01 + 105 \times 0.008 + 190 \times 0.005 + 75 \times 0.00}{1,625}$$

$$K_r = 0.18 ft/d$$

Assuming b = the thickness of transmissive intervals in borehole UE-25c #2:

$$\beta = \frac{K_z r^2}{K_r b^2} = \frac{0.015 ft/d \times (95 ft)^2}{0.18 ft/d \times (544 ft)^2} = 0.003$$

Fit to the type curve for ß = 0.004, the drawdown data from borehole UE-25c #2 after the pump was restarted (fig. 23) indicated the following values of transmissivity (T), storativity (S), specific yield (S_y), horizontal hydraulic conductivity, vertical hydraulic conductivity, and anisotropy (K_z/K_r):

$$T = \frac{Q \times W(\mu_A, \mu_B, \beta)}{4\pi s}$$

$$T = \frac{414 gal/min \times 192.5 ft^3/d \times 1}{4\pi \times 0.27 ft \times 1 gal/min} = 23,000 ft^2/d$$

$$S = \frac{4Tt\mu_A}{r^2} = \frac{4 \times 23,000 ft^2/d \times 0.6 min \times 1}{(95 ft)^2 \times 1,440 min/d} = 0.004$$

$$S_Y = \frac{4Tt\mu_B}{r^2} = \frac{4 \times 23,000 ft^2/d \times 9.7 min \times 1}{(95 ft)^2 \times 1,440 min/d} = 0.07$$

Assuming b = thickness of transmissive intervals:

$$K_r = T/b = \frac{23,000 ft^2/d}{544 ft} = 40 ft/d$$

$$K_z = \frac{K_r b^2 \beta}{r^2} = \frac{40 ft/d \times (544 ft)^2 \times 0.004}{(95 ft)^2}$$

$$K_z = 5 ft/d$$

$$K_z/K_r = \frac{5 ft/d}{40 ft/d} = 0.1$$

Both the drawdown data from borehole UE-25c #1 above the packers and the recovery data from borehole UE-25c #1 between the packers unambiguously conform to type curves of Neuman (1975) for an unconfined, anisotropic aquifer (figs. 24 and 25). From a heat-pulse flowmeter survey done in December 1991, it was estimated that tuffaceous rocks above the packers contribute four percent of the discharge from the entire thickness of rocks below casing and concrete in borehole UE-25c #1, and tuffaceous rocks between the packers contribute 0.5 percent of this discharge. Therefore, for the interval above the packers the following values of transmissivity (T) and specific yield (S_y) were calculated:

$$T = \frac{Q \times W(\mu_A, \mu_B, \beta)}{4\pi s} = \frac{(0.04 \times 418 gal/min \times 192.5 ft^3/d) \times 1}{(4\pi \times 4.5 ft) \times 1 gal/min} = 60 ft^2/$$

$$S_Y = \frac{4Tt\mu_B}{r^2} = \frac{4 \times 60 ft^2/d \times 480 min \times 1}{(256 ft)^2 \times 1440 min/d} = 0.001$$

For the interval between the packers, the following values of transmissivity and specific yield were calculated:

$$T = \frac{Q \times W(\mu_A, \mu_B, \beta)}{4\pi s} = \frac{(0.005 \times 418 gal/min \times 192.5 ft^3/d) \times 1}{(4\pi \times 0.74 ft) \times 1 gal/min} = 40 ft^2/$$

$$S_Y = \frac{4Tt\mu_B}{r^2} = \frac{4 \times 40 ft^2/d \times 1,100 min \times 1}{(259 ft)^2 \times 1,440 min/d} = 0.002$$

From the drawdown data and thickness of transmissive intervals above the packers,

$$\beta = r^2/b^2 \times K_z/K_r = 4.0$$

$$K_z/K_r = \frac{4.0 \times b^2}{r^2} = \frac{4.0 \times (182 ft)^2}{(256 ft)^2} = 2$$

Fracture data from between the packers were insufficient to calculate unequivocally the thickness of transmissive intervals between the packers. Therefore, average values of horizontal hydraulic conductivity (K_r) and vertical hydraulic conductivity (K_z) were calculated for the Calico Hills aquifer (the intervals above and between the packers in borehole UE-25c #1) by assuming that the value of anisotropy (K_z/K_r) obtained above the packers applies, also, to the interval between the packers.

Adding the transmissivity values for the intervals above and between the packers gives a composite transmissivity of 100 ft²/d for the Calico Hills aquifer. Dividing this transmissivity value by the known thickness of transmissive intervals above and between the packers, 198 ft, gives a horizontal hydraulic conductivity value of 0.5 ft/d for the Calico Hills aquifer. If $K_z/K_r = 2$, then the vertical hydraulic conductivity of the Calico Hills aquifer = 2 K_r = 2 × 0.5 ft/d = 1 ft/d.

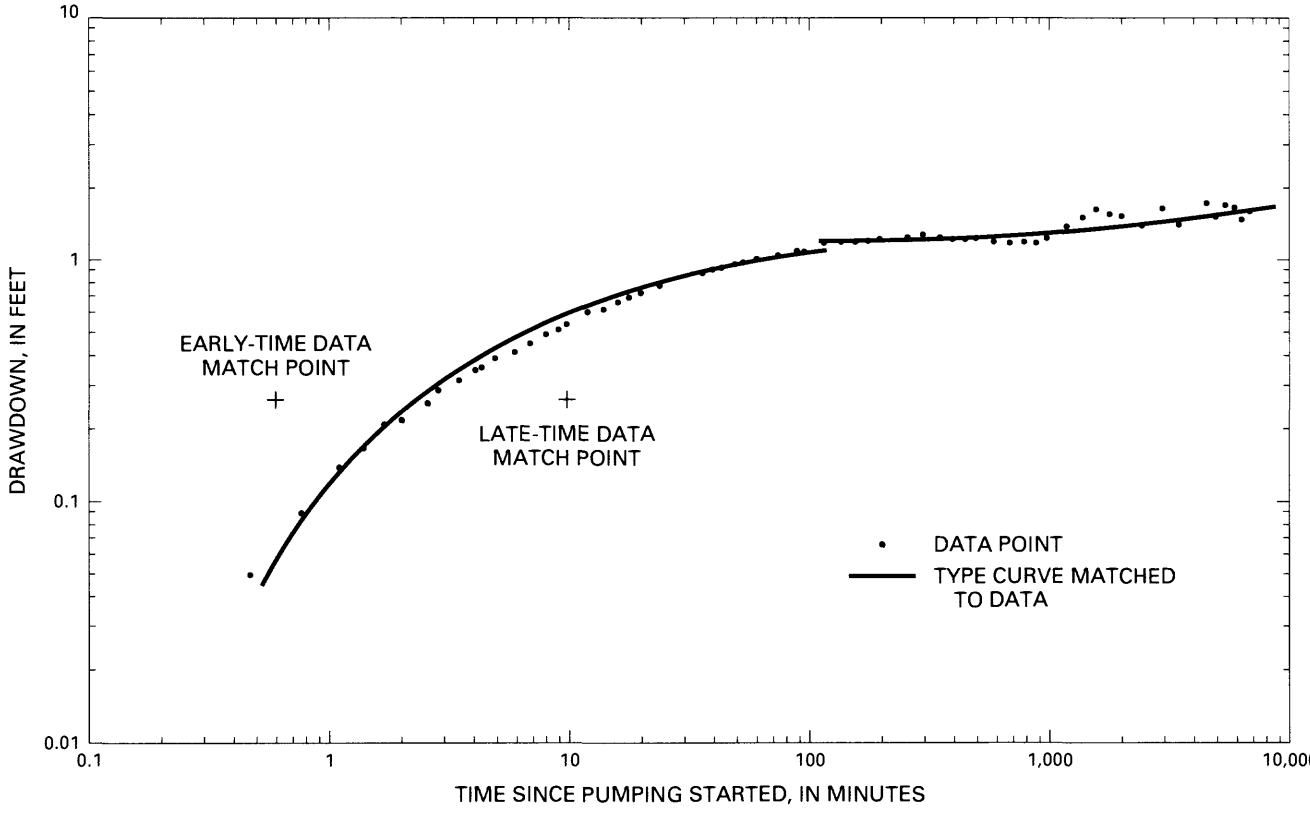

Figure 23. Analytical solution for drawdown data from borehole UE-25c #2 assuming an infinite, homogeneous, anisotropic, unconfined aquifer, pumping test in borehole UE-25c #3, May to June 1984.

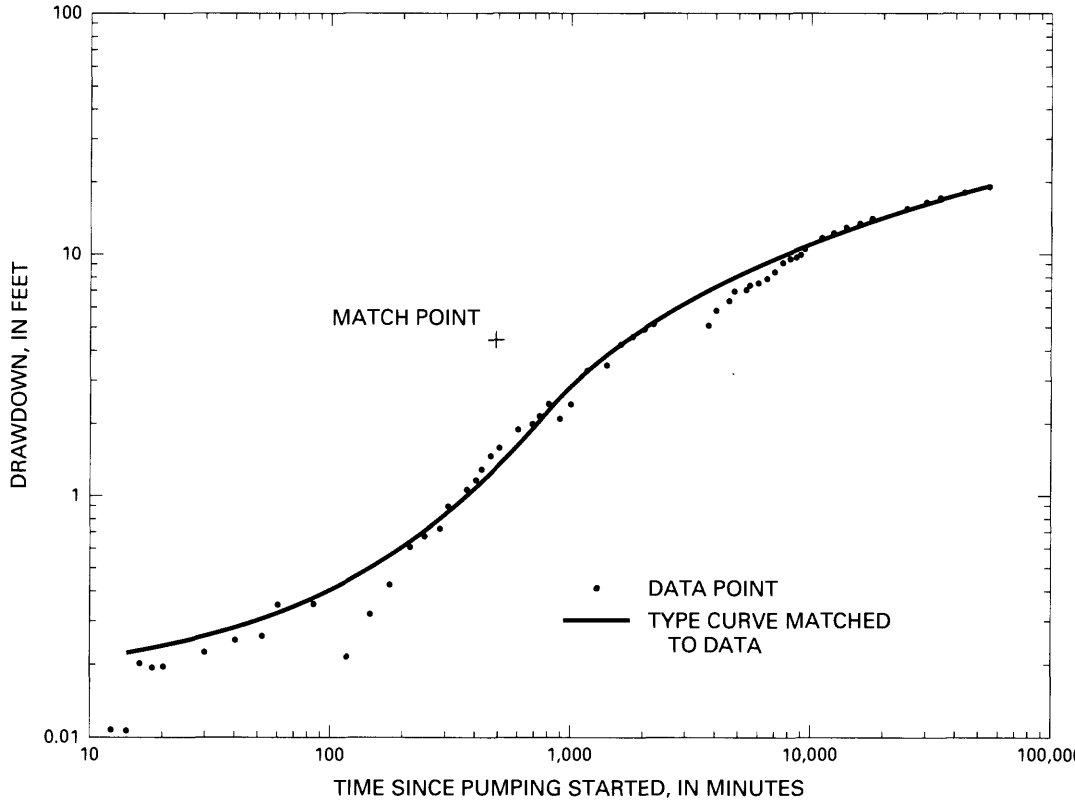

Figure 24. Analytical solution for drawdown data from borehole UE-25c #1 above the packers assuming an infinite, homogeneous, anisotropic, unconfined aquifer, pumping test in borehole UE-25c #3, May to June 1984.

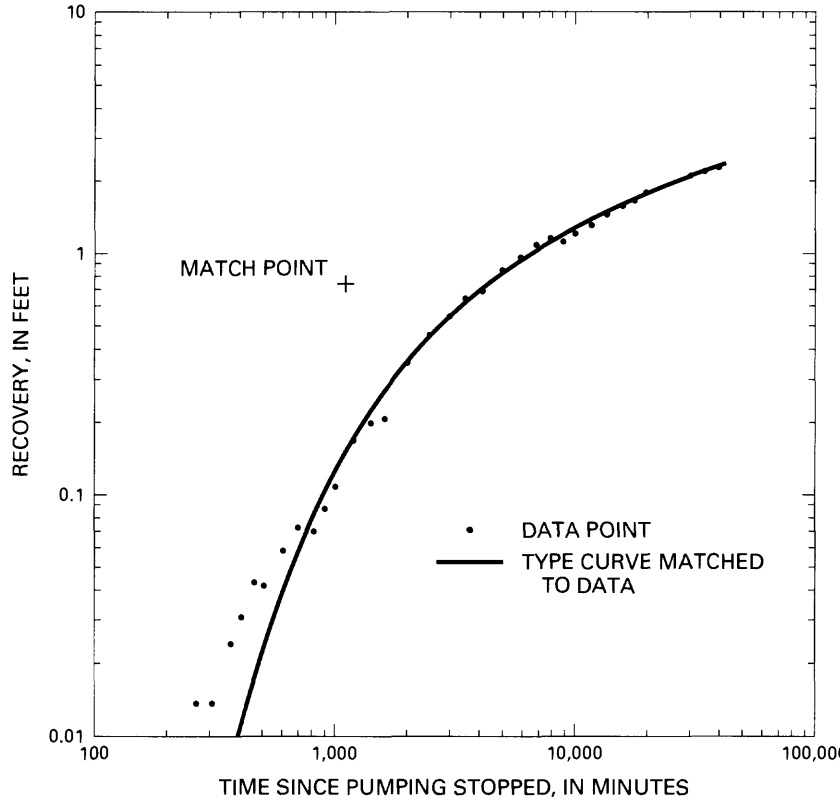

Figure 25. Analytical solution for recovery data from borehole UE-25c #1 between the packers assuming an infinite, homogeneous, anisotropic, unconfined aquifer, pumping test in borehole UE-25c #3, May to June 1984.

Injection Test in Borehole UE-25c #2

An injection test was conducted in borehole UE-25c #2 from 1351 to 1520 on October 30, 1984, to ascertain hydrologic properties of an interval in borehole UE-25c #2 that was thought to contain very permeable rock (the Bullfrog aquifer). The injection test was conducted using monitoring equipment installed for a pumping test in borehole UE-25c #3 that began 156 minutes after the injection test ended.

In the injection well, borehole UE-25c #2, straddle packers were installed on a 2.9-in-diameter plastic tube to isolate the Bullfrog aquifer (Fenix and Scisson, Inc., written commun., 1984). The interval between the packers extended from 2,364 to 2,475 ft below the land surface. Above the packers, from 1,365 to 2,355 ft below the land surface, the borehole was open in the Calico Hills aquifer, the Prow Pass-upper Bullfrog aquifer, and confining units between and below the two aquifers. Below the packers, from 2,484 to 2,990 ft below land surface, the borehole was open in the Tram aquifer and the overlying confining unit. Hydraulic heads above, between, and below the packers were monitored with GRC temperature-compensated, pressure transducers with recording ranges of 0 to 2,500 and 0 to 5,000 lb/in.^{2}, that were connected at the surface to a HP-85 data logger (USGS logbook for the c-holes, 1984–1985, unpublished). During the test, water was injected between the packers from a Baker tank to maintain a constant pressure head of 778 ft (USGS records, unpublished). Because the injection rate quickly stabilized at 167 gal/min (USGS logbook for the c-holes, 1984–1985, unpublished), what was intended to be a constant-head test was converted to a constant-flux test, and the effects of this flux were monitored in borehole UE-25c #1, UE-25c #2, and UE-25c #3 (Devin L. Galloway, USGS, oral commun., 1993).

Borehole UE-25c #1 was monitored above, between, and below straddle packers hung on a 2.9-in.-diameter plastic tube (Fenix and Scisson, Inc., written commun., 1984). Above the packers, from 1,371 to 2,514 ft below land surface, the borehole was open from the Calico Hills aquifer to the top of the Bullfrog aquifer. Between the packers, from 2,524 to 2,594 ft below land surface, the borehole was open in the Bullfrog aquifer. Below the packers, from 2,603 to 2,962 ft below land surface, the borehole was open in the Tram aquifer and overlying confining unit. Hydraulic heads in borehole UE-25c #1 were monitored with GRC temperature-compensated, pressure transducers with recording ranges of 0 to 2,500 and 0 to 5,000 lb/in.^{2}, that were connected at the surface to a HP-85 data logger (USGS logbook for the c-holes, 1984–1985, unpublished). Before the test began, borehole UE-25c #1 was shut in to minimize barometric effects.

Borehole UE-25c #3 was open in the tuffs and lavas of Calico Hills and the Crater Flat Tuff, from the bottom of concrete, at a depth of 1,368 ft, to the bottom of the borehole, at a depth of 2,976 ft. The pump installation was the same as it was in the May-June 1984 pumping test in borehole UE-25c #3. Depth to water in the borehole was monitored with a Bell and Howell pressure transducer with a recording range of 0 to 50 lb/in.^{2}, that was suspended inside a 2.4-in.-diameter access tube and connected at the surface to a Fluke data logger (USGS logbook for the c-holes, 1984–1985, unpublished). The calibrated depth of the transducer was 1,320 ft below the top of the access tube, 100 ft below the static water level inside the tube (USGS records, unpublished).

Injection of water between the packers in borehole UE-25c #2 caused the water level to rise about 4.0 ft in borehole UE-25c #2 above the packers (fig. 26), 0.7 ft in borehole UE-25c #1 between the packers, 0.1 ft in borehole UE-25c #1 above and below the packers, and 0.4 ft in borehole UE-25c #3 (fig. 27). After injection ended, water-level recovery to pre-test static levels was complete in all monitored intervals in boreholes UE-25c #1 and UE-25c #3 within 90 minutes. However, in borehole UE-25c #2, water level recovery above the packers was only 69 percent complete when a pumping test began in borehole UE-25c #3, 156 minutes after injection ended. As indicated in figure 26, residual drawdown from the injection test is estimated to have had an effect on the water level in borehole UE-25c #2 above the packers for the first 515 minutes of the pumping test. Possibly because injection changed fracture apertures in the injection interval, the hydraulic head between the packers was 1.6 ft lower than the pre-injection test static level and still falling when the pumping test in borehole UE-25c #3 started (fig. 27). Post-pumping test data indicate that the hydraulic head between the packers probably would have stabilized asymptotically with time at a level about 2.5 ft lower than before the injection test started, had the pumping test in borehole UE-25c #3 not been conducted.

Most of the data from the injection test were not analyzed. The head build-up in borehole UE-25c #2 above the packers (fig. 26) was erratic and indicative of possible mechanical problems. The head build-up in borehole UE-25c #1 above and below the packers (fig. 27) was insignificant. Although the head build-up in borehole UE-25c #1 between the packers (fig. 27) was large and steady enough to be analyzed, the data were considered less reliable than recovery data

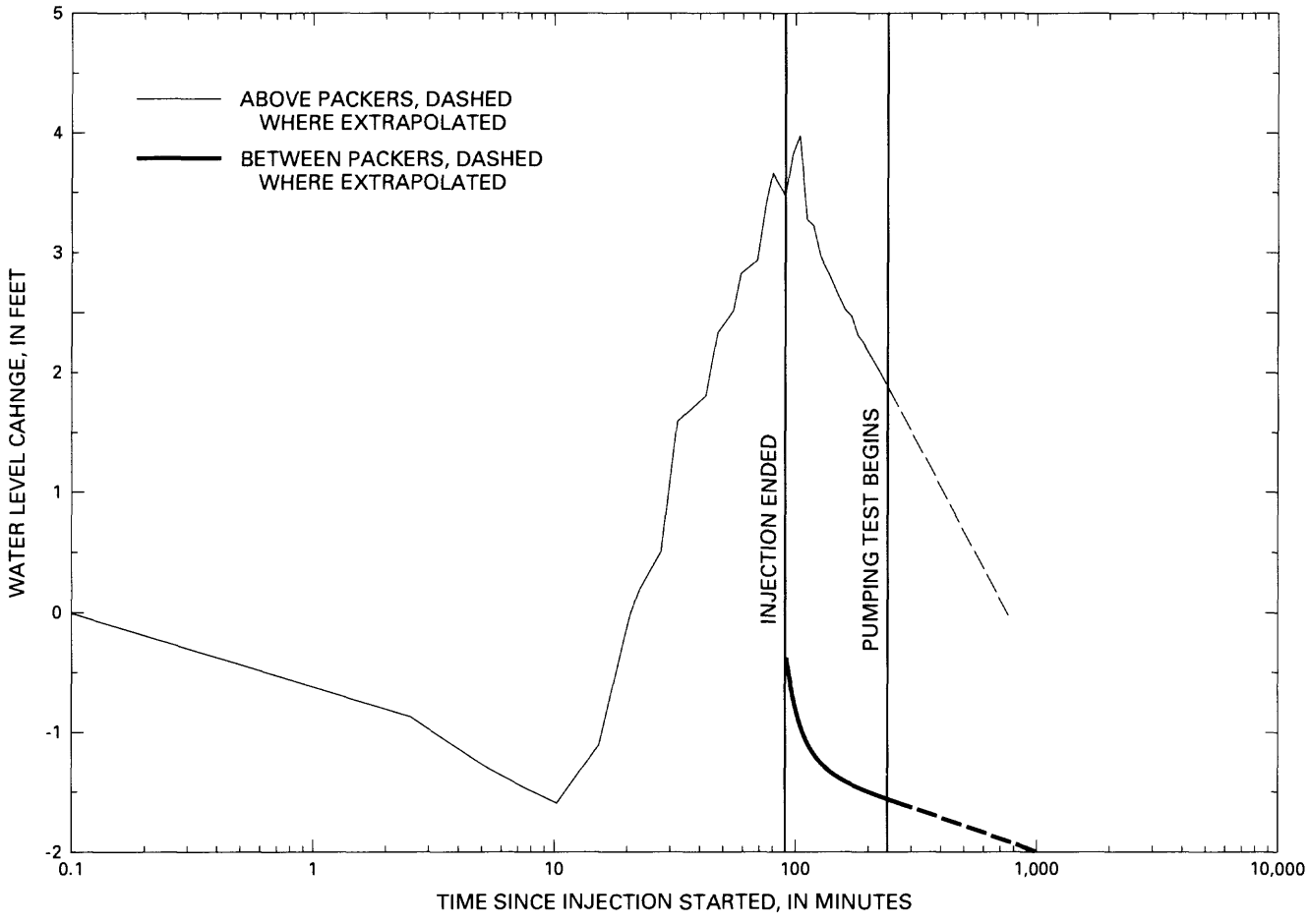

Figure 26. Water-level changes in borehole UE-25c #2 during and after injection of water between packers on October 30, 1984.

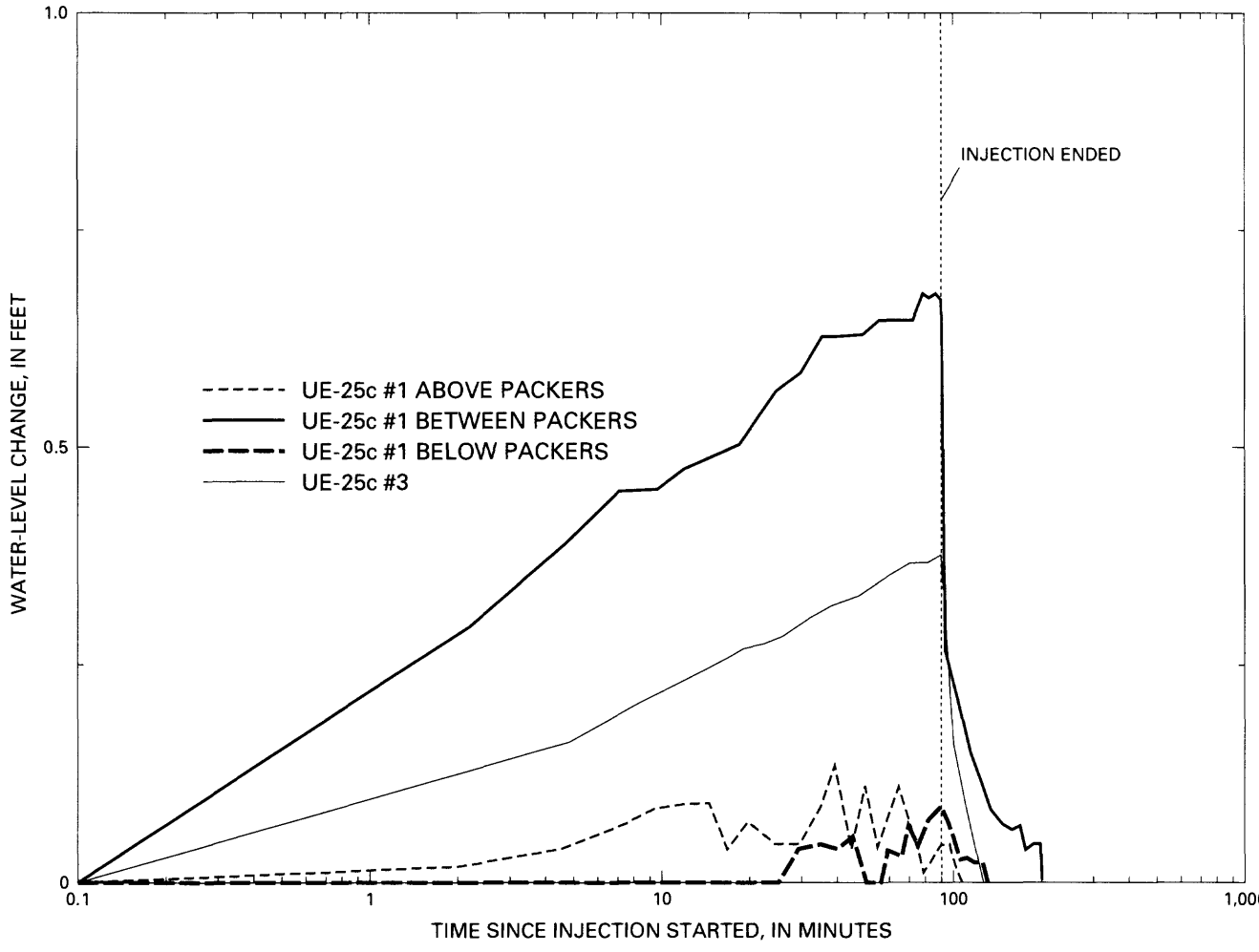

Figure 27. Water-level changes in boreholes UE-25c #1 and UE-25c #3 in response to injection of water into borehole UE-25c #2, October 30, 1984.

obtained from the same interval during the subsequent pumping test in borehole UE-25c #3. Consequently, the data from UE-25c #1 between the packers were not analyzed. Only the data from borehole UE-25c #3 were analyzed because no comparable data were obtained from this borehole in any other constant-flux tests (This was the only test in which borehole UE-25c #3 was used as an observation well).

The composite transmissivity (T), storativity (S), and hydraulic conductivity (K_r) of the tuffaceous rocks in borehole UE-25c #3 could be determined from the head build-up data shown in figure 27 assuming an infinite, homogeneous, isotropic, confined aquifer. Using the method of Cooper and Jacob (1946) and equations 12 and 13, the following calculations were made:

$$T = \frac{2.3Q}{4\pi\Delta s_d} = \frac{2.3 \times 167 gal/min \times 192.5 ft^3/d}{4\pi \times (0.40 - 0.23) ft \times 1 gal/min} = 35,000 ft^2/d$$

$$S = \frac{2.25Tt_o}{r^2} = \frac{2.25 \times 35,000 ft^2/d \times 0.42 min}{(95 ft)^2 \times 1,440 min/d} = 0.002$$

Assuming b to be the thickness of transmissive intervals:

$$K_r = T/b = \frac{35,000 ft^2/d}{899 ft} = 40 ft/d$$

Values of transmissivity and hydraulic conductivity determined for the rocks in borehole UE-25c #3 from the injection test are two orders of magnitude larger than values determined from the drawdown in borehole UE-25c #3 during the pumping test in this borehole in May-June 1984. Yet, the transmissivity determined from the pumping test in borehole UE-25c #3 is the same, to one significant figure, as the composite transmissivity determined in borehole UE-25c #1 from fluid-injection tests (261 ft^2/d). Larger values of transmissivity and hydraulic conductivity apparently are determined as the radius of investigation expands and encompasses more conduits for groundwater flow, such as faults and fracture zones. Cross-hole tests indicate site-scale hydrologic properties, whereas single-well tests indicate hydrologic properties within a small radius of the pumping or injection well. Consequently, the remainder of this report emphasizes analyses of data obtained from observation wells.

Second Pumping Test in Borehole UE-25c #3

A second pumping test was conducted in borehole UE-25c #3 from October-December 1984, primarily to determine vertical and lateral variations in hydrologic properties of the Crater Flat Tuff. In addition to the monitoring network for the injection test described in the previous section, a piezometer was monitored in borehole UE-25p #1, and a recording barometer was maintained at borehole USW H-4. Because the piezometer record from borehole UE-25p #1 indicated an erratic but progressive increase in hydraulic head throughout the entire two weeks that borehole UE-25c #3 was pumped, it is believed that the transducer installed in borehole UE-25p #1 was miscalibrated or malfunctioned during this pumping test. The barometric record obtained at borehole USW H-4 (fig. 28) was not used to correct drawdown data, because head changes in the c-holes were considered large enough that atmospheric pressure changes probably would have had little or no effect on data analyses.

Procedures and Problems

Pumping in borehole UE-25c #3 began at 1756 on October 30, 1984, and continued until 1342 on November 15, 1984, a period of about 15.8 days (USGS records, unpublished). The test was interrupted by an 8.3 minute pump failure on November 2, 1984 (3,839 minutes into the test), which caused a 97 percent recovery of the water level in the pumped well but only slight (4–8 percent) recovery in monitored intervals of boreholes UE-25c #1 and UE-25c #2 (USGS records, unpublished). During the first few hours of the test, the discharge rate varied from 400 to 410 gal/min, but for most of the test, the discharge rate varied from 422 to 429 gal/min (USGS logbook for the c-holes, 1984–1985, unpublished). At an average discharge rate of 425 gal/min, a volume of 9,675,942 gallons of water was withdrawn during the test (USGS logbook for the c-holes, 1984–1985, unpublished).

In addition to the pump failure, the second pumping test in borehole UE-25c #3 was hampered by several other mechanical problems and the short interval between the injection test in borehole UE-25c #2 described previously and the pumping test. The transducer in borehole UE-25c #2 below the packers was inoperative for the entire pumping test, and the transducer in borehole UE-25c #1 between the packers intermittently gave spurious readings (USGS logbook for the c-holes, 1984–1985, unpublished; USGS records unpublished). During the first few days of the test, the discharge meter was slightly inaccurate

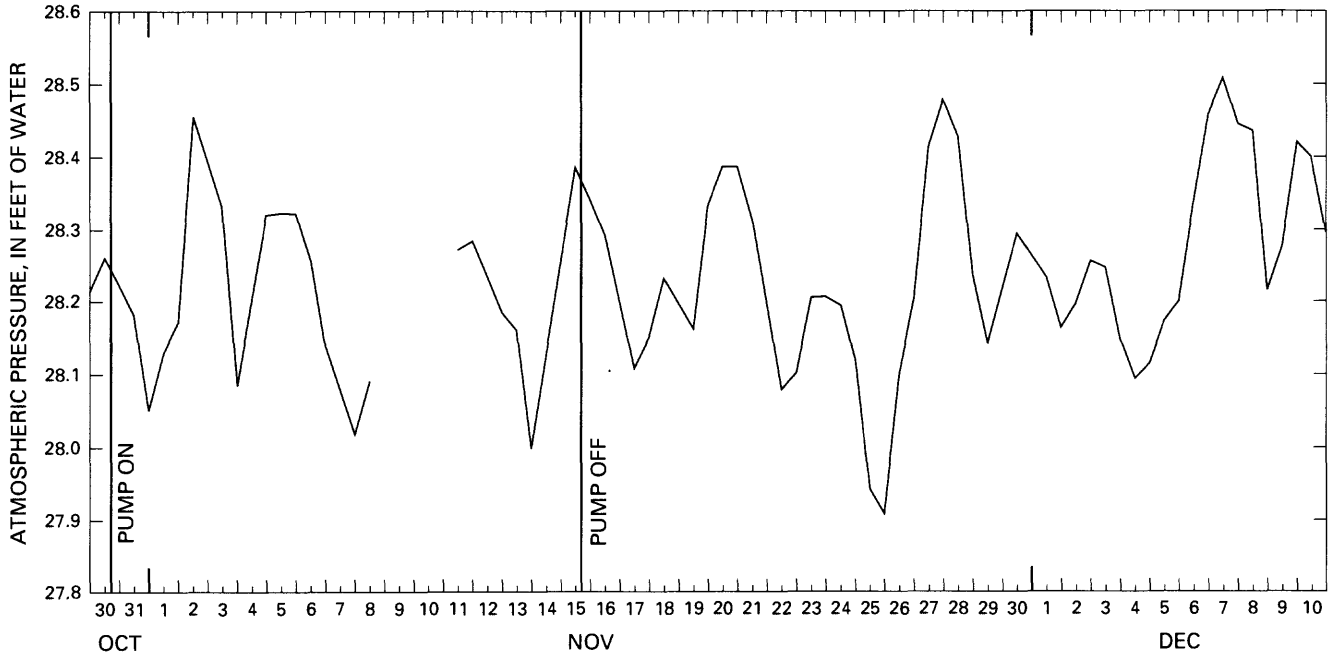

Figure 28. Atmospheric pressure at borehole USW H-4 during the pumping test in borehole UE-25c #3, October to December 1984.

because of leakage through a fitting in the discharge line (USGS logbook for the c-holes, 1984–1985, unpublished). Oscillations in the power supply coupled with Earth tides caused diurnal fluctuations in recorded drawdown (USGS records, unpublished). Problems with data loggers caused intermittent losses of drawdown and recovery data (USGS logbook for the c-holes, 1984–1985, unpublished). In borehole UE-25c #2 above the packers, a 13-ft head decrease followed by a 7-ft head increase occurred as borehole UE-25c #3 was being pumped. Regardless of whether the head increase during pumping resulted from antecedent effects of the preceding injection test, changing hydrologic conditions during pumping (e.g. boundary effects), or a transducer malfunction, the entire record from borehole UE-25c #2 above the packers is suspect. Consequently, this record could not be analyzed to determine hydrologic properties. Finally, antecedent drawdown from the injection test required a correction to the recorded drawdown data from borehole UE-25c #2 between the packers for these data to be used to calculate hydrologic properties. The antecedent drawdown trend was estimated by extrapolation between drawdown values recorded prior to pumping and apparent steady-state drawdown values obtained 23.7 days after pumping ceased.

As in the first pumping test in borehole UE-25c #3 (fig. 18A), turning the pump on and off during the second pumping test in this borehole caused rapid, large changes in the water level in the pumped well (fig. 29). Ten minutes after pumping began, the water level in borehole UE-25c #3 had decreased 61 ft; when the pump was turned off, the water level rose about 65 ft in ten minutes. Maximum drawdown in the pumped well during this test was about 65 ft (USGS records, unpublished).

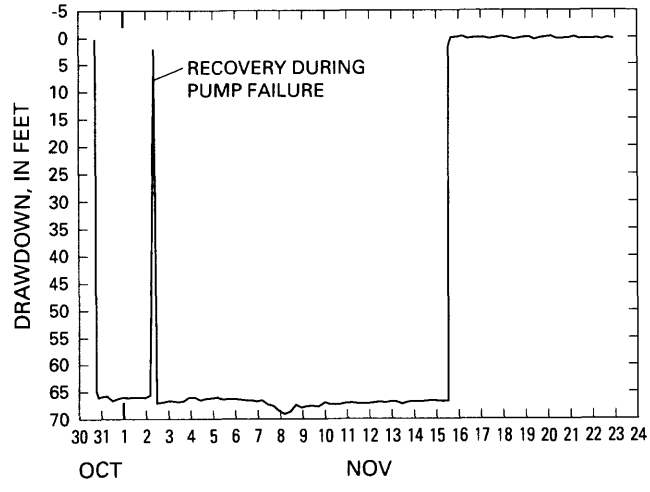

Figure 29. Drawdown as a function of time in borehole UE-25c #3 during the pumping test in borehole UE-25c #3, October to December 1984.

The drawdown in monitored intervals of borehole UE-25c #1 caused by pumping borehole UE-25c #3 was much slower and smaller than in the pumped well (USGS records, unpublished). The maximum drawdown in borehole UE-25c #1 above the packers was about 1.1 ft; the maximum drawdown between the packers was about 2.2 ft; and the maximum drawdown below the packers was about 3.15 ft (fig. 30). Water-level recovery in the pumped well was complete 444 minutes after pumping ceased (fig. 29), but complete recovery in monitored intervals of borehole UE-25c #1 required 20.7 to 21.7 days (fig. 30).

Similar to borehole UE-25c #1 between the packers, the maximum drawdown in borehole UE-25c #2 between the packers after correcting for residual drawdown from the injection test was about 2.3 ft (USGS records, unpublished). Complete recovery in borehole UE-25c #2 between the packers occurred 23.7 days after pumping ceased (fig. 31).

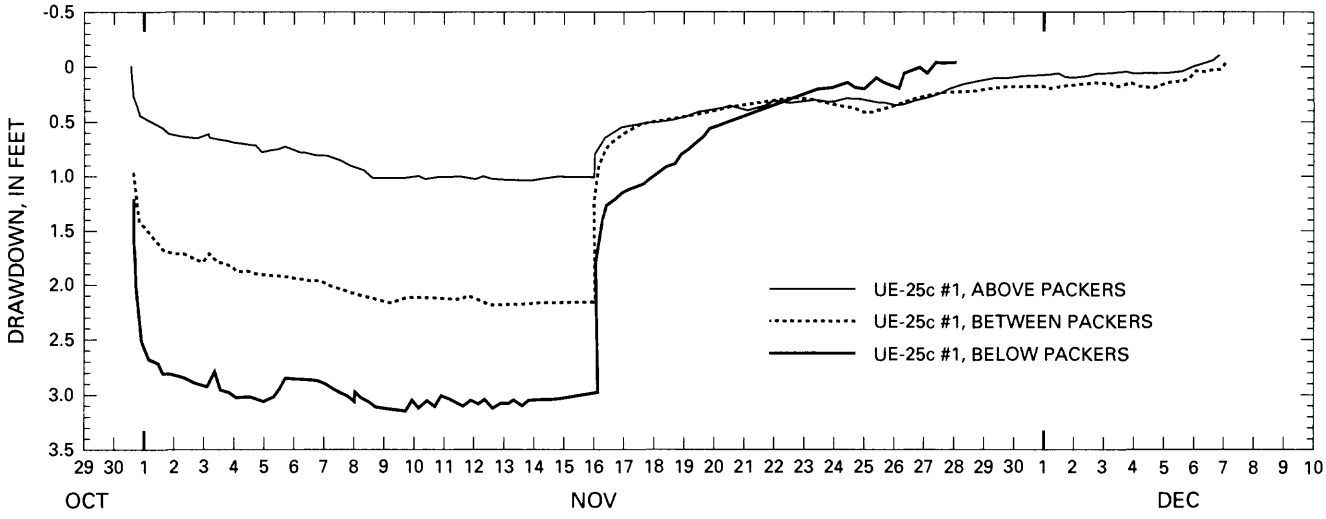

Figure 30. Drawdown as a function of time in borehole UE-25c #1 during the pumping test in borehole UE-25c #3, October to December 1984.

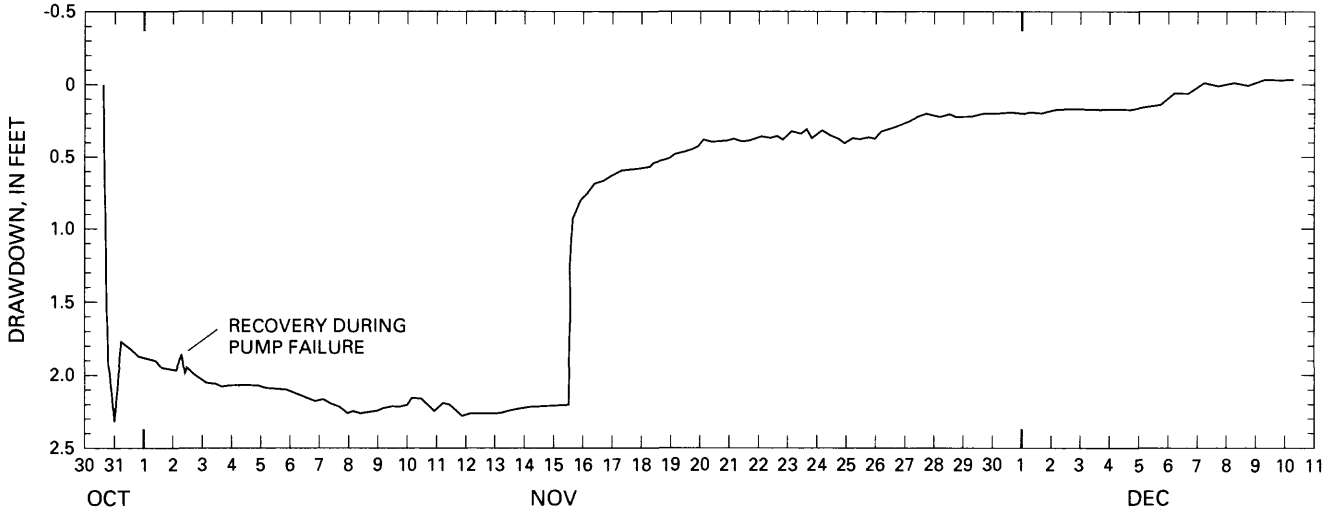

Figure 31. Drawdown as a function of time in borehole UE-25c #2 between the packers during the pumping test in borehole UE-25c #3, October to December 1984, with residual drawdown from a preceding injection test subtracted.

Test Analyses

The second pumping test in borehole UE-25c #3 produced analyzable data sets from boreholes UE-25c #3, UE-25c #2 between the packers, and UE-25c #1 above, between, and below the packers. Analyses of the data from the pumped well, borehole UE-25c #3, produced nearly identical results as analyses of data from this borehole obtained during the first pumping test in the borehole. To avoid redundancy, analyses of data from the pumped well obtained during the second pumping test in the borehole are not discussed further in this report. The remaining data sets are discussed with respect to the hydrogeologic intervals tested, instead of by borehole.

For drawdown and recovery data from borehole UE-25c #1 above the packers, the pumping test in borehole UE-25c #2 indicated that using the analytical solution of Neuman (1975) for an unconfined aquifer and matching the data curve to the type curve for ß = 0.06 provided the most reasonable calculations of hydrologic properties. Therefore, in the second pumping test in borehole UE-25c #3, drawdown data from borehole UE-25c #1 above the packers again were matched to the type curve of Neuman (1975) for ß = 0.06 (fig. 32), and the following values of transmissivity (T), storativity (S), specific yield (S_y), horizontal hydraulic conductivity (K_r), vertical hydraulic conductivity (K_z), and anisotropy (K_z/K_r) were calculated:

$$T = \frac{Q \times W\left(\mu_A, \mu_B, \beta\right)}{4\pi s} = \frac{\left(0.125 \times 425 gal/min \times 192.5 ft^3/d\right) \times 1}{(4\pi \times 0.21 ft) \times 1 gal/min} = 3,900 ft^2/d$$

$$S = \frac{4Tt\mu_A}{r^2} = \frac{4 \times 3,900 ft^2/d \times 6.1 min \times 1}{(267 ft)^2 \times 1,440 min/d} = 0.0009$$

$$S_Y = \frac{4Tt\mu_B}{r^2} = \frac{4 \times 3,900 ft^2/d \times 80 min \times 1}{(267 ft)^2 \times 1,440 min/d} = 0.01$$

$$K_r = T/b = \frac{3,900 ft^2/d}{528 ft} = 7 ft/d$$

$$K_z = \frac{K_r b^2 \beta}{r^2} = \frac{7 ft/d \times \left(528 ft^2\right) \times 0.06}{\left(267 ft^2\right)} = 2 ft/d$$

$$K_z/K_r = 2/7 = 0.3$$

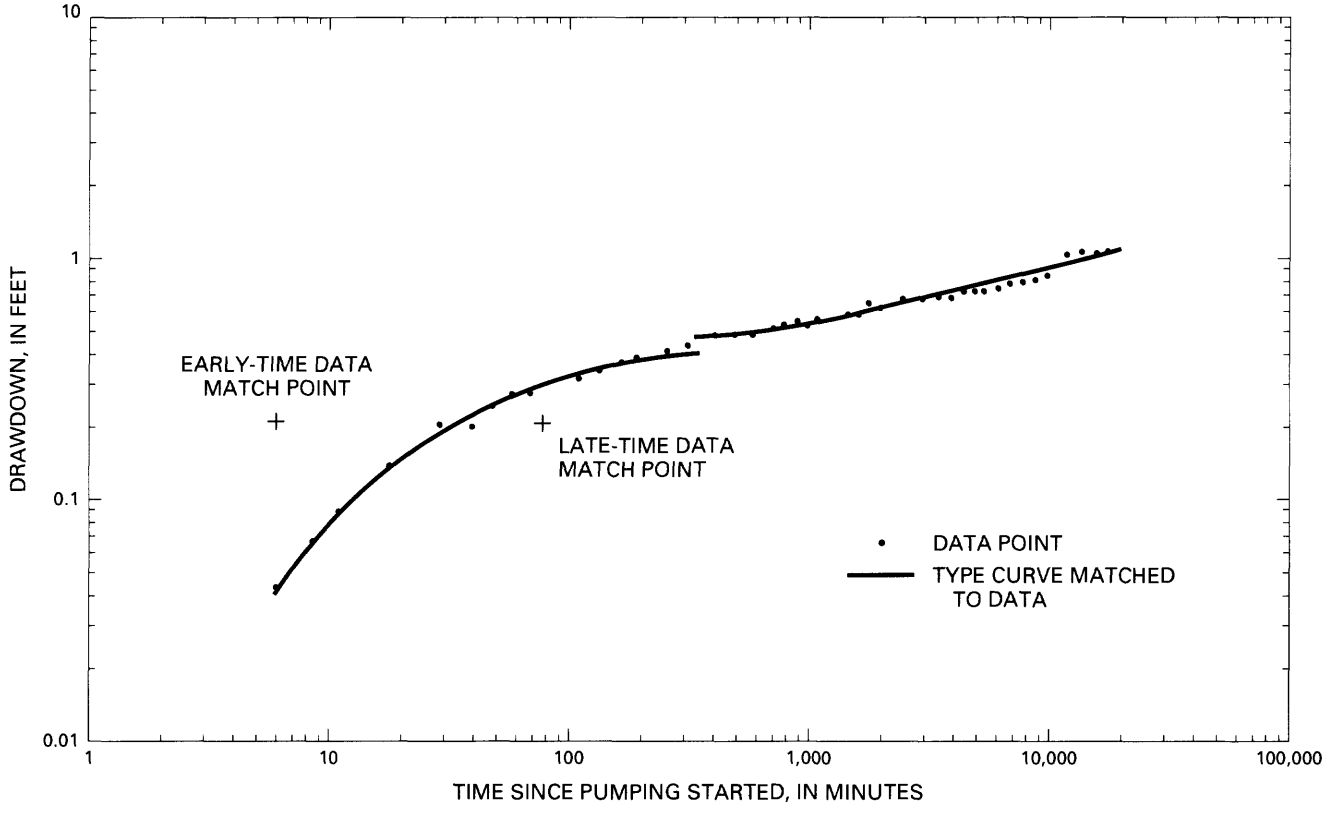

Figure 32. Analytical solution for drawdown data from borehole UE-25c #1 above the packers assuming an infinite, homogeneous, anisotropic, unconfined aquifer, pumping test in borehole UE-25c #3, October to December 1984.

The average transmissivity of the Prow Pass-upper Bullfrog aquifer was estimated to equal the average transmissivity of the rocks in borehole UE-25c #1 above the packers minus the transmissivity of the Calico Hills aquifer, which was calculated as follows:

	Transmissivity (ft^2/d)
UE-25c #1 above packers, pumping test in borehole UE-25c #2	2,900
UE-25c #1 above packers, second pumping test in borehole UE-25c #3	3,900
UE-25c #1 above packers, average	3,400
Calico Hills aquifer	−100
Prow Pass - upper Bullfrog aquifer	3,300

The average horizontal hydraulic conductivity of the Prow Pass-upper Bullfrog aquifer, then, would be 3,300 ft^2/d divided by 326 ft of transmissive rocks, which equals 10 ft/d. Multiplying the average horizontal hydraulic conductivity of the Prow Pass-upper Bullfrog aquifer by the average anisotropy in borehole UE-25c #1 above the packers, 0.2, indicates an average vertical hydraulic conductivity of 2 ft/d for the Prow Pass-upper Bullfrog aquifer.

As in the above calculations, the average specific yield of the Prow Pass-upper Bullfrog aquifer was estimated to equal the average specific yield of the rocks in borehole UE-25c #1 above the packers minus the specific yield of the Calico Hills aquifer, which was calculated as follows:

	Specific yield
UE-25c #1 above packers, pumping test in borehole UE-25c #2	0.004
UE-25c #1 above packers, second pumping test in borehole UE-25c #3	.01
UE-25c #1 above packers, average	0.007
Calico Hills aquifer	−.003
Prow Pass-upper Bullfrog aquifer	.004

Recovery data obtained from boreholes UE-25c #1 and UE-25c #2 between the packers, both,

conform to the type curve of Theis (1935) for an infinite, homogeneous, isotropic, confined aquifer (figs. 33 and 34) and indicate hydrologic properties for the Bullfrog aquifer. Based on heat-pulse flowmeter surveys done in December 1991, it was assumed that 29.5 percent of the flow in rocks below casing and concrete in borehole UE-25c #1 and 14 percent of the flow in rocks below casing and concrete in borehole UE-25c #2 come from the packed-off intervals in these boreholes. The following calculations of transmissivity (T), storativity (S), and horizontal hydraulic conductivity (K_r) were made:

UE-25c #1 Between Packers

$$T = \frac{Q \times W(\mu)}{4\pi s}$$

$$T = \frac{\left(0.295 \times 425 gal/min \times 192.5 ft^3/d\right) \times 1}{(4\pi \times 0.23 ft) \times 1 gal/min}$$

$$T = 8,400 ft^2/d$$

$$S = \frac{4Tt\mu}{r^2}$$

$$S = \frac{4 \times 8,400 ft^2/d \times 7.0 min \times 0.1}{(280 ft)^2 \times 1,440 min/d}$$

$$S = 0.0002$$

$$K_r = T/b$$

$$K_r = \frac{8,400 ft^2/d}{70 ft} = 100 ft/d$$

UE-25c #2 Between Packers

$$T = \frac{Q \times W(\mu)}{4\pi s}$$

$$T = \frac{\left(0.14 \times 425 gal/min \times 192.5 ft^3/d\right) \times 1}{(4\pi \times 0.22 ft) \times 1 gal/min}$$

$$T = 4,100 ft^2/d$$

$$S = \frac{4Tt\mu}{r^2}$$

$$S = \frac{4 \times 4,100 ft^2/d \times 5.6 min \times 0.1}{(92 ft)^2 \times 1440 min/d}$$

$$S = 0.0008$$

$$K_r = T/b$$

$$K_r = \frac{4,100 ft^2/d}{74 ft} = 60 ft/d$$

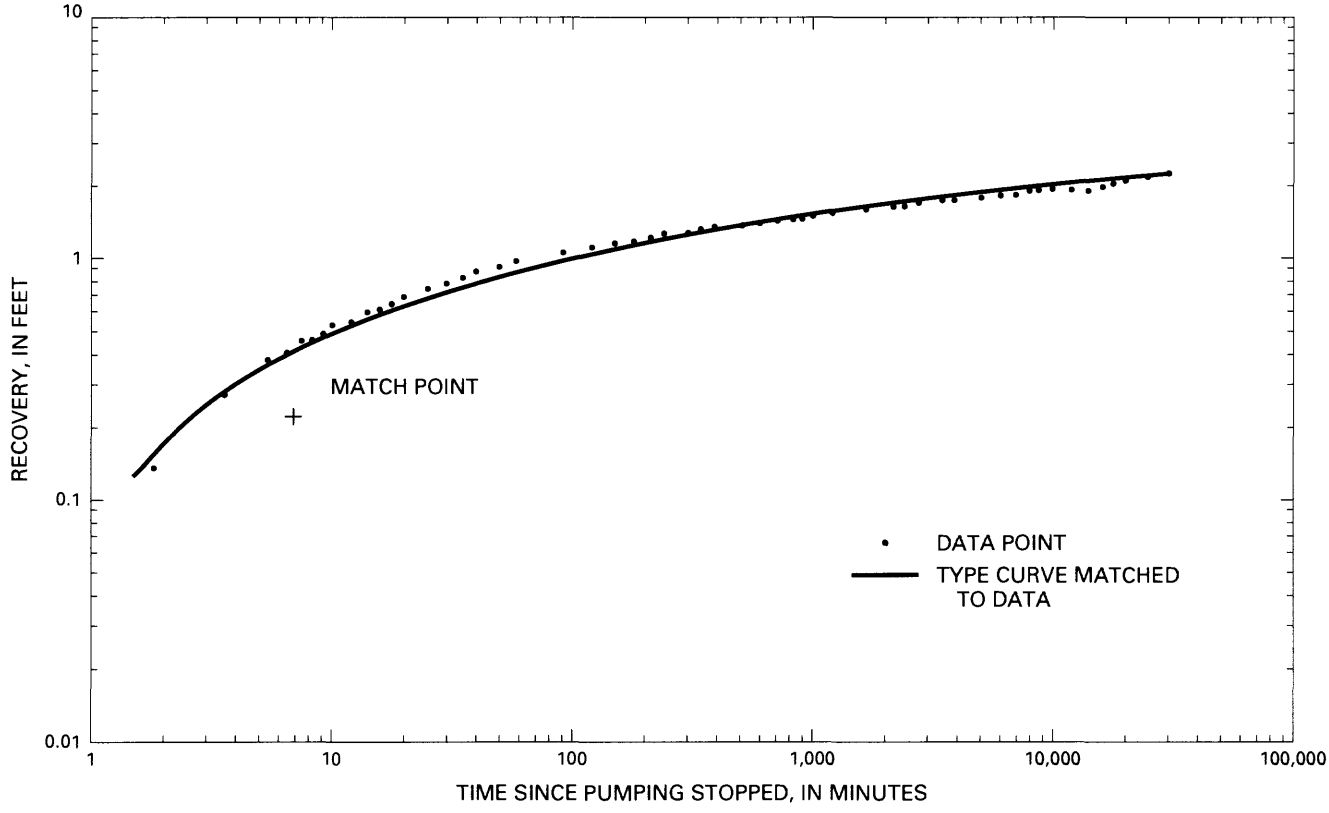

Figure 33. Analytical solution for recovery data from borehole UE-25c #1 between the packers assuming an infinite, homogeneous, isotropic, confined aquifer, pumping test in borehole UE-25c #3, October to December 1984.

Because of uncertainty regarding the estimate of flow contributed by rocks between the packers, calculated values of hydrologic properties presumably bracket the actual values.

Drawdown data obtained from borehole UE-25c #1 below the packers reveal the influence of fault boundaries on the Tram aquifer. Drawdown below the packers became essentially constant after about 5,000 minutes of pumping, indicating a constant flux to the Tram aquifer from that point until pumping ceased. The two faults that are shown in figure 7 cutting the Tram aquifer at the c-hole complex probably are the source of the water recharged to the aquifer during pumping. As discussed previously, a constant flux from a fault is analogous to constant leakage from a confining unit without storage. Hence, the drawdown data from borehole UE-25c #1 below the packers were matched to the type curve of Cooper (1963) for $v = 0.02$ (fig. 35), and values of transmissivity (T), storativity (S), and horizontal hydraulic conductivity (K_r) were then calculated. Based on a heat-pulse flowmeter survey done in December 1991, it was estimated that 58 percent of the flow from rocks below casing and concrete in borehole UE-25c #1 comes from the interval that was below the packers during this pumping test. The following calculations were made:

$$T = \frac{Q \times L(\mu v)}{4\pi s} = \frac{\left(0.58 \times 425 gal/min \times 192.5 ft^3/d\right) \times 1}{(4\pi \times 0.48 ft) \times 1 gal/min} = 7,900 ft^2/d$$

$$S = \frac{4Tt/r^2}{1/\mu} = \frac{4 \times 7,900 ft^2/d \times 0.00012 min/ft^2}{1 \times 1,440 min/d} = 0.003$$

$$K_r = T/b = \frac{7,900 ft^2/d}{208 ft} = 40 ft/d$$

As a check on the assumptions made regarding the percentage of flow contributed from rocks in borehole UE-25c #1 above, between, and below the packers, values of transmissivity, storativity, and hydraulic conductivity obtained for each interval from the second pumping test in borehole UE-25c #3 were added or averaged, as appropriate, and compared to composite values of hydrologic properties obtained from boreholes UE-25c #2 and UE-25c #3 during the first pump-

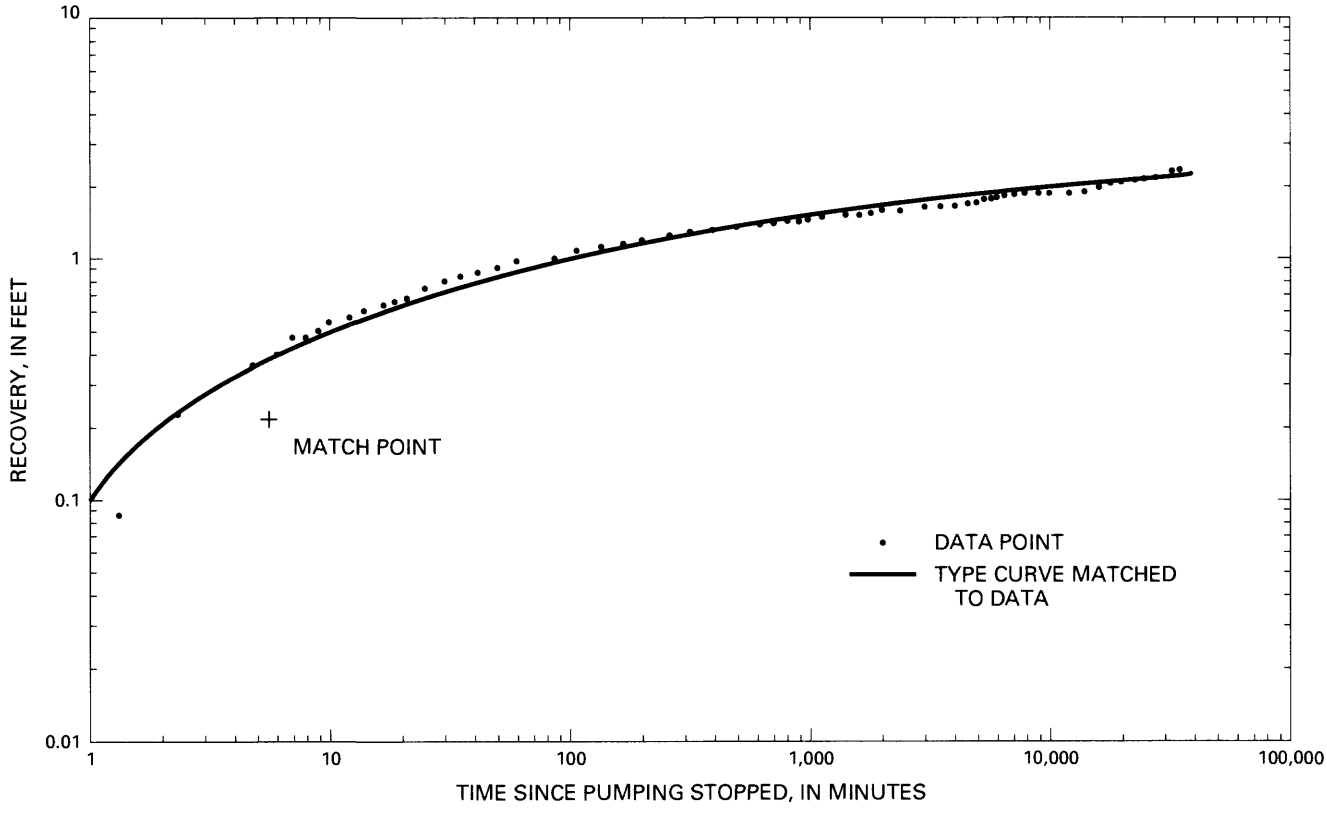

Figure 34. Analytical solution for recovery data from borehole UE-25c #2 between the packers assuming an infinite, homogeneous, isotropic, confined aquifer, pumping test in borehole UE-25c #3, October to December 1984.

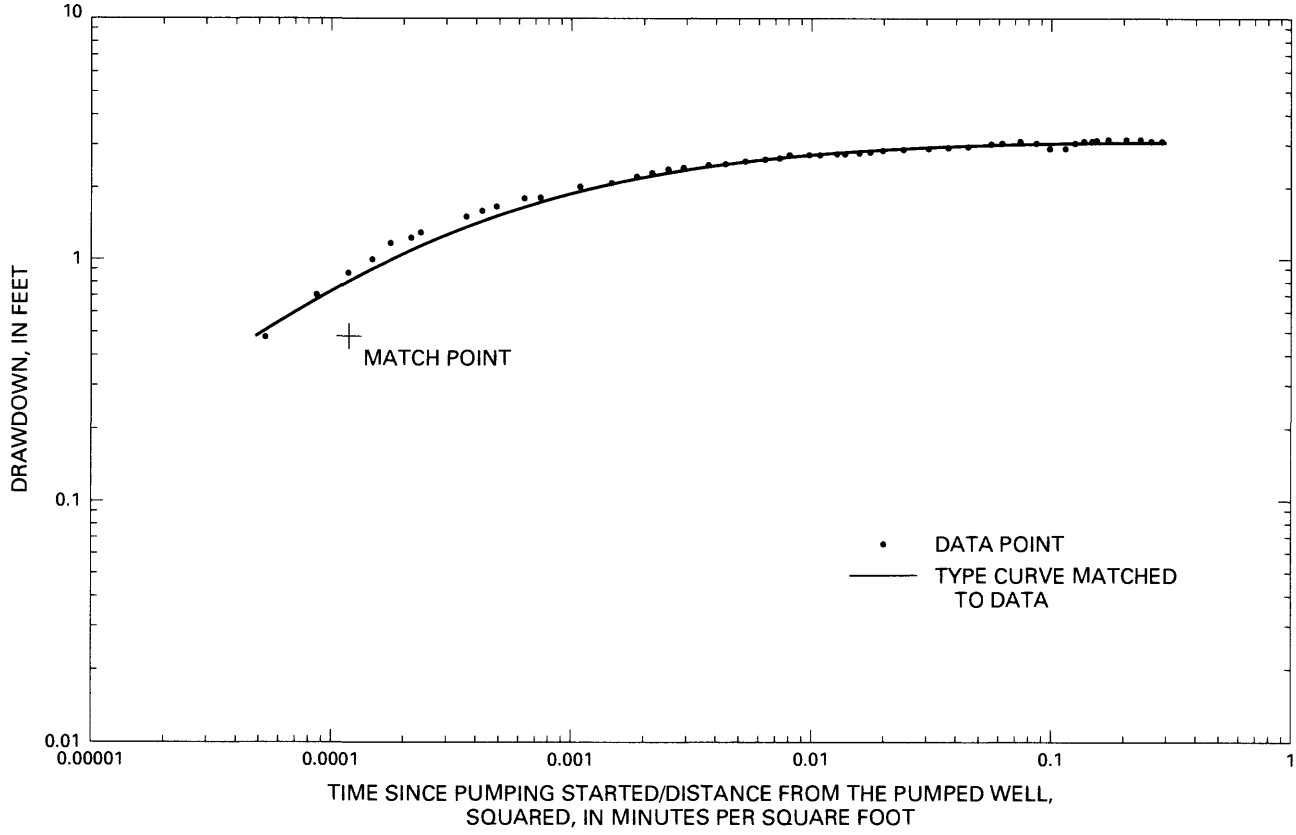

Figure 35. Analytical solution for drawdown data from borehole UE-25c #1 below the packers assuming an infinite, homogeneous, isotropic, confined aquifer with leakage from a confining unit without storage, pumping test in borehole UE-25c #3, October to December 1984.

ing test in borehole UE-25c #3 and the injection test in borehole UE-25c #2. As indicated in table 9, composite values of transmissivity = 20,000 ft^2/d, storativity = 0.004, horizontal hydraulic conductivity = 30 ft/d, and vertical hydraulic conductivity = 2 ft/d calculated for borehole UE-25c #1 compare favorably with composite values of transmissivity, storativity, and hydraulic conductivity obtained for rocks in boreholes UE-25c #2 and UE-25c #3. Therefore, calculations of hydrologic properties of the four aquifers penetrated by borehole UE-25c #1 can be considered reasonable estimates.

SUMMARY AND CONCLUSIONS

Fluid-injection and pumping tests conducted in 1983 and 1984 in boreholes UE-25c #1, UE-25c #2, and UE-25c #3 (the c-holes) on the east side of Yucca Mountain, Nev., were analyzed and interpreted in the context of other hydrogeologic information obtained from lithologic logs, borehole geophysical logs, core permeameter tests, and borehole flow surveys.

The c-holes, each of which is about 3,000 ft deep, are 100 to 251 ft apart at the surface. The three boreholes are completed in a 5,000-ft-thick sequence of Miocene tuffaceous rocks that is underlain by Paleozoic carbonate rocks and transected by high-angle, north-northeasterly and northwesterly striking faults. The contact between the Miocene and Paleozoic rocks generally is believed to be a detachment fault, into which the north-northeasterly striking faults merge listrically. A pumping test conducted in borehole UE-25c #2 indicated hydraulic connection between the Miocene and Paleozoic rocks, possibly through the network of faults cutting these rocks.

The depth to water at the c-hole complex ranges from 1,312 to 1,320 ft below land surface. The c-holes are open in the saturated zone below an average depth of about 1,370 ft from the land surface. Each of the c-holes is open in the tuffs and lavas of Calico Hills and the Prow Pass, Bullfrog, and Tram Members of the Crater Flat Tuff. These geologic units consist mostly of nonwelded to densely welded ash-flow tuff with interlayered ash-fall tuff and volcaniclastic rocks. A tuff breccia occurs in the Tram Member where the unit is transected by the Paintbrush Canyon Fault and another high-angle, north-northeasterly striking fault.

Tectonic and cooling fractures pervade the tuffaceous rocks penetrated by the c-holes, although fractures are distributed unevenly, and intervals range from unfractured to very fractured. Because of the fault brecciation, fracture frequency is greatest in the Tram Member. The bedded zone of the tuffs and lavas of Calico Hills, also, is very fractured. On the average, moderately to densely welded zones of the Prow Pass and Bullfrog Members are more fractured than bedded zones which, in turn, are more fractured than nonwelded to partially welded zones. Most fractures strike approximately south and dip westward at angles of 50°–87°. The least common fractures strike generally east or west, and many of these are shallow-dipping or mineralized.

Within the saturated zone open to the c-holes, the tuffaceous rocks display layered heterogeneity. Permeameter tests indicate a vertical range in matrix permeability of 0.001 to 20 mD, with slightly larger permeability horizontally than vertically. Falling-head and pressure-injection tests in borehole UE-25c #1 indicate a vertical range in hydraulic conductivity of 0.003 to 2 ft/d. The average hydraulic conductivity in the horizontal direction in borehole UE-25c #1 is 0.2 ft/d, whereas the average hydraulic conductivity in the vertical direction is 0.02 ft/d.

Fluid-injection tests and single-well pumping tests in boreholes UE-25c #1 and UE-25c #3 indicate a composite transmissivity of about 300 ft^2/d for the tuffs and lavas of Calico Hills and the Crater Flat Tuff. However, multiple-well, constant-flux tests in the c-holes indicate that single-well injection and withdrawal tests are not reliable indicators of site-scale hydrologic properties. For the entire thickness of rocks below casing and concrete in a borehole, cross-hole tests generally indicate values of transmissivity and hydraulic conductivity that are about two orders of magnitude larger than values obtained in single-well tests. This dependence of results on the radius of investigation can be interpreted as an effect of encompassing more conduits for ground-water flow, such as faults or fracture zones, as a larger volume of aquifer is investigated.

In the c-holes, eleven transmissive intervals were identified on the basis of fracture and matrix permeability distributions, borehole resistivity, temperature, and caliper logs, and heat-pulse flowmeter and tracejector surveys. The heat-pulse flowmeter surveys indicated downward flow in the upper parts and upward flow in the lower parts of boreholes UE-25c #1 and UE-25c #2, but upward flow through the entire surveyed section of borehole UE-25c #3 (below a depth of about 1,500 ft). The eleven transmissive intervals at the c-hole complex were grouped for purposes of investigation and discussion into four informal aquifers with intercalated confining units. In descending order, the four aquifers are the Calico Hills, Prow Pass-upper Bullfrog, Bullfrog, and Tram.

The Calico Hills aquifer is unconfined and anisotropic. The aquifer has a transmissivity of 100 ft^2/d, a specific yield of 0.003, a horizontal hydraulic conduc-

Table 9. Summary of analyses of 1984 constant-flux aquifer tests in boreholes UE-25c #1, UE-25c #2, and UE-25c #3

[Values of transmissivity rounded to two significant figures; other hydrologic properties rounded to one significant figure]

Monitored interval or borehole	Transmissivity (feet squared per day)	Storativity	Fracture storativity	Block storativity	Specific yield	Hydraulic conductivity (feet per day)			
						Horizontal	Vertical	Fracture	Block
UE-25c #1									
Calico Hills aquifer	100				0.003	0.5	1	7	0.01
Prow Pass-Upper Bullfrog aquifer	3,300	0.0005			0.004	10	2		
Bullfrog aquifer	8,400	.0002				100	100		
Tram aquifer	7,900	.003				40	40		
Composite	20,000	.004				30	2		
UE-25c #2									
Composite (Neuman, 1975)	23,000	.004			.07	40	5		
Composite (Streltsova-Adams, 1978)	29,000		.004	.04				50	0.01
UE-25c #3									
Composite (Cooper-Jacob, 1946)	35,000	.002				40			

tivity of 0.5 ft/d, and a vertical hydraulic conductivity of about 1 ft/d.

The Prow Pass-upper Bullfrog aquifer may be either an unconfined, anisotropic aquifer or a fissure-block aquifer. If unconfined, the aquifer has an average transmissivity in pumping tests of 3,300 ft^2/d, a specific yield of 0.004, a storativity, combined with the Calico Hills aquifer, of 0.0005, a horizontal hydraulic conductivity of 10 ft/d, and a vertical hydraulic conductivity of 2 ft/d.

The Bullfrog aquifer is confined, nonleaky, and isotropic. The aquifer has a transmissivity that in borehole UE-25c #1 was determined to be 8,400 ft^2/d and in borehole UE-25c #2 was determined to be 4,100 ft^2/d. Assuming the larger value to be correct, the aquifer has a storativity of 0.0002, and a hydraulic conductivity of 100 ft/d.

The Tram aquifer, although confined, is recharged by leakage from faults. The aquifer has a transmissivity of 7,900 ft^2/d, a storativity of 0.003, and a hydraulic conductivity of 40 ft/d.

Composite values of hydrologic properties determined for rocks in borehole UE-25c #1 by adding or averaging interval values, as appropriate, compare favorably with composite values determined by monitoring borehole UE-25c #2 during a pumping test in borehole UE-25 c#3 and by monitoring borehole UE-25c #3 during an injection test in borehole UE-25c #2. For the entire thickness of rocks penetrated by the c-holes, transmissivity was determined to be between 20,000 and 35,000 ft^2/d, storativity was determined to be between 0.002 and 0.004, horizontal hydraulic conductivity was determined to be between 30 and 40 ft/d, and vertical hydraulic conductivity was determined to be between 2 and 5 ft/d.

SELECTED REFERENCES

Barker, J.A., and Black, J.H., 1983, Slug tests in fissured aquifers: American Geophysical Union, Water Resources Research, v. 19, no. 6, p. 1558–1564.

Bredehoeft, J.D., and Papadopulos, S.S., 1980, A method for determining the hydraulic properties of tight formations: American Geophysical Union, Water Resources Research, v. 16, no. 1, p. 233–238.

Carr, M.D., Waddell, S.J., Vick, G.S., Stock, J.M., Monsen, S.A., Harris, A.G., Cork, B.W., and Byers, F.M., Jr., 1986, Geology of drill hole UE-25p #1: A test hole into pre-Tertiary rocks near Yucca Mountain, southern Nevada: U.S. Geological Survey Open-File Report 86-175, 87 p.

Carr, W.J., 1990, Styles of extension in the Nevada Test Site region, southern Walker Lane Belt; An integration of volcano-tectonic and detachment fault models, *in* Wernicke, B.P., ed., Basin and Range extensional tectonics near the latitude of Las Vegas, Nevada: Boulder, Colo., Geological Society of America Memoir 176, p. 283–303.

Cooper, H.H., Jr., 1963, Type curves for nonsteady radial flow in an infinite leaky artesian aquifer, *in* Bentall, Ray, Compiler, Shortcuts and special problems in aquifer tests: U.S. Geological Survey Water-Supply Paper 1545-C, p. 48–55.

Cooper, H.H., Jr., and Jacob, C.E., 1946, A generalized graphical method for evaluating formation constants and summarizing well-field history: American Geophysical Union Transactions, v. 27, no. 4, p. 526–534.

Cooper, H.H., Jr., Bredehoeft, J.D., and Papadopulos, I.S., 1967, Response of a finite-diameter well to an instantaneous charge of water: American Geophysical Union, Water Resources Research, v. 3, no. 1, p. 263–269.

Driscoll, F.G., 1986, Groundwater and wells: St. Paul, Minnesota, Johnson Division, 1089 p.

Fenix and Scisson, Inc., 1986, NNWSI hole histories UE-25c #1, UE-25c #2, UE-25c #3: Tulsa, Okla., 60 p.

Freeze, R.A., and Cherry, J.A., 1979, Groundwater: Englewood Cliffs, N.J., Prentice-Hall, Inc., 604 p.

Frizzell, V.A., Jr., and Shulters, Jacqueline, 1990, Geologic map of the Nevada Test Site, southern Nevada: U.S. Geological Survey Miscellaneous Investigations Map I-2046, scale 1:100,000.

Galloway, D.L., and Rojstaczer, Stuart, 1988, Analysis of the frequency response of water levels in wells to Earth tides and atmospheric loading, *in* Hitchon, Brian, and Bachu, Stefan, eds., Proceedings Fourth Canadian/American Conference on Hydrogeology - Fluid flow, heat transfer, and mass transport in fractured rocks: Dublin, Ohio, National Water Well Association, p. 100–113.

Geldon, A.L., 1993, Preliminary hydrogeologic assessment of boreholes UE-25c #1, UE-25c #2, and UE-25c #3, Yucca Mountain, Nye County, Nevada: U.S. Geological Survey Water-Resources Investigations Report 92-4016, 85 p.

Gringarten, A.C., 1982, Flow-test evaluation of fractured reservoirs, *in* Narasimhan, T.N., ed., Recent trends in hydrogeology: Boulder, Colo., Geological Society of America Special Paper 189, p. 237–263.

Hess, A.E., 1990, Thermal-pulse flowmeter for measuring slow velocities in boreholes: U.S. Geological Survey Open-File Report 87-121, 70 p.

Lobmeyer, D.H., Whitfield, M.S., Lahoud, R.R., and Bruckheimer, Laura, 1983, Geohydrologic data for test well UE-25b #1, Nevada Test Site, Nye County, Nevada: U.S. Geological Survey Open-File Report 83-855, 48 p.

Lohman, S.W., 1979, Ground-water hydraulics: U.S. Geological Survey Professional Paper 708, 70 p.

Nelson, P.H., Muller, D.C., Schimschal, Ulrich, and Kibler, J.E., 1991, Geophysical logs and core measurements from forty boreholes at Yucca Mountain, Nevada: U.S. Geological Survey Geophysical Investigations Map GP-1001.

Neuman, Shlomo, 1975, Analysis of pumping test data from anisotropic unconfined aquifers considering delayed gravity response: American Geophysical Union, Water Resources Research, v. 11, no. 2, p. 329–342.

Neuzil, C.E., 1982, On conducting the modified "slug" test in tight formations: American Geophysical Union, Water Resources Research, v. 18, no. 2, p. 439–441.

Reed, J.E., 1980, Type curves for selected problems of flow to wells in confined aquifers: U.S. Geological Survey Techniques of Water-Resources Investigations, book 3, chap. B3.

Robison, J.H., and Craig, R.W., 1991, Geohydrology of rocks penetrated by test well USW H-5, Yucca Mountain, Nye County, Nevada: U.S. Geological Survey Water-Resources Investigations Report 88-4168, 44 p.

Robison, J.H., Stephens, D.M., Luckey, R.R., and Baldwin, D.A., 1988, Water levels in periodically measured wells in the Yucca Mountain area, Nevada, 1981–87: U.S. Geological Survey Open-File Report 88-468, 132 p.

Rush, F.E., Thordarson, William, and Bruckheimer, Laura, 1983, Geohydrologic and drill-hole data for test well USW H-1, adjacent to Nevada Test Site, Nye County, Nevada: U.S. Geological Survey Open-File Report 83-141, 38 p.

Scott, R.B., 1990, Tectonic setting of Yucca Mountain, southwest Nevada in Wernicke, B.P., ed., Basin and Range extensional tectonics near the latitude of Las Vegas, Nevada: Boulder, Colo., Geological Society of America Memoir 176, p. 251–282.

Scott, R.B., and Bonk, Jerry, 1984, Preliminary geologic map of Yucca Mountain, Nye County, Nevada, with geologic sections: U.S. Geological Survey Open-File Report 84-494, scale 1:12,000.

Streltsova-Adams, T.D., 1978, Well testing in heterogeneous aquifer formations, *in* Chow, V.T., ed., Advances in hydroscience: New York, Academic Press, v. 11, p. 357–423.

Theis, C.V., 1935, The relation between the lowering of the piezometric surface and the rate and duration of discharge of a well using ground-water storage: American Geophysical Union Transactions, v. 16, p. 519–524.

SUPPLEMENTAL DATA

TABLE 10. SUMMARY OF INFORMATION FROM LITHOLOGIC (L), TELEVISION (TV), ACOUSTIC TELEVIEWER (AT), CALIPER (C), AND TEMPERATURE (TEMP) LOGS FOR BOREHOLE UE-25C #1

[Abbreviations for tables 10, 11, and 12: SG, casing; NW, nonwelded; NW-PW, nonwelded to partially welded; MW, moderately welded; MW-DW, moderately to densely welded; PW-NW, partially welded to nonwelded; PW, partially welded; N.VERT, near vertical; LITH, lithologic; TD, total depth; N, north, S, south; SW, southwest, SE, southeast; SSW, south-southwest]

DEPTH BLW CASING (FEET)		GEOLOGIC UNIT	LITHOLOGIC ZONE	FEATURE	DIP AZIMUTH	DIP ANGLE	STRIKE AZIMUTH	REMARKS	LOG
TOP	BOTTOM								
1313		TOPOPAH SPRING	BASAL	WATER TABLE				ABRUPT INCREASE IN TEMPERATURE	TEMP
1332		CALICO HILLS	NW	CONTACT					L
1362				BOTTOM OF CSG				TEXTURE CHANGE FROM SMOOTH TO ROUGH BLW CSG	TV
1362	1371			CONCRETE				ABRUPT INCREASE IN DIAMETER BELOW CONCRETE	TV/C
1427	1428			FRACTURE	265	N. VERT	175	HOLE SKEWED AND VISIBILITY POOR 1371-1505	TV
1461	1461			FRACTURE	225	SHALLOW	135		TV
1486	1486			FRACTURE	280	N. VERT	190		TV
1486	1487			FRACTURE	225	SHALLOW	135		TV
1505	1506			FRACTURE	20	STEEP	290		TV
1506	1506			FRACTURE	30	STEEP	300		TV
1510	1511			LEDGE				HOLE DIAMETER REDUCED	TV
1515	1516			FRACTURE	95	STEEP	5		TV
1521	1523			FRACTURE	180	STEEP	90		TV
1522	1524			FRACTURE	210	STEEP	120		TV
1523	1525			FRACTURE	95	STEEP	5		TV
1523	1534			FRACTURE	275	VERTICAL	185	SPLAYS WITH INTERSTITIAL CAVITIES	TV
1525	1528			FRACTURE	95	N. VERT	5		TV
1530	1534			FRACTURE	105	N. VERT	15		TV
1530	1531			FRACTURE	270	STEEP	180		TV
1531	1532			FRACTURE	260	STEEP	170		TV
1532	1532			FRACTURE	260	STEEP	170		TV
1535	1541			FRACTURE	350	VERTICAL	260		TV
1535	1535			FRACTURE	145	STEEP	55		TV
1541	1544			FRACTURE	270	N. VERT	180		TV
1561	1562			FRACTURE	255	SHALLOW	165		TV
1582	1584			FRACTURE	170	STEEP	80		TV

TABLE 10. SUMMARY OF INFORMATION FROM LITHOLOGIC (L), TELEVISION (TV), ACOUSTIC TELEVIEWER (AT), CALIPER (C), AND TEMPERATURE (TEMP) LOGS FOR BOREHOLE UE-25C #1 --Continued

DEPTH BLW CASING (FEET)		GEOLOGIC UNIT	LITHOLOGIC ZONE	FEATURE	DIP AZIMUTH	DIP ANGLE	STRIKE AZIMUTH	REMARKS	LOG
TOP	BOTTOM								
1592	1593	CALICO HILLS	NW	FRACTURE	285	VERTICAL	195		TV
1593			BEDDED	CONTACT				TEXTURE ROUGHER AND VISIBILITY POORER	L
1623	1630			FRACTURE	287	83	197		AT
1636	1637			FRACTURE	270	N. VERT	180		TV
1636	1637			FRACTURE	180	SHALLOW	90		TV
1638	1639			FRACTURE	285	N. VERT	195		TV
1672	1673			FRACTURE	170	N. VERT	90		TV
1691	1692	PROW PASS	NW-PW	CONTACT				OPEN PARTING	TV/L
1693	1694			FRACTURE	117	27	27		AT
1722	1722			FRACTURE	305	STEEP	215		TV
1759	1765			FRACTURE	309	80	219		AT
1767	1768			FRACTURE	315	N. VERT	225		TV
1778	1778			FRACTURE	285	STEEP	195		TV
1785	1785			FRACTURE	230	SHALLOW	140		TV
1791	1791			FRACTURE	210	SHALLOW	120		TV
1802	1802			FRACTURE	230	SHALLOW	140	MINERALIZED	TV
1803	1804			FRACTURE	315	SHALLOW	225		TV
1805	1806			FRACTURE	230	N. VERT	140		TV
1806	1806			FRACTURE	125	SHALLOW	35		TV
1806	1807			FRACTURE	230	STEEP	140		TV
1806	1808			FRACTURE	245	STEEP	155		TV
1808	1809			FRACTURE	190	N. VERT	100		TV
1809	1810			FRACTURE	250	N. VERT	160		TV
1809	1813			FRACTURE	298	76	208		AT
1811	1817			FRACTURE	300	VERTICAL	210		TV
1815	1821			FRACTURE	215	VERTICAL	125		TV

TABLE 10. SUMMARY OF INFORMATION FROM LITHOLOGIC (L), TELEVISION (TV), ACOUSTIC TELEVIEWER (AT), CALIPER (C), AND TEMPERATURE (TEMP) LOGS FOR BOREHOLE UE-25C #1 --Continued

DEPTH BLW CASING (FEET)		GEOLOGIC UNIT	LITHOLOGIC ZONE	FEATURE	DIP AZIMUTH	DIP ANGLE	STRIKE AZIMUTH	REMARKS	LOG
TOP	BOTTOM								
1817	1818	PROW PASS	NW-PW	FRACTURE	255	STEEP	165		TV
1818	1819			FRACTURE	235	N. VERT	145		TV
1818	1819			FRACTURE	245	N. VERT	155		TV
1819	1819			FRACTURE	245	N. VERT	155		TV
1819	1821			FRACTURE	235	N. VERT	145		TV
1820	1821			FRACTURE	250	N. VERT	160		TV
1821	1821			FRACTURE	235	N. VERT	145		TV
1821	1823			FRACTURE	105	N. VERT	15	OPEN AT UPTOE	TV
1822	1822			FRACTURE	110	N. VERT	20		TV
1822	1822			FRACTURE	100	N. VERT	10		TV
1823	1823			FRACTURE	105	N. VERT	15		TV
1823	1823			FRACTURE	200	N. VERT	110		TV
1823	1824			FRACTURE	285	STEEP	195		TV
1825	1825			FRACTURE	15	N. VERT	285	OPEN AT DOWNTOE	TV
1825	1825			FRACTURE	240	N. VERT	150		TV
1828	1828			FRACTURE	250	VERTICAL	160		TV
1830	1830			FRACTURE	175	N. VERT	85		TV
1831	1833			FRACTURE	35	STEEP	305		TV
1832	1833			FRACTURE	5	N. VERT	275		TV
1833	1834			FRACTURE	255	VERTICAL	165		TV
1834	1835			FRACTURE	330	STEEP	240		TV
1834	1835			FRACTURE	100	STEEP	10		TV
1835	1837			FRACTURE	235	N. VERT	145	CAVED AT UPTOE	TV
1835	1836			FRACTURE	110	N. VERT	20		TV
1835	1840			FRACTURE	284	79	194		AT
1836	1836			FRACTURE	260	N. VERT	170		TV
1836	1836			FRACTURE	145	N. VERT	55		TV
1837	1837			FRACTURE	190	N. VERT	100		TV
1837	1839			FRACTURE	245	N. VERT	155		TV

TABLE 10. SUMMARY OF INFORMATION FROM LITHOLOGIC (L), TELEVISION (TV), ACOUSTIC TELEVIEWER (AT), CALIPER (C), AND TEMPERATURE (TEMP) LOGS FOR BOREHOLE UE-25C #1 --Continued

DEPTH BLW CASING (FEET)		GEOLOGIC UNIT	LITHOLOGIC ZONE	FEATURE	DIP AZI-MUTH	DIP ANGLE	STRIKE AZI-MUTH	REMARKS	LOG
TOP	BOT-TOM								
1838		PROW PASS	MW	CONTACT					L
1839	1841			FRACTURE	285	N. VERT	195		TV
1839	1839			FRACTURE	110	N. VERT	20		TV
1839	1840			FRACTURE	165	N. VERT	75		TV
1840	1840			FRACTURE	95	STEEP	5		TV
1840	1841			FRACTURE	295	N. VERT	205		TV
1840	1846			FRACTURE	260	82	170		AT
1841	1841			FRACTURE	115	SHALLOW	25		TV
1841	1843			FRACTURE	200	STEEP	110		TV
1842	1842			FRACTURE	75	N. VERT	345		TV
1843	1843			FRACTURE	285	N. VERT	195		TV
1843	1843			FRACTURE	265	N. VERT	175		TV
1844	1844			FRACTURE	235	N. VERT	145		TV
1844	1845			FRACTURE	235	N. VERT	145		TV
1860	1860			FRACTURE	275	SHALLOW	185		TV
1860	1860			FRACTURE	220	SHALLOW	130		TV
1860	1861		PW-NW	CONTACT				OPEN PARTING	TV/L
1866	1871			FRACTURE	263	80	173		AT
1871	1872			FRACTURE	240	STEEP	150		TV
1879	1883			FRACTURE	273	79	183		AT
1884	1884			FRACTURE	260	N. VERT	170		TV
1887	1888			FRACTURE	235	STEEP	145		TV
1890	1892			FRACTURE	272	70	182		AT
1892	1893			FRACTURE	200	N. VERT	110		TV
1893	1895			FRACTURE	258	N. VERT	168		TV
1896	1898			FRACTURE	281	58	191		AT
1898	1899			FRACTURE	105	N. VERT	15		TV
1899	1901			FRACTURE	277	64	187		AT

TABLE 10. SUMMARY OF INFORMATION FROM LITHOLOGIC (L), TELEVISION (TV), ACOUSTIC TELEVIEWER (AT), CALIPER (C), AND TEMPERATURE (TEMP) LOGS FOR BOREHOLE UE-25C #1 --Continued

DEPTH BLW CASING (FEET)		GEOLOGIC UNIT	LITHOLOGIC ZONE	FEATURE	DIP AZIMUTH	DIP ANGLE	STRIKE AZIMUTH	REMARKS	LOG
TOP	BOTTOM								
1902	1903	PROW PASS	PW-NW	FRACTURE	295	STEEP	205	MANY SPLAYS	TV
1907	1909			FRACTURE	262	STEEP	172		TV
1910	1910			FRACTURE	195	SHALLOW	105		TV
1911	1913			FRACTURE	260	STEEP	170		TV
1919	1922			FRACTURE	275	STEEP	185	BOTH TOES OPEN (CAVED)	TV
1920	1921			FRACTURE	180	STEEP	90	OPEN AT UPTOE	TV
1921	1922			FRACTURE	105	SHALLOW	15		TV
1924	1925			FRACTURE	105	SHALLOW	15		TV
1939	1942			FRACTURE	275	N. VERT	185		TV
1940	1941			FRACTURE	280	STEEP	190	OPEN	TV
1942	1948			FRACTURE	280	VERTICAL	190		TV
1943	1945			FRACTURE	290	63	200		AT
1947	1950			FRACTURE	322	74	232		AT
1963	1964			FRACTURE	105	28	15	OPEN	AT
1974	1975			FRACTURE	110	44	20	OPEN	AT
1982	1985			FRACTURE	273	73	183		AT
2071	2071			FRACTURE	265	SHALLOW	175	VISIBILITY POOR 2061-2118 BECAUSE OF SKEWED HOLE	TV
2079	2079			FRACTURE	180	VERTICAL	90		TV
2081	2081			FRACTURE	215	VERTICAL	125		TV
2087	2087			FRACTURE	145	VERTICAL	55		TV
2114	2115			FRACTURE	25	N. VERT	295		TV
2115	2118			FRACTURE	285	VERTICAL	195	OPEN	TV
2118			BEDDED	CONTACT				SMOOTHER TEXTURE, CORRUGATIONS AT CONTACT	TV/L
2118	2119			FRACTURE	270	N. VERT	180		TV
2119	2119			FRACTURE	235	N. VERT	145		TV
2121	2122			FRACTURE	272	30	182		AT
2122	2122			FRACTURE	260	22	170		AT
2124	2124			FRACTURE	280	SHALLOW	190		TV

TABLE 10. SUMMARY OF INFORMATION FROM LITHOLOGIC (L), TELEVISION (TV), ACOUSTIC TELEVIEWER (AT), CALIPER (C), AND TEMPERATURE (TEMP) LOGS FOR BOREHOLE UE-25C #1 --Continued

DEPTH BLW CASING (FEET)		GEOLOGIC UNIT	LITHOLOGIC ZONE	FEATURE	DIP AZI-MUTH	DIP ANGLE	STRIKE AZI-MUTH	REMARKS	LOG
TOP	BOT-TOM								
2125	2125	PROW PASS	BEDDED	FRACTURE	325	N. VERT	235		TV
2127	2129			FRACTURE	274	58	184		AT
2130	2131			FRACTURE	265	42	175		AT
2130	2131			FRACTURE	35	VERTICAL	305		TV
2137	2138			FRACTURE	145	49	55	OPEN	AT
2140	2141			FRACTURE	291	59	201		AT
2146	2147			FRACTURE	259	30	169		AT
2150	2150			FRACTURE	120	SHALLOW	30		TV
2151	2152			FRACTURE	160	SHALLOW	70		TV
2152	2152			FRACTURE	120	VERTICAL	30		TV
2152	2153	BULLFROG	NW-PW	CONTACT				OPEN PARTING	TV/L
2153	2156			FRACTURE	131	25	41		AT
2181	2182			FRACTURE	5	SHALLOW	275		TV
2182	2183			FRACTURE	5	SHALLOW	275		TV
2201	2202			FRACTURE	175	N. VERT	85		TV
2204	2204			FRACTURE	320	SHALLOW	230		TV
2204	2204			FRACTURE	95	SHALLOW	5		TV
2206	2206			FRACTURE	285	N. VERT	195		TV
2209	2209			FRACTURE	220	SHALLOW	130		TV
2209	2210			FRACTURE	225	SHALLOW	135		TV
2215	2215			FRACTURE	110	N. VERT	20		TV
2216	2216			FRACTURE	265	SHALLOW	175		TV
2216	2218			FRACTURE	220	N. VERT	130	OPEN	TV
2217	2222			FRACTURE	283	78	193		AT
2219	2220			FRACTURE	260	VERTICAL	170		TV
2230	2230			FRACTURE	220	N. VERT	130		TV
2234	2234			FRACTURE	90	VERTICAL	0		TV
2238	2238			FRACTURE	240	N. VERT	150	OPEN UPTOE	TV

TABLE 10. SUMMARY OF INFORMATION FROM LITHOLOGIC (L), TELEVISION (TV), ACOUSTIC TELEVIEWER (AT), CALIPER (C), AND TEMPERATURE (TEMP) LOGS FOR BOREHOLE UE-25C #1 --Continued

DEPTH BLW CASING (FEET)		GEOLOGIC UNIT	LITHOLOGIC ZONE	FEATURE	DIP AZIMUTH	DIP ANGLE	STRIKE AZIMUTH	REMARKS	LOG
TOP	BOTTOM								
2239	2240	BULLFROG	NW-PW	FRACTURE	210	N. VERT	120		TV
2241	2241			FRACTURE	240	N. VERT	150		TV
2241	2243			FRACTURE	267	67	177		AT
2260		BULLFROG	MW-DW	CONTACT					L
2270	2274			FRACTURE	235	N. VERT	145	MINERALIZED	TV
2281	2281			FRACTURE	265	N. VERT	175	MINERALIZED	TV
2301	2304			FRACTURE	250	N. VERT	160	MINERALIZED	TV
2311	2314			FRACTURE	280	N. VERT	190	MINERALIZED	TV
2312	2313			FRACTURE	55	N. VERT	325	MINERALIZED	TV
2315	2318			FRACTURE	10	N. VERT	280		TV
2318	2318			FRACTURE	245	N. VERT	155	MINERALIZED	TV
2320	2326			FRACTURE	190	VERTICAL	100		TV
2327	2328			FRACTURE	10	STEEP	280		TV
2332	2333			FRACTURE	270	N. VERT	180		TV
2342	2344			FRACTURE	190	N. VERT	100	MINERALIZED	TV
2352	2358			FRACTURE	265	VERTICAL	175	MINERALIZED	TV
2362	2364			FRACTURE	260	N. VERT	170	MINERALIZED	TV
2363	2363			FRACTURE	270	N. VERT	180		TV
2365	2370			FRACTURE	255	VERTICAL	165	MINERALIZED	TV
2366	2366			FRACTURE	225	N. VERT	135	MINERALIZED	TV
2368	2370			FRACTURE	230	N. VERT	140	MINERALIZED	TV
2378	2381			FRACTURE	205	N. VERT	115	MINERALIZED	TV
2385	2385			FRACTURE	260	N. VERT	170	MINERALIZED	TV
2387	2388			FRACTURE	245	N. VERT	155	MINERALIZED	TV
2390	2391			FRACTURE	250	N. VERT	160	MINERALIZED	TV
2392	2397			FRACTURE	190	VERTICAL	100	PARTLY MINERALIZED	TV
2407	2411			FRACTURE	255	N. VERT	165	MINERALIZED	TV
2424	2427			FRACTURE	267	67	177	MINERALIZED	AT
2432	2436			FRACTURE	275	N. VERT	185		TV
2436	2439			FRACTURE	285	VERTICAL	195	MINERALIZED	TV

TABLE 10. SUMMARY OF INFORMATION FROM LITHOLOGIC (L), TELEVISION (TV), ACOUSTIC TELEVIEWER (AT), CALIPER (C), AND TEMPERATURE (TEMP) LOGS FOR BOREHOLE UE-25C #1 --Continued

DEPTH BLW CASING (FEET)		GEOLOGIC UNIT	LITHOLOGIC ZONE	FEATURE	DIP AZIMUTH	DIP ANGLE	STRIKE AZIMUTH	REMARKS	LOG
TOP	BOTTOM								
2449	2450	BULLFROG	MW-DW	FRACTURE	260	N. VERT	170		TV
2450	2453			FRACTURE	265	N. VERT	175	MINERALIZED	TV
2454	2457			FRACTURE	258	N. VERT	168	PARTLY MINERALIZED	TV
2463	2476			FRACTURE	190	VERTICAL	100		TV
2466	2466			FRACTURE	145	VERTICAL	55		TV
2469	2471			FRACTURE	245	VERTICAL	155		TV
2476	2478			FRACTURE	185	VERTICAL	95		TV
2479	2483			FRACTURE	287	78	197	OPEN	AT
2479	2484			FRACTURE	293	80	203	OPEN	AT
2480			PW-NW	CONTACT					L
2482	2486			FRACTURE	291	79	201	OPEN	AT
2489	2490			FRACTURE	200	N. VERT	110		TV
2498	2504			FRACTURE	282	81	192	OPEN	AT
2498	2499			FRACTURE	220	VERTICAL	130		TV
2502	2508			FRACTURE	278	81	188	OPEN	AT
2516	2518			FRACTURE	235	N. VERT	145		TV
2525	2527			FRACTURE	215	STEEP	125		TV
2526	2529			FRACTURE	264	68	174		AT
2534	2535			FRACTURE	220	N. VERT	130	OPEN	TV
2535	2535			FRACTURE	85	N. VERT	355	OPEN	TV
2537	2541			FRACTURE	270	VERTICAL	180	OPEN	TV
2542	2543			FRACTURE	240	N. VERT	150		TV
2543	2544			FRACTURE	260	N. VERT	170		TV
2544	2545			FRACTURE	215	N. VERT	125		TV
2547	2548			FRACTURE	200	STEEP	110	TERMINATED BY SSW-STRIKING FRACTURE	TV
2548	2550			FRACTURE	282	67	192		AT
2549	2550			FRACTURE	220	STEEP	130		TV

TABLE 10. SUMMARY OF INFORMATION FROM LITHOLOGIC (L), TELEVISION (TV), ACOUSTIC TELEVIEWER (AT), CALIPER (C), AND TEMPERATURE (TEMP) LOGS FOR BOREHOLE UE-25C #1 --Continued

DEPTH BLW CASING (FEET)		GEOLOGIC UNIT	LITHOLOGIC ZONE	FEATURE	DIP AZIMUTH	DIP ANGLE	STRIKE AZIMUTH	REMARKS	LOG
TOP	BOTTOM								
2554	2556	BULLFROG	PW-NW	FRACTURE	260	N. VERT	170		TV
2558	2560			FRACTURE	277	70	187	OPEN, CAVING	AT
2565	2566			FRACTURE	205	N. VERT	115		TV
2568	2569			FRACTURE	135	STEEP	45		TV
2572	2572			FRACTURE	295	SHALLOW	205	OPEN; HOLE ENLARGED BY FRACTURES 2572-2573	TV
2572	2572			FRACTURE	80	SHALLOW	350	OPEN	TV
2572	2573			FRACTURE	165	VERTICAL	75	OPEN	TV
2572	2573			FRACTURE	195	VERTICAL	105	OPEN	TV
2574	2575			FRACTURE	150	SHALLOW	60	OPEN; HOLE ENLARGED BY FRACTURES 2574-2575	TV
2574	2575			FRACTURE	150	SHALLOW	60	OPEN	TV
2574	2575			FRACTURE	90	N. VERT	0		TV
2574	2575			FRACTURE	83	32	353	OPEN	AT
2577	2578			FRACTURE	105	SHALLOW	15	OPEN; HOLE ENLARGED BY FRACTURES 2577-2579	TV
2578	2578			FRACTURE	110	SHALLOW	20	OPEN	TV
2578	2579			FRACTURE	110	SHALLOW	20	OPEN	TV
2588	2589			FRACTURE	122	SHALLOW	32		TV
2590	2591			FRACTURE	85	SHALLOW	355		TV
2590	2591			FRACTURE	85	SHALLOW	355		TV
2594	2595			FRACTURE	110	SHALLOW	20		TV
2603	2604			FRACTURE	105	SHALLOW	15		TV
2656	2657			FRACTURE	80	SHALLOW	350		TV
2677	2679			FRACTURE	110	STEEP	20		TV
2682	2684			FRACTURE	108	STEEP	18		TV
2694	2695			FRACTURE	108	SHALLOW	18		TV
2695			BEDDED	CONTACT					L
2698	2699			FRACTURE	95	SHALLOW	5		TV
2703	2704			FRACTURE	110	SHALLOW	20		TV

TABLE 10. SUMMARY OF INFORMATION FROM LITHOLOGIC (L), TELEVISION (TV), ACOUSTIC TELEVIEWER (AT), CALIPER (C), AND TEMPERATURE (TEMP) LOGS FOR BOREHOLE UE-25C #1 --Continued

DEPTH BLW CASING (FEET)		GEOLOGIC UNIT	LITHOLOGIC ZONE	FEATURE	DIP AZIMUTH	DIP ANGLE	STRIKE AZIMUTH	REMARKS	LOG
TOP	BOTTOM								
2708	2709	BULLFROG	BEDDED	FRACTURE	105	SHALLOW	15		TV
2715	2715			FRACTURE	110	SHALLOW	20		TV
2716		TRAM	UPPER (NW-PW)	CONTACT					TV
2718	2718			FRACTURE	285	N. VERT	195	MINERALIZED	L
2729	2729			FRACTURE	325	N. VERT	235		TV
2730	2731			FRACTURE	105	SHALLOW	15		TV
2730	2731			FRACTURE	300	VERTICAL	210		TV
2731	2733			FRACTURE	127	56	37		TV
2731	2734			FRACTURE	297	68	207		AT
2732	2733			FRACTURE	285	N. VERT	195		AT
2733	2733			FRACTURE	210	VERTICAL	120		TV
2734	2734			FRACTURE	205	STEEP	115	MINERALIZED	TV
2735	2738			FRACTURE	304	66	214		AT
2742	2743			FRACTURE	85	SHALLOW	355		TV
2742	2742			FRACTURE	5	SHALLOW	275	OPEN	TV
2742	2743			FRACTURE	195	N. VERT	105	OPEN	TV
2743	2750			FRACTURE	355	VERTICAL	265	CAVERNOUS; HOLE FOLLOWS FRACTURE	TV
2750	2752			FRACTURE	300	55	210		AT
2759	2760			FRACTURE	290	N. VERT	200	OPEN	TV
2761	2761			FRACTURE	305	SHALLOW	215	OPEN	TV
2762	2763			FRACTURE	305	SHALLOW	215		TV
2762	2764			FRACTURE	280	64	190		AT
2763	2764			FRACTURE	205	STEEP	115	CAVERNOUS UPTOE	TV
2763	2764			FRACTURE	35	SHALLOW	305		TV
2764	2765			FRACTURE	305	64	215		AT
2765	2766			FRACTURE	0	SHALLOW	270		TV
2766	2767			FRACTURE	293	62	203		AT

TABLE 10. SUMMARY OF INFORMATION FROM LITHOLOGIC (L), TELEVISION (TV), ACOUSTIC TELEVIEWER (AT), CALIPER (C), AND TEMPERATURE (TEMP) LOGS FOR BOREHOLE UE-25C #1 --Continued

DEPTH BLW CASING (FEET)		GEOLOGIC UNIT	LITHOLOGIC ZONE	FEATURE	DIP AZIMUTH	DIP ANGLE	STRIKE AZIMUTH	REMARKS	LOG
TOP	BOTTOM								
2766	2768	TRAM	UPPER (NW-PW)	FRACTURE	299	64	209		AT
2767	2768			FRACTURE	303	64	213		AT
2768	2768			FRACTURE	330	STEEP	240		TV
2768	2768			FRACTURE	335	STEEP	245		TV
2768	2770			FRACTURE	279	61	189		AT
2770	2771			FRACTURE	266	59	176		AT
2770	2772			FRACTURE	278	66	188		AT
2772	2773			FRACTURE	289	58	199		AT
2773	2774			FRACTURE	284	57	194		AT
2774	2775			FRACTURE	291	53	201		AT
2775			TUFF BRECCIA	CONTACT					L
2776	2776			FRACTURE	260	SHALLOW	170		TV
2777	2777			FRACTURE	305	STEEP	215	OPEN; HOLE ENLARGED BY FRACTURES 2777-2779	TV
2777	2779			FRACTURE	300	STEEP	210		TV
2777	2779			FRACTURE	260	STEEP	170		TV
2780	2782			FRACTURE	281	63	191		AT
2782	2783			FRACTURE	287	51	197		AT
2784	2784			FRACTURE	50	SHALLOW	320		TV
2784	2786			FRACTURE	293	64	203		AT
2784	2786			FRACTURE	266	48	176		AT
2784	2784			FRACTURE	240	STEEP	150		TV
2787	2789			FRACTURE	275	65	185	PAINTBRUSH CANYON FAULT ON LITH LOG	AT/L
2788	2790			FRACTURE	282	64	192		AT
2790	2791			FRACTURE	110	N. VERT	20		TV
2791	2791			FRACTURE	345	N. VERT	255		TV
2791	2791			FRACTURE	30	N. VERT	300		TV
2794	2795			FRACTURE	195	N. VERT	105		TV
									TV

TABLE 10. SUMMARY OF INFORMATION FROM LITHOLOGIC (L), TELEVISION (TV), ACOUSTIC TELEVIEWER (AT), CALIPER (C), AND TEMPERATURE (TEMP) LOGS FOR BOREHOLE UE-25C #1 --Continued

DEPTH BLW CASING (FEET)		GEOLOGIC UNIT	LITHOLOGIC ZONE	FEATURE	DIP AZIMUTH	DIP ANGLE	STRIKE AZIMUTH	REMARKS	LOG
TOP	BOTTOM								
2794	2794	TRAM	TUFF BRECCIA	FRACTURE	200	N. VERT	110		TV
2794	2795			FRACTURE	200	N. VERT	110		TV
2795	2795			FRACTURE	345	VERTICAL	255		TV
2795	2795			FRACTURE	155	N. VERT	65		TV
2796	2796			FRACTURE	205	N. VERT	115		TV
2796	2797			FRACTURE	320	N. VERT	230		TV
2796	2802			FRACTURE	116	82	26	OPEN	AT
2802	2802			FRACTURE	175	N. VERT	85		TV
2803	2804			FRACTURE	200	N. VERT	110		TV
2804	2804			FRACTURE	200	N. VERT	110		TV
2814	2816			FRACTURE	220	N. VERT	130		TV
2816	2820			FRACTURE	255	76	165		AT
2817	2818			FRACTURE	230	STEEP	140	OPEN	TV
2820	2822			FRACTURE	270	64	180		AT
2822	2822			FRACTURE	265	STEEP	175		TV
2822	2828			FRACTURE	225	VERTICAL	135	SPLAYED	TV
2828	2830			FRACTURE	198	STEEP	108	TRUNCATES SE-STRIKING FRACTURE ABOVE IT	TV
2832	2833			FRACTURE	65	N. VERT	335	CAVING ALONG FRACTURE FACE	TV
2836	2837			FRACTURE	50	N. VERT	320		TV
2836	2838			FRACTURE	70	N. VERT	340		TV
2837	2838			FRACTURE	10	STEEP	280	MINERALIZED	TV
2838	2839			FRACTURE	164	56	74		AT
2840	2840			FRACTURE	285	N. VERT	195		TV
2843	2844			FRACTURE	35	SHALLOW	305	MINERALIZED	TV
2843	2844			FRACTURE	20	SHALLOW	290	MINERALIZED	TV
2845	2845			FRACTURE	15	SHALLOW	285	MINERALIZED	TV
2845	2847			FRACTURE	20	STEEP	290	MINERALIZED	TV
2850	2851			FRACTURE	15	STEEP	285	MINERALIZED	TV

TABLE 10. SUMMARY OF INFORMATION FROM LITHOLOGIC (L), TELEVISION (TV), ACOUSTIC TELEVIEWER (AT), CALIPER (C), AND TEMPERATURE (TEMP) LOGS FOR BOREHOLE UE-25C #1 --Continued

DEPTH BLW CASING (FEET)		GEOLOGIC UNIT	LITHOLOGIC ZONE	FEATURE	DIP AZIMUTH	DIP ANGLE	STRIKE AZIMUTH	REMARKS	LOG
TOP	BOTTOM								
2854	2857	TRAM	TUFF BRECCIA	FRACTURE	80	N. VERT	350		TV
2854	2857			FRACTURE	75	N. VERT	345		TV
2856	2856			FRACTURE	35	SHALLOW	305	MINERALIZED	TV
2857	2858			FRACTURE	255	N. VERT	165		TV
2858	2859			FRACTURE	65	SHALLOW	335	PARTLY MINERALIZED	TV
2859	2860			FRACTURE	265	N. VERT	175		TV
2860	2860			FRACTURE	65	SHALLOW	335	MINERALIZED	TV
2860	2863			FRACTURE	60	N. VERT	330	OPEN	TV
2863	2866			FRACTURE	121	71	31		AT
2865	2867			FRACTURE	270	STEEP	160		TV
2866	2868			FRACTURE	115	N. VERT	25	MINERALIZED	TV
2867	2870			FRACTURE	279	68	189		AT
2868	2868			FRACTURE	125	N. VERT	35	MINERALIZED	TV
2868	2870			FRACTURE	70	STEEP	340		TV
2870	2870			FRACTURE	5	SHALLOW	275	MINERALIZED	TV
2870	2872			FRACTURE	55	SHALLOW	325		AT
2872	2873			FRACTURE	119	64	29		TV
2872	2872			FRACTURE	270	VERTICAL	180		TV
2872	2872			FRACTURE	95	VERTICAL	5		TV
2872	2876			FRACTURE	65	N. VERT	335		TV
2873	2873			FRACTURE	180	N. VERT	90		TV
2874	2874			FRACTURE	265	VERTICAL	175		TV
2875	2878			FAULT	320	VERTICAL	230	OFFSETS SE-STRIKING FRACTURE AT 2877	TV
2875	2875			FRACTURE	290	VERTICAL	200		TV
2876	2876			FRACTURE	180	SHALLOW	90	PARTLY MINERALIZED	TV
2876	2876			FRACTURE	250	N. VERT	160		TV
2877	2877			FRACTURE	0	SHALLOW	270	PARTLY MINERALIZED	TV
2877	2880			FRACTURE	210	N. VERT	120		TV
2878	2879			FRACTURE	95	N. VERT	5		TV
2879	2879			FRACTURE	305	VERTICAL	215		TV

TABLE 10. SUMMARY OF INFORMATION FROM LITHOLOGIC (L), TELEVISION (TV), ACOUSTIC TELEVIEWER (AT), CALIPER (C), AND TEMPERATURE (TEMP) LOGS FOR BOREHOLE UE-25C #1 --Continued

DEPTH BLW CASING (FEET)		GEOLOGIC UNIT	LITHOLOGIC ZONE	FEATURE	DIP AZI-MUTH	DIP ANGLE	STRIKE AZI-MUTH	REMARKS	LOG
TOP	BOT-TOM								
2879	2880	TRAM	TUFF BRECCIA	FRACTURE	260	N. VERT	170	PARTLY MINERALIZED	TV
2879	2880			FRACTURE	350	SHALLOW	260	MINERALIZED	TV
2880	2881			FRACTURE	50	STEEP	320		TV
2881	2882			FRACTURE	310	SHALLOW	220	MINERALIZED	TV
2881	2884			FRACTURE	120	72	30		TV
2881	2881			FRACTURE	110	SHALLOW	20	MINERALIZED	TV
2882	2884			FRACTURE	35	STEEP	305		TV
2884	2884			FRACTURE	135	N. VERT	45		TV
2884	2884			FRACTURE	210	STEEP	120		TV
2886	2886			FRACTURE	35	SHALLOW	305	PARTLY MINERALIZED	TV
2888	2889			FRACTURE	50	SHALLOW	320	PARTLY MINERALIZED	TV
2889	2889			FRACTURE	40	SHALLOW	310	MINERALIZED	TV
2889	2890			FRACTURE	285	SHALLOW	195	MINERALIZED	TV
2890	2891			FRACTURE	25	SHALLOW	295	MINERALIZED	TV
2890	2893			FRACTURE	175	N. VERT	85		TV
2892	2892			FRACTURE	300	N. VERT	210		TV
2893	2893			FRACTURE	280	SHALLOW	190		TV
2893	2893			FRACTURE	260	N. VERT	170		TV
2893	2896			FRACTURE	290	74	200		AT
2894	2894			FRACTURE	0	SHALLOW	270	MINERALIZED	TV
2899	2900			FRACTURE	25	N. VERT	295	CAVING ALONG FRACTURE FACE	TV
2901	2901			FRACTURE	255	N. VERT	165		TV
2901	2909			FRACTURE	155	VERTICAL	65		TV
2902	2902			FRACTURE	85	N. VERT	355		TV
2908	2908			FRACTURE	130	N. VERT	40		TV
2911	2912			FRACTURE	220	N. VERT	130		TV
2912	2912			FRACTURE	225	VERTICAL	135		TV
2913	2913			FRACTURE	105	N. VERT	15	MINERALIZED	TV
2914	2915			FRACTURE	245	N. VERT	155		TV

TABLE 10. SUMMARY OF INFORMATION FROM LITHOLOGIC (L), TELEVISION (TV), ACOUSTIC TELEVIEWER (AT), CALIPER (C), AND TEMPERATURE (TEMP) LOGS FOR BOREHOLE UE-25C #1 --Continued

DEPTH BLW CASING (FEET)		GEOLOGIC UNIT	LITHOLOGIC ZONE	FEATURE	DIP AZIMUTH	DIP ANGLE	STRIKE AZIMUTH	REMARKS	LOG
TOP	BOTTOM								
2921	2921	TRAM	TUFF BRECCIA	FRACTURE	55	VERTICAL	325		TV
2921	2922			FRACTURE	15	N. VERT	285		TV
2922	2923			FRACTURE	265	STEEP	175		TV
2923	2924			FRACTURE	260	STEEP	170		TV
2924	2924			FRACTURE	80	N. VERT	350		TV
2924	2925			FRACTURE	260	STEEP	170		TV
2925	2925			FRACTURE	60	STEEP	330		TV
2925	2927			FRACTURE	60	STEEP	330		TV
2926	2926			FRACTURE	50	STEEP	320		TV
2926	2926			FRACTURE	90	N. VERT	0		TV
2929	2930			FRACTURE	115	N. VERT	25		TV
2930	2930			FRACTURE	105	N. VERT	15		TV
2930	2931			FRACTURE	310	SHALLOW	220		TV
2933	2933			FRACTURE	280	N. VERT	190		TV
2935	2935			FRACTURE	70	SHALLOW	340	OPEN	TV
2935	2936			FRACTURE	130	N. VERT	40		TV
2936	2937			FRACTURE	185	N. VERT	95		TV
2937	2937			FRACTURE	65	N. VERT	335		TV
2940	2940			FRACTURE	305	N. VERT	215		TV
2941	2941			FRACTURE	250	N. VERT	160		TV
2954	2955			FRACTURE	285	N. VERT	195		TV
2962				BOTTOM				HOLE CAVED TO ORIGINAL TD AT 3000	TV

TABLE 11. SUMMARY OF INFORMATION FROM LITHOLOGIC (L), TELEVISION (TV), ACOUSTIC TELEVIEWER (AT), CALIPER (C), AND TEMPERATURE (TEMP) LOGS FOR BOREHOLE UE-25C #2

[Abbreviations for tables 10, 11, and 12: CSG, casing; NW, nonwelded; NW-PW, nonwelded to partially welded; MW, moderately welded; MW-DW, moderately to densely welded; PW-NW, partially welded to nonwelded; PW, partially welded; N.VERT, near vertical; LITH, lithologic; TD, total depth; N, north, S, south; SW, southwest, SE, southeast; SSW, south-southwest]

DEPTH BLW CASING (FEET)		GEOLOGIC UNIT	LITHOLOGIC ZONE	FEATURE	DIP AZIMUTH	DIP ANGLE	STRIKE AZIMUTH	REMARKS	LOG
TOP	BOTTOM								
1315		TOPOPAH SPRING	BASAL	WATER TABLE					TV
1316		CALICO HILLS	NW	CONTACT					L
1360				CSG BOTTOM					TV
1360	1365			CONCRETE				ROUGH; SPALLED; HOLE ABRUPTLY WIDENS BELOW	TV/C
1395	1396			FRACTURE	235	35	145	VISIBILITY IMPAIRED 1365-1515 BY SKEWED HOLE	AT
1461	1469			FRACTURE	65	81	335		AT
1461	1470			FRACTURE	65	82	335		AT
1465	1472			FRACTURE	95	79	5		AT
1467	1477			FRACTURE	75	82	345		AT
1510	1511			FRACTURE	255	>35	165		TV
1514	1534			FRACTURE	65	86	335	OPEN	AT/TV
1515	1515			LEDGE				HOLE DIAMETER REDUCED	TV
1518	1539			FRACTURE	70	87	340	OPEN	AT/TV
1550	1555			FRACTURE	90	>78	0		TV
1552	1552			FRACTURE	120	VERTICAL	30		TV
1570			BEDDED	CONTACT					L
1600	1600			FRACTURE	120	32	30		TV
1624	1625			FRACTURE	120	43	30		TV
1624	1625			FRACTURE	120	27	30		TV
1626	1626			FRACTURE	120	27	30		TV
1626	1626			FRACTURE	115	43	25		TV
1627	1627			FRACTURE	105	36	15		TV
1627	1628			FRACTURE	110	36	20		TV
1628	1629			FRACTURE	120	45	30	MINERALIZED	TV
1629	1630			FRACTURE	75	35	345		AT
1630	1631			FRACTURE	100	48	10	PARTLY MINERALIZED	TV

TABLE 11. SUMMARY OF INFORMATION FROM LITHOLOGIC (L), TELEVISION (TV), ACOUSTIC TELEVIEWER (AT), CALIPER (C), AND TEMPERATURE (TEMP) LOGS FOR BOREHOLE UE-25C #2 --Continued

DEPTH BLW CASING (FEET)		GEOLOGIC UNIT	LITHOLOGIC ZONE	FEATURE	DIP AZIMUTH	DIP ANGLE	STRIKE AZIMUTH	REMARKS	LOG
TOP	BOTTOM								
1631	1632	CALICO HILLS	BEDDED	FRACTURE	110	48	20	MINERALIZED	TV
1632	1633			FRACTURE	110	40	20	MINERALIZED	TV
1633	1634			FRACTURE	105	42	15		AT
1644	1645			FRACTURE	110	40	20	OPEN	TV
1645	1645			FRACTURE	145	VERTICAL	55		TV
1645	1650			FRACTURE	75	78	345	OPEN AT INTERSECTION WITH SE-STRIKING FRACTURE	TV
1646	1650			FRACTURE	225	74	135	OPEN AT INTERSECTION WITH N-STRIKING FRACTURE	TV
1650	1653			FRACTURE	255	68	165		AT
1652	1652			FRACTURE	115	27	25	MINERALIZED	TV
1652	1653			FRACTURE	15	VERTICAL	285		TV
1653	1653			FRACTURE	225	VERTICAL	135		TV
1653	1653			FRACTURE	320	VERTICAL	230		TV
1653	1654			FRACTURE	270	27	180	ROCK CHANGES COLOR BELOW FRACTURE	TV
1654	1654			FRACTURE	20	27	290	MINERALIZED	TV
1655	1655			FRACTURE	75	22	345	MINERALIZED	TV
1655	1656			FRACTURE	155	STEEP	65	MINERALIZED	TV
1655	1656			FRACTURE	115	26	25	MINERALIZED	TV
1655	1656			FRACTURE	115	26	25	MINERALIZED	TV
1656	1656			FRACTURE	120	26	30	MINERALIZED	TV
1656	1657			FRACTURE	120	26	30	MINERALIZED	TV
1658	1658			FRACTURE	120	30	30	MINERALIZED	TV
1658	1659			FRACTURE	120	30	30	MINERALIZED	TV
1659	1659			FRACTURE	125	16	35	MINERALIZED	TV
1659	1660			FRACTURE	125	16	35	MINERALIZED	TV
1660	1660			FRACTURE	125	21	35	MINERALIZED	TV
1661	1662			FRACTURE	130	34	40	MINERALIZED	TV
1663	1664			FRACTURE	130	26	40	MINERALIZED	TV
1664	1665			FRACTURE	315	22	225		TV

TABLE 11. SUMMARY OF INFORMATION FROM LITHOLOGIC (L), TELEVISION (TV), ACOUSTIC TELEVIEWER (AT), CALIPER (C), AND TEMPERATURE (TEMP) LOGS FOR BOREHOLE UE-25C #2 --Continued

DEPTH BLW CASING (FEET)		GEOLOGIC UNIT	LITHOLOGIC ZONE	FEATURE	DIP AZIMUTH	DIP ANGLE	STRIKE AZIMUTH	REMARKS	LOG
TOP	BOTTOM								
1665	1665	CALICO HILLS	BEDDED	FRACTURE	130	11	40		TV
1665	1666			FRACTURE	110	N. VERT	20		TV
1666	1666			FRACTURE	135	39	45		TV
1670	1670			FRACTURE	190	VERTICAL	100		TV
1671	1672			FRACTURE	60	47	330	MINERALIZED	TV
1672	1673	PROW PASS	NW-PW	CONTACT				OPEN PARTING; DEAD LIZARD ON TOP OF PROW PASS	TV/L
1676	1676			FRACTURE	115	16	25		TV
1676	1677			FRACTURE	280	N. VERT	190	TERMINATES AT SE-STRIKING FRACTURE	TV
1676	1678			FRACTURE	202	46	112		TV
1677	1678			FRACTURE	120	STEEP	30		TV
1679	1679			FRACTURE	255	SHALLOW	165		TV
1681	1683			FRACTURE	270	>64	180		TV
1704	1710			FRACTURE	180	79	90	OPEN TOWARD DOWNTOE	TV
1709	1710			FRACTURE	10	VERTICAL	280		TV
1787	1788			FRACTURE	300	VERTICAL	210		TV
1789	1789			FRACTURE	80	VERTICAL	350	MINERALIZED	TV
1790	1790			FRACTURE	35	VERTICAL	305		TV
1798	1800			FRACTURE	270	65	180	MINERALIZED	TV
1801	1803			FRACTURE	200	VERTICAL	110	MINERALIZED	TV
1802	1803			CORRUGATED				HORIZONTAL WASHOUTS	TV
1810	1811		MW	CONTACT				TEXTURE BECOMES SMOOTHER	TV/L
1812	1817			FRACTURE	262	80	172	OPEN DOWNTOE	TV
1812	1818			FRACTURE	262	81	172	OPEN DOWNTOE	TV
1812	1815			FRACTURE	315	VERTICAL	225	PARTLY MINERALIZED	TV
1818	1820			FRACTURE	280	69	190		TV

TABLE 11. SUMMARY OF INFORMATION FROM LITHOLOGIC (L), TELEVISION (TV), ACOUSTIC TELEVIEWER (AT), CALIPER (C), AND TEMPERATURE (TEMP) LOGS FOR BOREHOLE UE-25C #2 --Continued

DEPTH BLW CASING (FEET)		GEOLOGIC UNIT	LITHOLOGIC ZONE	FEATURE	DIP AZIMUTH	DIP ANGLE	STRIKE AZIMUTH	REMARKS	LOG
TOP	BOTTOM								
1822	1826	PROW PASS	MW	FRACTURE	270	77	180		TV
1823	1824			FRACTURE	265	N. VERT	175	MINERALIZED	TV
1826	1830			FRACTURE	275	78	185		TV
1834	1836			FRACTURE	275	VERTICAL	185		TV
1836	1839			FRACTURE	263	72	173		TV
1840			PW-NW	CONTACT					L
1846	1849			FRACTURE	260	75	170		TV
1848	1851			FRACTURE	248	74	158		TV
1848	1848			FRACTURE	150	18	60		TV
1848	1849			FRACTURE	5	VERTICAL	275	MINERALIZED	TV
1849	1853			FRACTURE	270	74	180		AT
1851	1854			FRACTURE	260	75	170		AT
1857	1861			FRACTURE	245	77	155		TV
1866	1870			FRACTURE	215	77	125		TV
1881	1883			FRACTURE	100	>57	10		TV
1958	1959			FRACTURE	220	38	130		TV
1960	1961			WASHOUT?				HOLE OUT OF ROUND BUT NO FRACTURES VISIBLE	TV
1995	1995			FRACTURE	260	52	170		TV
2021	2022			FRACTURE	270	STEEP	180		TV
2022	2023			FRACTURE	305	N. VERT	215		TV
2025	2027			FRACTURE	305	74	215		AT
2032	2033			FRACTURE	220	28	130		TV
2035	2037			FRACTURE	285	VERTICAL	195		TV
2110			BEDDED	CONTACT				VISIBILITY IMPAIRED 2055-2122 BY SKEWED HOLE	L
2131	2132			FRACTURE	240	28	150		TV
2132	2132			FRACTURE	242	32	152	MINERALIZED	TV
2132	2133			FRACTURE	245	36	155		TV

TABLE 11. SUMMARY OF INFORMATION FROM LITHOLOGIC (L), TELEVISION (TV), ACOUSTIC TELEVIEWER (AT), CALIPER (C), AND TEMPERATURE (TEMP) LOGS FOR BOREHOLE UE-25C #2 --Continued

DEPTH BLW CASING (FEET)		GEOLOGIC UNIT	LITHOLOGIC ZONE	FEATURE	DIP AZIMUTH	DIP ANGLE	STRIKE AZIMUTH	REMARKS	LOG
TOP	BOTTOM								
2134	2134	PROW PASS	BEDDED	FRACTURE	245	36	155	MINERALIZED	TV
2134	2135			FRACTURE	165	45	75	MINERALIZED	TV
2138	2139	BULLFROG	NW-PW	CONTACT				OPEN PARTING	TV/L
2173	2174			FRACTURE	285	VERTICAL	195		TV
2194	2199			FRACTURE	270	VERTICAL	180	MINERALIZED	TV
2240			MW-DW	CONTACT					L
2252	2256			FRACTURE	280	77	190		TV
2258	2263			FRACTURE	270	80	180	OPEN	TV
2262	2267			FRACTURE	255	79	165		AT
2297	2298			FRACTURE	300	N. VERT	210	MINERALIZED	TV
2298	2298			FRACTURE	275	N. VERT	185		TV
2298	2300			FRACTURE	275	59	185		TV
2299	2300			FRACTURE	275	59	185		TV
2299	2302			FRACTURE	225	75	135		TV
2300	2303			FRACTURE	225	74	135		TV
2300	2303			FRACTURE	225	71	135		TV
2300	2301			FRACTURE	195	N. VERT	105		TV
2302	2304			FRACTURE	230	70	140		TV
2304	2305			FRACTURE	275	N. VERT	185		TV
2306	2309			FRACTURE	275	75	185		AT
2314	2315			FRACTURE	220	N. VERT	130	OPEN	TV
2330	2332			FRACTURE	270	N. VERT	180		TV
2335	2339			FRACTURE	285	77	195	MINERALIZED; INTERSECTING FRACTURES 2335-2342	AT
2336	2337			FRACTURE	280	N. VERT	190		TV
2338	2340			FRACTURE	180	VERTICAL	90	MINERALIZED	TV
2340	2340			FRACTURE	270	N. VERT	180		TV

TABLE 11. SUMMARY OF INFORMATION FROM LITHOLOGIC (L), TELEVISION (TV), ACOUSTIC TELEVIEWER (AT), CALIPER (C), AND TEMPERATURE (TEMP) LOGS FOR BOREHOLE UE-25C #2 --Continued

DEPTH BLW CASING (FEET)		GEOLOGIC UNIT	LITHOLOGIC ZONE	FEATURE	DIP AZIMUTH	DIP ANGLE	STRIKE AZIMUTH	REMARKS	LOG
TOP	BOTTOM								
2340	2340	BULLFROG	MW-DW	FRACTURE	300	N. VERT	210		TV
2340	2341			FRACTURE	275	N. VERT	185		TV
2341	2342			FRACTURE	300	N. VERT	210		TV
2342	2345			FRACTURE	95	77	5		AT
2344	2345			FRACTURE	250	VERTICAL	160		TV
2345	2346			FRACTURE	275	VERTICAL	185		TV
2345	2347			FRACTURE	260	VERTICAL	170		TV
2346	2348			FRACTURE	272	51	182		TV
2347	2349			FRACTURE	300	STEEP	210		TV
2348	2349			FRACTURE	300	STEEP	210		TV
2348	2348			FRACTURE	230	N. VERT	140		TV
2348	2350			FRACTURE	300	STEEP	210		TV
2348	2352			FRACTURE	295	69	205		TV
2350	2350			FRACTURE	210	N. VERT	120		TV
2350	2352			FRACTURE	350	N. VERT	260		TV
2350	2358			FRACTURE	265	84	175		AT
2351	2355			FRACTURE	270	77	180		TV
2352	2353			FRACTURE	205	N. VERT	115	MINERALIZED	TV
2352	2352			FRACTURE	155	VERTICAL	65		TV
2352	2355			FRACTURE	255	69	165		AT
2353	2356			FRACTURE	265	69	175	MINERALIZED	AT/TV
2356	2359			FRACTURE	260	77	170	MINERALIZED	AT/TV
2356	2358			FRACTURE	270	71	180	MINERALIZED	TV
2357	2360			FRACTURE	255	73	165	MINERALIZED	TV
2357	2361			FRACTURE	278	75	188	MINERALIZED	TV
2358	2358			FRACTURE	260	N. VERT	170		TV
2358	2361			FRACTURE	295	72	205	PARTLY MINERALIZED	TV
2359	2364			FRACTURE	275	79	185	PARTLY MINERALIZED	TV
2361	2361			FRACTURE	295	STEEP	205		TV
2361	2362			FRACTURE	295	STEEP	205		TV
2361	2363			FRACTURE	260	74	170		AT

TABLE 11. SUMMARY OF INFORMATION FROM LITHOLOGIC (L), TELEVISION (TV), ACOUSTIC TELEVIEWER (AT), CALIPER (C), AND TEMPERATURE (TEMP) LOGS FOR BOREHOLE UE-25C #2 --Continued

DEPTH BLW CASING (FEET)		GEOLOGIC UNIT	LITHOLOGIC ZONE	FEATURE	DIP AZI-MUTH	DIP ANGLE	STRIKE AZI-MUTH	REMARKS	LOG
TOP	BOT-TOM								
2362	2365	BULLFROG	MW-DW	FRACTURE	278	71	188		TV
2363	2366			FRACTURE	270	74	180		TV
2365	2367			FRACTURE	310	61	220		AT
2366	2366			FRACTURE	282	45	192		TV
2366	2369			FRACTURE	265	74	175		AT
2367	2371			FRACTURE	250	79	160	PARTLY MINERALIZED	AT/TV
2368	2368			FRACTURE	285	34	195	MINERALIZED	TV
2372	2375			FRACTURE	262	74	172	MINERALIZED	TV
2373	2376			FRACTURE	262	75	172	MINERALIZED	TV
2376	2379			FRACTURE	245	71	155		AT
2378	2378			FRACTURE	295	34	205	MINERALIZED	TV
2378	2380			FRACTURE	250	62	160	MINERALIZED	TV
2380	2383			FRACTURE	255	72	165	OPEN	TV
2381	2384			FRACTURE	250	66	160		TV
2382	2387			FRACTURE	275	77	185	CAVERNOUS INTERSECTION OF FRACTURES 2382-2390	TV
2382	2388			FRACTURE	70	80	340	OPEN	TV
2387	2390			FRACTURE	200	74	110	OPEN	TV
2388	2389			FRACTURE	255	STEEP	165		TV
2388	2390			FRACTURE	205	63	115		TV
2389	2395			FRACTURE	130	>81	40	OPEN	TV
2390	2391			FRACTURE	250	STEEP	160		TV
2390	2391			FRACTURE	210	STEEP	120	INTERSECTS S-STRIKING FRACTURE	TV
2390	2393			FRACTURE	270	71	180	MINERALIZED	TV
2391	2391			FRACTURE	250	STEEP	160		TV
2391	2394			FRACTURE	78	67	348		TV
2391	2392			FRACTURE	110	VERTICAL	20		TV
2392	2398			FRACTURE	272	80	182	OPEN	TV

TABLE 11. SUMMARY OF INFORMATION FROM LITHOLOGIC (L), TELEVISION (TV), ACOUSTIC TELEVIEWER (AT), CALIPER (C), AND TEMPERATURE (TEMP) LOGS FOR BOREHOLE UE-25C #2 --Continued

DEPTH BLW CASING (FEET)		GEOLOGIC UNIT	LITHOLOGIC ZONE	FEATURE	DIP AZI-MUTH	DIP ANGLE	STRIKE AZI-MUTH	REMARKS	LOG
TOP	BOT-TOM								
2394	2396	BULLFROG	MW-DW	FRACTURE	68	64	338	CAVERNOUS WHERE FRACTURES INTERSECT 2394-2397	TV
2395	2396			FRACTURE	215	STEEP	125		TV
2395	2396			FRACTURE	120	VERTICAL	30		TV
2396	2397			FRACTURE	130	VERTICAL	40		TV
2396	2396			FRACTURE	320	38	230		TV
2396	2397			FRACTURE	245	45	155		TV
2396	2397			FRACTURE	255	N. VERT	165		TV
2397	2399			FRACTURE	305	N. VERT	215	OPEN	TV
2398	2403			FRACTURE	270	79	180	OPEN	TV
2399	2404			FRACTURE	260	80	170		TV
2399	2405			FRACTURE	240	80	150		TV
2399	2401			FRACTURE	105	VERTICAL	15		TV
2402	2405			FRACTURE	240	71	150	OPEN UPTOE	TV
2404	2412			FRACTURE	265	83	175	OPEN	TV
2408	2408			FRACTURE	70	VERTICAL	340		TV
2408	2416			FRACTURE	260	82	170		AT
2410	2416			FRACTURE	68	81	338	OPEN, WITH CAVITIES	TV
2413	2413			FRACTURE	100	VERTICAL	10		TV
2416	2416			FRACTURE	280	N. VERT	190		TV
2416	2417			FRACTURE	295	STEEP	205		TV
2417	2418			FRACTURE	220	STEEP	130		TV
2417	2418			FRACTURE	280	STEEP	190		TV
2418	2419			FRACTURE	270	STEEP	180		TV
2420	2421			FRACTURE	275	51	165		AT
2420	2422			FRACTURE	295	49	205		AT
2422	2424			FRACTURE	295	64	205		AT
2424	2426			FRACTURE	190	N. VERT	100		TV
2425	2426			FRACTURE	285	STEEP	195		TV
2426	2427			FRACTURE	250	N. VERT	160		TV
2427	2428			FRACTURE	260	VERTICAL	170		TV

TABLE 11. SUMMARY OF INFORMATION FROM LITHOLOGIC (L), TELEVISION (TV), ACOUSTIC TELEVIEWER (AT), CALIPER (C), AND TEMPERATURE (TEMP) LOGS FOR BOREHOLE UE-25C #2 --Continued

DEPTH BLW CASING (FEET)		GEOLOGIC UNIT	LITHOLOGIC ZONE	FEATURE	DIP AZIMUTH	DIP ANGLE	STRIKE AZIMUTH	REMARKS	LOG
TOP	BOTTOM								
2429	2432	BULLFROG	MW-DW	FRACTURE	300	STEEP	210		TV
2429	2432			FRACTURE	270	72	180		AT
2430	2431			FRACTURE	280	24	190		TV
2431	2432			FRACTURE	315	STEEP	225		TV
2432	2432			FRACTURE	285	41	195		TV
2432	2433			FRACTURE	282	62	192		TV
2432	2433			FRACTURE	160	N. VERT	70		TV
2432	2435			FRACTURE	280	N. VERT	190		TV
2432	2434			FRACTURE	250	N. VERT	160	MINERALIZED	TV
2434	2435			FRACTURE	60	SHALLOW	330	MINERALIZED	TV
2434	2435			FRACTURE	245	VERTICAL	155	MINERALIZED	TV
2434	2435			FRACTURE	255	64	165		AT
2435	2437			FRACTURE	285	66	195		TV
2435	2437			FRACTURE	280	N. VERT	190		TV
2436	2438			FRACTURE	240	53	160		TV
2436	2438			FRACTURE	280	N. VERT	190		TV
2437	2437			FRACTURE	205	N. VERT	115		TV
2437	2441			FRACTURE	275	>75	185	ROCK BROKEN UP WHERE FRACTURES INTERSECT 2437-2444	TV
2439	2440			FRACTURE	60	71	330	OPEN	TV
2439	2440			FRACTURE	220	N. VERT	130		TV
2439	2442			FRACTURE	278	70	188	OPEN	TV
2441	2444			FRACTURE	240	72	150	OPEN	TV
2441	2443			FRACTURE	245	55	155	OPEN	TV
2444	2445			FRACTURE	110	52	20		TV
2445	2448			FRACTURE	285	72	195		TV
2446	2448			FRACTURE	265	60	175		TV
2449	2459			FRACTURE	300	85	210	OPEN	TV/AT
2449	2451			FRACTURE	310	N. VERT	220		TV

TABLE 11. SUMMARY OF INFORMATION FROM LITHOLOGIC (L), TELEVISION (TV), ACOUSTIC TELEVIEWER (AT), CALIPER (C), AND TEMPERATURE (TEMP) LOGS FOR BOREHOLE UE-25C #2 --Continued

DEPTH BLW CASING (FEET)		GEOLOGIC UNIT	LITHOLOGIC ZONE	FEATURE	DIP AZIMUTH	DIP ANGLE	STRIKE AZIMUTH	REMARKS	LOG
TOP	BOTTOM								
2451	2452	BULLFROG	MW-DW	FRACTURE	255	VERTICAL	165		TV
2452	2453			FRACTURE	265	VERTICAL	175		TV
2453	2462			FRACTURE	285	84	195		AT
2454	2455			FRACTURE	260	VERTICAL	170		TV
2456	2457			FRACTURE	260	VERTICAL	170		TV
2460		BULLFROG	PW-NW	CONTACT					L
2470	2473			FRACTURE	270	>74	180	MINERALIZED	TV
2473	2477			FRACTURE	268	78	178	OPEN	TV
2473	2479			FRACTURE	320	81	230	OPEN	TV
2475	2476			FRACTURE	110	24	20		TV
2478	2483			FRACTURE	300	80	210		AT
2489	2489			FRACTURE	240	VERTICAL	150		TV
2492	2492			FRACTURE	195	VERTICAL	105		TV
2492	2492			FRACTURE	160	N. VERT	70		TV
2495	2499			FRACTURE	250	>75	160		TV
2499	2500			FRACTURE	270	VERTICAL	180	MINERALIZED	TV
2500	2500			FRACTURE	260	VERTICAL	170	MINERALIZED	TV
2506	2506			FRACTURE	300	VERTICAL	210	MINERALIZED	TV
2510	2517			FRACTURE	258	82	168	MINERALIZED	TV
2530	2534			FRACTURE	UNK	VERTICAL	UNK		TV
2532	2533			FRACTURE	255	VERTICAL	165		TV
2539	2544			FRACTURE	280	>80	190		TV
2539	2548			FRACTURE	280	>84	190		TV
2548	2551			FRACTURE	92	68	2		TV
2555	2556			FRACTURE	270	VERTICAL	180	MINERALIZED	TV
2556	2560			FRACTURE	268	75	178	MINERALIZED	TV
2558	2559			FRACTURE	245	VERTICAL	155	MINERALIZED	TV
2561	2562			FRACTURE	145	46	55	MINERALIZED	TV
2561	2561			FRACTURE	135	17	45	MINERALIZED	TV

TABLE 11. SUMMARY OF INFORMATION FROM LITHOLOGIC (L), TELEVISION (TV), ACOUSTIC TELEVIEWER (AT), CALIPER (C), AND TEMPERATURE (TEMP) LOGS FOR BOREHOLE UE-25C #2 --Continued

DEPTH BLW CASING (FEET)		GEOLOGIC UNIT	LITHOLOGIC ZONE	FEATURE	DIP AZIMUTH	DIP ANGLE	STRIKE AZIMUTH	REMARKS	LOG
TOP	BOTTOM								
2561	2562	BULLFROG	PW-NW	FRACTURE	335	46	245	CAVITY FORMED BY INTERSECTING FRACTURES 2561-2562	TV
2662	2663			FRACTURE	8	36	278	MINERALIZED	TV
2663	2663			FRACTURE	5	32	275	MINERALIZED	TV
2664	2665			FRACTURE	275	43	185	MINERALIZED	TV
2675		BULLFROG	BEDDED	CONTACT					L
2686	2691			FRACTURE	245	>81	155	MINERALIZED	TV
2691	2694			FAULT	280	75-90	190	PARTLY MINERALIZED	TV/L
2704	2705			FRACTURE	255	32	165	MINERALIZED	TV
2706	2706			FRACTURE	115	STEEP	25	MINERALIZED	TV
2707	2708			FRACTURE	325	VERTICAL	235		TV
2708	2709			FRACTURE	265	STEEP	175	MINERALIZED	TV
2708	2708			FRACTURE	265	VERTICAL	175		TV
2709	2712			FRACTURE	265	70	175	OPEN; HOLE ENLARGED BY FRACTURES 2709-2724	TV/C
2709	2719			FRACTURE	60	84	330	OPEN	TV
2710	2710			FRACTURE	335	STEEP	245		TV
2710	2710			FRACTURE	210	STEEP	120		TV
2710	2713			FRACTURE	260	70	170	OPEN	TV
2712	2713			FRACTURE	215	STEEP	125		TV
2712	2713			FRACTURE	325	STEEP	235	OPEN	TV
2713	2719			FRACTURE	260	78	170	OPEN	TV/C
2714	2715			FRACTURE	150	N. VERT	60		TV
2717	2717			FRACTURE	25	VERTICAL	295		TV
2717	2718			FRACTURE	205	N. VERT	115	OPEN	TV
2717	2723			FRACTURE	250	77	160	OPEN	TV
2718	2718			FRACTURE	210	STEEP	120	OPEN	TV
2718	2719			FRACTURE	0	VERTICAL	270		TV

TABLE 11. SUMMARY OF INFORMATION FROM LITHOLOGIC (L), TELEVISION (TV), ACOUSTIC TELEVIEWER (AT), CALIPER (C), AND TEMPERATURE (TEMP) LOGS FOR BOREHOLE UE-25C #2 --Continued

DEPTH BLW CASING (FEET)		GEOLOGIC UNIT	LITHOLOGIC ZONE	FEATURE	DIP AZI-MUTH	DIP ANGLE	STRIKE AZI-MUTH	REMARKS	LOG
TOP	BOT-TOM								
2718	2720	BULLFROG	BEDDED	FRACTURE	330	VERTICAL	240	OPEN	TV
2718	2719			FRACTURE	215	STEEP	125		TV
2719		TRAM	UPPER (NW-PW)	CONTACT					L
2720	2724			FRACTURE	272	72	182	OPEN	TV
2722	2725			FRACTURE	250	70	160	OPEN	TV/C
2722	2726			FRACTURE	285	74	195		TV/C
2728	2729			FRACTURE	285	47	195		AT
2729	2729			FRACTURE	105	N. VERT	15		TV
2730	2732			FRACTURE	282	64	192		TV
2731	2732			FRACTURE	100	VERTICAL	10		TV
2732	2732			FRACTURE	0	VERTICAL	270		TV
2732	2733			FRACTURE	110	SHALLOW	20		TV
2733	2733			FRACTURE	105	SHALLOW	15	MINERALIZED	TV
2733	2734			FRACTURE	95	SHALLOW	5		TV
2734	2735			FRACTURE	240	58	150		TV
2734	2735			FRACTURE	250	62	160		TV
2734	2739			FRACTURE	245	79	155		TV
2736	2738			FRACTURE	90	>64	0		TV
2737	2741			FRACTURE	278	77	188		TV
2739	2740			FRACTURE	280	N. VERT	190		TV
2739	2744			FRACTURE	245	79	155		AT
2749	2751			FRACTURE	90	62	0		TV
2751	2754			FRACTURE	92	72	2	OPEN	TV
2752	2752			FRACTURE	275	N. VERT	185		TV
2752	2754			FRACTURE	265	66	175	OPEN	TV
2754	2755			FRACTURE	115	N. VERT	25		TV
2755	2759			FRACTURE	90	>78	0	OPEN	TV
2757	2757			FRACTURE	255	VERTICAL	165		TV
2757	2758			FRACTURE	265	VERTICAL	175		TV
2757	2761			FRACTURE	115	76	25		AT

TABLE 11. SUMMARY OF INFORMATION FROM LITHOLOGIC (L), TELEVISION (TV), ACOUSTIC TELEVIEWER (AT), CALIPER (C), AND TEMPERATURE (TEMP) LOGS FOR BOREHOLE UE-25C #2 --Continued

DEPTH BLW CASING (FEET)		GEOLOGIC UNIT	LITHOLOGIC ZONE	FEATURE	DIP AZI-MUTH	DIP ANGLE	STRIKE AZI-MUTH	REMARKS	LOG
TOP	BOT-TOM								
2758	2760	TRAM	UPPER (NW-PW)	FRACTURE	250	VERTICAL	160		TV
2758	2759			FRACTURE	255	VERTICAL	165		TV
2759	2759			FRACTURE	250	N. VERT	160		TV
2765	2766			FRACTURE	280	58	190		TV
2765	2766			FRACTURE	90	43	0		TV
2767	2768			FRACTURE	90	N. VERT	0	MINERALIZED	TV
2771	2772			FRACTURE	270	N. VERT	180		TV
2773	2774			FRACTURE	270	N. VERT	180		TV
2774	2774			FRACTURE	300	N. VERT	210		TV
2775			TUFF BRECCIA	CONTACT				ROCK VISIBLY BRECCIATED	TV/L
2776	2778			FRACTURE	270	59	180		TV
2777	2779			FRACTURE	295	69	205		TV
2780	2780			FRACTURE	170	SHALLOW	80	MINERALIZED	TV
2780	2780			FRACTURE	170	SHALLOW	80	MINERALIZED	TV
2781	2783			FRACTURE	255	63	165	MINERALIZED	TV
2781	2784			FRACTURE	262	73	172	INTERSECTS N-STRIKING FRACTURE AT 2782	TV
2782	2782			FRACTURE	80	VERTICAL	0		TV
2783	2784			FRACTURE	260	64	180		TV
2784	2787			FRACTURE	280	72	190		TV
2785	2787			FRACTURE	255	60	165		TV
2786	2789			FRACTURE	268	73	178		TV
2786	2788			FRACTURE	75	61	345		AT
2788	2790			FRACTURE	270	49	180	PARTLY MINERALIZED	TV
2789	2789			FRACTURE	0	SHALLOW	270	PARTLY MINERALIZED	TV
2789	2790			FRACTURE	270	SHALLOW	180	PARTLY MINERALIZED	TV
2790	2790			FRACTURE	270	SHALLOW	180		TV
2790	2790			FRACTURE	290	19	200	MINERALIZED	TV

TABLE 11. SUMMARY OF INFORMATION FROM LITHOLOGIC (L), TELEVISION (TV), ACOUSTIC TELEVIEWER (AT), CALIPER (C), AND TEMPERATURE (TEMP) LOGS FOR BOREHOLE UE-25C #2 --Continued

DEPTH BLW CASING (FEET)		GEOLOGIC UNIT	LITHOLOGIC ZONE	FEATURE	DIP AZIMUTH	DIP ANGLE	STRIKE AZIMUTH	REMARKS	LOG
TOP	BOTTOM								
2791	2792	TRAM	TUFF BRECCIA	FRACTURE	300	SHALLOW	210		TV
2793	2794			FRACTURE	278	56	188	OPEN; PAINTBRUSH CANYON FAULT ZONE 2793-2795	TV/L
2793	2794			FRACTURE	275	49	185		TV
2794	2795			FRACTURE	268	54	178	OPEN	TV
2795	2796			FRACTURE	25	STEEP	295		TV
2795	2797			FRACTURE	20	66	290	PARTLY MINERALIZED	TV
2796	2797			FRACTURE	280	56	190		AT
2796	2799			FRACTURE	286	72	196		AT
2796	2797			FRACTURE	315	STEEP	225		TV
2799	2799			FRACTURE	335	STEEP	245	MINERALIZED	TV
2799	2800			FRACTURE	225	N. VERT	135		TV
2800	2800			FRACTURE	250	STEEP	160	MINERALIZED	TV
2800	2800			FRACTURE	160	STEEP	70	MINERALIZED	TV
2800	2800			FRACTURE	355	STEEP	265	MINERALIZED	TV
2802	2802			FRACTURE	155	STEEP	65		TV
2802	2802			FRACTURE	270	STEEP	180	MINERALIZED	TV
2802	2802			FRACTURE	250	N. VERT	160		TV
2802	2803			FRACTURE	270	N. VERT	180		TV
2804	2804			FRACTURE	90	STEEP	0		TV
2804	2804			FRACTURE	215	N. VERT	125	MINERALIZED	TV
2805	2805			FRACTURE	260	N. VERT	170		TV
2805	2806			FRACTURE	340	N. VERT	250		TV
2806	2807			FRACTURE	240	N. VERT	150		TV
2806	2807			FRACTURE	260	N. VERT	170		TV
2807	2807			FRACTURE	300	STEEP	210		TV
2807	2808			FRACTURE	220	N. VERT	130		TV
2807	2808			FRACTURE	270	N. VERT	180		TV
2808	2810			FRACTURE	250	N. VERT	160		TV
2809	2810			FRACTURE	150	N. VERT	60		TV
2810	2812			FRACTURE	145	VERTICAL	55	MINERALIZED	TV

TABLE 11. SUMMARY OF INFORMATION FROM LITHOLOGIC (L), TELEVISION (TV), ACOUSTIC TELEVIEWER (AT), CALIPER (C), AND TEMPERATURE (TEMP) LOGS FOR BOREHOLE UE-25C #2 --Continued

DEPTH BLW CASING (FEET)		GEOLOGIC UNIT	LITHOLOGIC ZONE	FEATURE	DIP AZI-MUTH	DIP ANGLE	STRIKE AZI-MUTH	REMARKS	LOG
TOP	BOT-TOM								
2810	2811	TRAM	TUFF BRECCIA	FRACTURE	25	STEEP	295	MINERALIZED	TV
2811	2812			FRACTURE	295	SHALLOW	205	MINERALIZED	TV
2812	2813			FRACTURE	70	49	340	MINERALIZED	TV
2813	2814			FRACTURE	270	VERTICAL	180	MINERALIZED	TV
2814	2816			FRACTURE	265	STEEP	175		TV
2815	2816			FRACTURE	60	STEEP	330		TV
2815	2816			FRACTURE	270	STEEP	180		TV
2816	2816			FRACTURE	255	N. VERT	165		TV
2818	2818			FRACTURE	295	SHALLOW	205	MINERALIZED	TV
2821	2822			FRACTURE	270	N. VERT	180		TV
2822	2822			FRACTURE	270	N. VERT	180		TV
2822	2822			FRACTURE	270	N. VERT	180		TV
2822	2823			FRACTURE	305	N. VERT	215		TV
2822	2823			FRACTURE	350	N. VERT	260		TV
2824	2824			FRACTURE	280	N. VERT	190	MINERALIZED	TV
2824	2824			FRACTURE	345	42	255	MINERALIZED	TV
2824	2824			FRACTURE	85	N. VERT	355		TV
2824	2825			FRACTURE	270	N. VERT	180		TV
2824	2825			FRACTURE	345	SHALLOW	255	MINERALIZED	TV
2824	2825			FRACTURE	350	49	260	MINERALIZED	TV
2825	2826			FRACTURE	340	SHALLOW	250		TV
2825	2826			FRACTURE	175	SHALLOW	85	MINERALIZED	TV
2826	2826			FRACTURE	135	STEEP	45		TV
2826	2826			FRACTURE	300	N. VERT	210	MINERALIZED	TV
2826	2827			FRACTURE	340	STEEP	250	MINERALIZED	TV
2828	2829			FRACTURE	310	64	220		TV
2833	2833			FRACTURE	90	VERTICAL	0		TV
2833	2834			FRACTURE	35	N. VERT	305		TV
2834	2835			FRACTURE	100	N. VERT	10		TV

TABLE 11. SUMMARY OF INFORMATION FROM LITHOLOGIC (L), TELEVISION (TV), ACOUSTIC TELEVIEWER (AT), CALIPER (C), AND TEMPERATURE (TEMP) LOGS FOR BOREHOLE UE-25C #2 --Continued

DEPTH BLW CASING (FEET)		GEOLOGIC UNIT	LITHOLOGIC ZONE	FEATURE	DIP AZI-MUTH	DIP ANGLE	STRIKE AZI-MUTH	REMARKS	LOG
TOP	BOT-TOM								
2840	2842	TRAM	TUFF BRECCIA	FRACTURE	80	VERTICAL	350		TV
2840	2841			FRACTURE	325	N. VERT	235		TV
2841	2842			FRACTURE	335	VERTICAL	245		TV
2842	2842			FRACTURE	120	SHALLOW	30		TV
2843	2843			FRACTURE	90	VERTICAL	0		TV
2844	2844			FRACTURE	80	VERTICAL	350		TV
2845	2847			FRACTURE	0	65	270	MINERALIZED	TV
2861	2862			FRACTURE	235	STEEP	145		TV
2868	2869			FRACTURE	120	N. VERT	30	MINERALIZED	TV
2873	2875			FRACTURE	275	61-65	185		TV
2874	2875			FRACTURE	292	54	202		TV
2874	2876			FRACTURE	290	60	200		TV
2875	2876			FRACTURE	285	30	195		TV
2876	2876			FRACTURE	285	25	195		TV
2877	2878			FRACTURE	355	N. VERT	265		TV
2880	2880			FRACTURE	345	N. VERT	255		TV
2881	2882			FRACTURE	310	N. VERT	220		TV
2881	2882			FRACTURE	270	N. VERT	180		TV
2882	2883			FRACTURE	355	N. VERT	265		TV
2882	2883			FRACTURE	275	N. VERT	185		TV
2882	2883			FRACTURE	340	N. VERT	250		TV
2883	2883			FRACTURE	300	34	210		TV
2883	2884			FRACTURE	70	54	340		TV
2884	2884			FRACTURE	300	SHALLOW	210		TV
2884	2884			FRACTURE	70	STEEP	340		TV
2884	2884			FRACTURE	155	34	65		TV
2884	2885			FRACTURE	125	STEEP	35		TV
2885	2885			FRACTURE	225	SHALLOW	135		TV
2886	2887			FRACTURE	255	N. VERT	165		TV
2888	2889			FRACTURE	326	59	236		AT
2888	2888			FRACTURE	115	30	25		TV

TABLE 11. SUMMARY OF INFORMATION FROM LITHOLOGIC (L), TELEVISION (TV), ACOUSTIC TELEVIEWER (AT), CALIPER (C), AND TEMPERATURE (TEMP) LOGS FOR BOREHOLE UE-25C #2 --Continued

DEPTH BLW CASING (FEET)		GEOLOGIC UNIT	LITHOLOGIC ZONE	FEATURE	DIP AZI-MUTH	DIP ANGLE	STRIKE AZI-MUTH	REMARKS	LOG
TOP	BOT-TOM								
2889	2890	TRAM	TUFF BRECCIA	FRACTURE	90	30	0	MINERALIZED	TV
2890	2891			FRACTURE	295	35	205	MINERALIZED	TV
2892	2894			FRACTURE	265	69	175		TV
2893	2893			FRACTURE	250	STEEP	160		TV
2893	2893			FRACTURE	250	STEEP	160		TV
2893	2894			FRACTURE	280	58	190		TV
2896	2898			FRACTURE	282	71	192	OPEN	AT/TV
2897	2897			FRACTURE	110	43	20	MINERALIZED	TV
2897	2898			FRACTURE	270	N. VERT	180		TV
2897	2897			FRACTURE	115	19	25	MINERALIZED	TV
2897	2898			FRACTURE	300	30	210	MINERALIZED	TV
2898	2899			FRACTURE	295	35	205	MINERALIZED	TV
2899	2900			FRACTURE	295	30	205	MINERALIZED	TV
2900	2900			FRACTURE	295	30	205	MINERALIZED	TV
2901	2902			FRACTURE	155	46	65		TV
2901	2902			FRACTURE	280	39	190		TV
2902	2903			FRACTURE	270	SHALLOW	180	MINERALIZED	TV
2902	2903			FRACTURE	125	35	35		TV
2904	2904			FRACTURE	90	35	0		TV
2904	2904			FRACTURE	125	SHALLOW	35		TV
2904	2905			FRACTURE	60	N. VERT	330		TV
2905	2905			FRACTURE	180	STEEP	90		TV
2906	2906			FRACTURE	270	SHALLOW	180		TV
2906	2908			FRACTURE	270	58	180	OPEN	TV
2907	2907			FRACTURE	340	SHALLOW	250	MINERALIZED	TV
2907	2908			FRACTURE	275	35	185		TV
2907	2908			FRACTURE	300	SHALLOW	210	MINERALIZED	TV
2907	2908			FRACTURE	315	54	225	MINERALIZED	TV
2907	2908			FRACTURE	275	STEEP	185	OPEN	TV

TABLE 11. SUMMARY OF INFORMATION FROM LITHOLOGIC (L), TELEVISION (TV), ACOUSTIC TELEVIEWER (AT), CALIPER (C), AND TEMPERATURE (TEMP) LOGS FOR BOREHOLE UE-25C #2 --Continued

DEPTH BLW CASING (FEET)		GEOLOGIC UNIT	LITHOLOGIC ZONE	FEATURE	DIP AZIMUTH	DIP ANGLE	STRIKE AZIMUTH	REMARKS	LOG
TOP	BOTTOM								
2908	2908	TRAM	TUFF BRECCIA	FRACTURE	322	46	232	MINERALIZED	TV
2908	2909			FRACTURE	300	30	210		TV
2909	2909			FRACTURE	300	25	210		TV
2909	2909			FRACTURE	60	SHALLOW	330		TV
2910	2910			FRACTURE	315	N. VERT	225		TV
2910	2910			FRACTURE	355	N. VERT	265	MINERALIZED	TV
2910	2910			FRACTURE	300	SHALLOW	210	MINERALIZED	TV
2910	2910			FRACTURE	30	STEEP	300	MINERALIZED	TV
2910	2911			FRACTURE	345	STEEP	255	MINERALIZED	TV
2910	2911			FRACTURE	285	54	195		AT
2910	2911			FRACTURE	205	STEEP	115		TV
2910	2911			FAULT	90	VERTICAL	0	OFFSETS SW-STRIKING FRACTURE AT 2911	TV
2911	2911			FRACTURE	300	SHALLOW	210	OFFSET BY FAULT	TV
2912	2913			FRACTURE	30	N. VERT	300	MINERALIZED	TV
2912	2913			FRACTURE	45	STEEP	315		TV
2912	2914			FRACTURE	5	52	275	MINERALIZED	TV
2913	2914			FRACTURE	0	55	270	MINERALIZED	TV
2914	2914			FRACTURE	255	SHALLOW	165		TV
2914	2915			FRACTURE	70	SHALLOW	340		TV
2914	2914			FRACTURE	200	SHALLOW	110		TV
2914	2915			FRACTURE	100	SHALLOW	10		TV
2915	2916			FRACTURE	195	SHALLOW	105	MINERALIZED	TV
2916	2917			FRACTURE	50	55	320	MINERALIZED	TV
2918	2919			FRACTURE	10	57	280		TV
2919	2920			FRACTURE	2	25	272	MINERALIZED	TV
2920	2920			FRACTURE	2	25	272	MINERALIZED	TV
2921	2921			FRACTURE	105	25	15	MINERALIZED	TV
2922	2922			FRACTURE	165	25	75		TV
2922	2923			FRACTURE	295	SHALLOW	205		TV
2923	2923			FRACTURE	355	19	265		TV

TABLE 11. SUMMARY OF INFORMATION FROM LITHOLOGIC (L), TELEVISION (TV), ACOUSTIC TELEVIEWER (AT), CALIPER (C), AND TEMPERATURE (TEMP) LOGS FOR BOREHOLE UE-25C #2 --Continued

DEPTH BLW CASING (FEET)		GEOLOGIC UNIT	LITHOLOGIC ZONE	FEATURE	DIP AZI-MUTH	DIP ANGLE	STRIKE AZI-MUTH	REMARKS	LOG
TOP	BOT-TOM								
2923	2925	TRAM	TUFF BRECCIA	FRACTURE	85	59	355		TV
2923	2924			FRACTURE	300	25	210		TV
2924	2925			FRACTURE	25	52	295		TV
2925	2926			FRACTURE	165	>43	75		TV
2925	2926			FRACTURE	55	STEEP	325		TV
2926	2926			FRACTURE	355	43	265		TV
2926	2927			FRACTURE	355	43	265		TV
2927	2928			FRACTURE	348	43	258		TV
2927	2929			FRACTURE	65	69	235	OPEN	TV
2933	2933			FRACTURE	355	30	265		TV
2933	2934			FRACTURE	340	30	250		TV
2935			LOWER (PW)	CONTACT					L
2936	2937			FRACTURE	325	35	235		TV
2937	2938			FRACTURE	165	N. VERT	75		TV
2939	2942			FRACTURE	160	>76	70		TV
2943	2943			FRACTURE	300	SHALLOW	210	MINERALIZED	TV
2945	2946			FRACTURE	340	VERTICAL	255		TV
2946	2946			FRACTURE	260	25	170		TV
2960	2961			FRACTURE	265	25	175	OPEN	TV
2986				BOTTOM				HOLE CAVED TO ORIGINAL TD AT 3000	TV

TABLE 12. SUMMARY OF INFORMATION FROM LITHOLOGIC (L), TELEVISION (TV), ACOUSTIC TELEVIEWER (AT), CALIPER (C), AND TEMPERATURE (TEMP) LOGS FOR BOREHOLE UE-25C #3

[Abbreviations for tables 10, 11, and 12: CSG, casing; NW, nonwelded; NW-PW, nonwelded to partially welded; MW, moderately welded; MW-DW, moderately to densely welded; PW-NW, partially welded to nonwelded; PW, partially welded; N.VERT, near vertical; LITH, lithologic; TD, total depth; N, north, S, south; SW, southwest, SE, southeast; SSW, south-southwest]

DEPTH BLW CASING (FEET)		GEOLOGIC UNIT	LITHOLOGIC ZONE	FEATURE	DIP AZIMUTH	DIP ANGLE	STRIKE AZIMUTH	REMARKS	LOG
TOP	BOTTOM								
1316		CALICO HILLS	NW	WATER TABLE				DEAD INSECT ON WATER SURFACE	TV
1320	1368			CONCRETE				SPALLED, ROUGH; HOLE ABRUPTLY ENLARGED BELOW	TV/C
1370	1372			GOUGED ZONE				SPIRALED WASHOUTS	TV/AT
1382	1383			CORRUGATED				HORIZONTAL WASHOUTS	TV
1389	1406			GOUGED ZONE				SPIRALED WASHOUTS	TV/AT
1413	1414			FRACTURE	93	N. VERT	3		TV
1416	1418			CORRUGATED				HORIZONTAL WASHOUTS	TV
1433	1435			FRACTURE	82	54	352	OPEN AT UPTOE	TV
1444	1445			FRACTURE	68	>48	338		TV
1444	1445			FRACTURE	310	N. VERT	220		TV
1445	1449			FRACTURE	65	>73	335		TV
1446	1450			FRACTURE	58	>74	328		TV
1483	1490			FRACTURE	90	>79	0		TV
1491	1493			FRACTURE	90	51	0		TV
1492	1498			FRACTURE	232	77	142	OPEN AT DOWNTOE	TV
1493	1495			FRACTURE	88	50	358		TV
1493	1498			FRACTURE	268	75	178	OPEN AT DOWNTOE	TV
1495	1499			FRACTURE	263	70	173	OPEN AT DOWNTOE	TV
1496	1504			FRACTURE	75	>79	345	OPEN	TV
1499	1501			FRACTURE	275	>57	185	OPEN AT DOWNTOE	TV
1499	1502			FRACTURE	263	61	173	OPEN AT DOWNTOE	TV
1505	1510			FRACTURE	98	77	8		TV
1512	1513			FRACTURE	315	44	225		TV
1513	1514			LEDGE				HOLE DIAMETER REDUCED	TV
1514	1514			FRACTURE	325	SHALLOW	235		TV
1516	1519			FRACTURE	110	>68	20		TV
1518	1520			FRACTURE	100	N. VERT	10		TV
1520	1521			FRACTURE	95	N. VERT	5		TV
1521	1522			FRACTURE	UNK	N. VERT	UNK		TV
1534	1541			FRACTURE	270	>82	180		TV

TABLE 12. SUMMARY OF INFORMATION FROM LITHOLOGIC (L), TELEVISION (TV), ACOUSTIC TELEVIEWER (AT), CALIPER (C), AND TEMPERATURE (TEMP) LOGS FOR BOREHOLE UE-25C #3 --Continued

DEPTH BLW CASING (FEET)		GEOLOGIC UNIT	LITHOLOGIC ZONE	FEATURE	DIP AZIMUTH	DIP ANGLE	STRIKE AZIMUTH	REMARKS	LOG
TOP	BOTTOM								
1536	1542	CALICO HILLS	NW	FRACTURE	255	>81	165		TV
1543	1543			FRACTURE	200	23	110		TV
1552	1553			FRACTURE	200	23	110		TV
1560			BEDDED	CONTACT					L
1569	1569			FRACTURE	200	23	110		TV
1581	1582			FRACTURE	200	23	110		TV
1581	1582			FRACTURE	200	23	110		TV
1582	1582			FRACTURE	115	SHALLOW	25		TV
1582	1584			FRACTURE	170	64	80		TV
1585	1586			FRACTURE	210	24	120		TV
1615	1618			FRACTURE	115	71	25	CAVERNOUS INTERSECTION WITH SSW FRACTURE AT 1616	TV
1616	1617			FRACTURE	292	41	202		TV
1616	1616			FRACTURE	230	33	140		TV
1616	1617			FRACTURE	230	23	140		TV
1616	1617			FRACTURE	230	23	140		TV
1617	1617			FRACTURE	235	24	145		TV
1619	1620			FRACTURE	105	29	15		AT
1620	1620			FRACTURE	95	38	5		AT
1622	1623			FRACTURE	260	N. VERT	170		TV
1622	1625			FRACTURE	145	>69	55	OPEN; HOLE ENLARGED BY FRACTURES 1622-1625	TV
1623	1624			FRACTURE	2	37	272	OPEN	TV
1624	1625			FRACTURE	95	N. VERT	5	OPEN	TV
1624	1625			FRACTURE	140	N. VERT	50		TV
1624	1624			FRACTURE	280	N. VERT	190	OPEN	TV
1624	1625			FRACTURE	245	STEEP	155		TV
1624	1625			FRACTURE	255	>47	165		TV

TABLE 12. SUMMARY OF INFORMATION FROM LITHOLOGIC (L), TELEVISION (TV), ACOUSTIC TELEVIEWER (AT), CALIPER (C), AND TEMPERATURE (TEMP) LOGS FOR BOREHOLE UE-25C #3 --Continued

DEPTH BLW CASING (FEET)		GEOLOGIC UNIT	LITHOLOGIC ZONE	FEATURE	DIP AZIMUTH	DIP ANGLE	STRIKE AZIMUTH	REMARKS	LOG
TOP	BOTTOM								
1625	1627	CALICO HILLS	BEDDED	FRACTURE	245	>57	155	MINERALIZED	TV
1626	1627			FRACTURE	75	53	345	MINERALIZED	AT/TV
1628	1629			FRACTURE	265	58	175	MINERALIZED	AT/TV
1628	1628			FRACTURE	235	25	145	MINERALIZED	TV
1629	1630			FRACTURE	105	54	15	OPEN	TV
1629	1631	PROW PASS	NW-PW	CONTACT				OPEN PARTING AT CONTACT	TV
1631	1631			FRACTURE	75	35	345	HOLE ENLARGED BY FRACTURES 1631-1638	TV
1633	1633			FRACTURE	170	>33	80		TV
1633	1634			FRACTURE	335	>45	245		TV
1634	1635			FRACTURE	155	SHALLOW	65		TV
1635	1636			FRACTURE	325	SHALLOW	235	MINERALIZED	TV
1638	1638			FRACTURE	350	SHALLOW	260	MINERALIZED	TV
1639	1639			FRACTURE	25	SHALLOW	295		AT
1640	1640			FRACTURE	130	27	40		TV
1651	1652			FRACTURE	95	SHALLOW	5	MINERALIZED	TV
1657	1658			FRACTURE	60	33	330	MINERALIZED	TV
1666	1669			FRACTURE	300	70	210		TV
1668	1669			FRACTURE	190	N. VERT	100		TV
1672	1674			FRACTURE	265	N. VERT	175		TV
1750	1751			FRACTURE	326	58	236		TV
1751	1752			FRACTURE	335	>52	245		TV
1751	1752			FRACTURE	91	>50	1		TV
1752	1752			FRACTURE	150	STEEP	60		TV
1753	1755			FRACTURE	205	>59	115	MINERALIZED	TV
1760	1760			FRACTURE	323	49	233	MINERALIZED	AT/TV
1761	1761			FRACTURE	60	34	330	MINERALIZED	TV
1771	1773			FRACTURE	100	61	10	MINERALIZED	AT/TV
1776	1776			FRACTURE	268	SHALLOW	178	MINERALIZED	TV
1778	1782			FRACTURE	305	76	215		AT

TABLE 12. SUMMARY OF INFORMATION FROM LITHOLOGIC (L), TELEVISION (TV), ACOUSTIC TELEVIEWER (AT), CALIPER (C), AND TEMPERATURE (TEMP) LOGS FOR BOREHOLE UE-25C #3 --Continued

DEPTH BLW CASING (FEET)		GEOLOGIC UNIT	LITHOLOGIC ZONE	FEATURE	DIP AZIMUTH	DIP ANGLE	STRIKE AZIMUTH	REMARKS	LOG
TOP	BOTTOM								
1779	1779	PROW PASS	NW-PW	FRACTURE	325	N. VERT	235		TV
1780			MW	CONTACT					L
1795	1797			FRACTURE	260	68	170	MINERALIZED	TV
1796	1796			FRACTURE	130	N. VERT	40		TV
1804	1806			FRACTURE	300	72	210		AT
1805	1806			FRACTURE	180	N. VERT	90		TV
1806	1807			FRACTURE	55	>58	325		TV
1813	1814			FRACTURE	310	STEEP	220	MINERALIZED	TV
1814	1815			FRACTURE	270	STEEP	180	MINERALIZED	TV
1814	1815			FRACTURE	200	N. VERT	110	MINERALIZED	TV
1815	1817			FRACTURE	285	66	195	MINERALIZED	AT/TV
1820	1823			FRACTURE	250	73	160		AT
1825	1825			FRACTURE	140	19	50		TV
1825	1826			FRACTURE	145	19	55	MINERALIZED	TV
1829	1830			FRACTURE	50	35	320		TV
1830			PW-NW	CONTACT					L
1830	1831			FRACTURE	262	N. VERT	172		TV
1831	1833			FRACTURE	245	N. VERT	155		TV
1835	1835			FRACTURE	135	>25	45		TV
1835	1835			FRACTURE	285	SHALLOW	195	MINERALIZED	TV
1837	1839			FRACTURE	20	>58	290		TV
1846	1847			FRACTURE	160	N. VERT	70		TV
1849	1852			FRACTURE	268	75	178		TV
1855	1860			FRACTURE	270	>80	180		TV
1863	1865			FRACTURE	245	N. VERT	155		TV
1938	1938			FRACTURE	355	30	265	MINERALIZED	TV
2085			BEDDED	CONTACT					L

TABLE 12. SUMMARY OF INFORMATION FROM LITHOLOGIC (L), TELEVISION (TV), ACOUSTIC TELEVIEWER (AT), CALIPER (C), AND TEMPERATURE (TEMP) LOGS FOR BOREHOLE UE-25C #3 --Continued

DEPTH BLW CASING (FEET)		GEOLOGIC UNIT	LITHOLOGIC ZONE	FEATURE	DIP AZIMUTH	DIP ANGLE	STRIKE AZIMUTH	REMARKS	LOG
TOP	BOTTOM								
2112		BULLFROG	NW-PW	CONTACT				TEXTURE BECOMES COARSER	TV/L
2116	2117			FRACTURE	350	23	260		TV
2116	2117			FRACTURE	350	23	260		TV
2117	2117			FRACTURE	350	18	260		TV
2117	2117			FRACTURE	350	24	260		TV
2117	2118			FRACTURE	350	24	260		TV
2118	2118			FRACTURE	350	38	260		TV
2119	2119			FRACTURE	350	29	260		TV
2119	2119			FRACTURE	350	24	260		TV
2120	2120			FRACTURE	350	24	260		TV
2120	2121			FRACTURE	350	29	260		TV
2121	2121			FRACTURE	350	24	260		TV
2122	2123			FRACTURE	345	18	255		TV
2123	2124			FRACTURE	345	29	255		TV
2124	2125			FRACTURE	345	38	255		TV
2125	2125			FRACTURE	345	24	255		TV
2126	2126			FRACTURE	345	29	255	MINERALIZED	TV
2128	2129			FRACTURE	275	29	185	MINERALIZED	TV
2128	2129			FRACTURE	110	48	20	MINERALIZED	TV
2128	2129			FRACTURE	345	38	255	MINERALIZED	TV
2129	2130			FRACTURE	290	N. VERT	200		TV
2129	2130			FRACTURE	285	N. VERT	195		TV
2130	2131			FRACTURE	275	N. VERT	185		TV
2130	2132			FRACTURE	285	64	195		TV
2143	2147			FRACTURE	245	>77	155		TV
2174	2177			FRACTURE	270	75	180	MINERALIZED	TV
2210		BULLFROG	MW-DW	CONTACT					L
2258	2268			FRACTURE	280	85	190	MINERALIZED	AT/TV
2263	2269			FRACTURE	275	82	185	MINERALIZED	AT/TV
2267	2271			FRACTURE	285	76	195	MINERALIZED	AT/TV
2286	2292			FRACTURE	260	81	170	MINERALIZED	AT/TV

TABLE 12. SUMMARY OF INFORMATION FROM LITHOLOGIC (L), TELEVISION (TV), ACOUSTIC TELEVIEWER (AT), CALIPER (C), AND TEMPERATURE (TEMP) LOGS FOR BOREHOLE UE-25C #3 --Continued

DEPTH BLW CASING (FEET)		GEOLOGIC UNIT	LITHOLOGIC ZONE	FEATURE	DIP AZIMUTH	DIP ANGLE	STRIKE AZIMUTH	REMARKS	LOG
TOP	BOTTOM								
2294	2302	BULLFROG	MW-DW	FRACTURE	255	83	165	MINERALIZED	AT/TV
2298	2308			FRACTURE	175	85	85	MINERALIZED	TV
2333	2333			FRACTURE	315	SHALLOW	225	MINERALIZED	TV
2337	2342			FRACTURE	255	83	165	MINERALIZED	AT/TV
2340	2342			FRACTURE	295	58	205	MINERALIZED	AT/TV
2343	2344			FRACTURE	285	56	195	MINERALIZED	AT/TV
2347	2348			FRACTURE	280	54	190	MINERALIZED	AT/TV
2349	2353			FRACTURE	270	78	180	MINERALIZED	AT/TV
2352	2353			FRACTURE	285	N. VERT	195	MINERALIZED	TV
2353	2356			FRACTURE	295	>72	205	MINERALIZED	TV
2354	2354			FRACTURE	295	35	205		AT
2356	2357			FRACTURE	180	52	90		TV
2368	2369			FRACTURE	235	N. VERT	145	MINERALIZED	TV
2368	2372			FRACTURE	260	80	170	MINERALIZED	AT/TV
2372	2373			FRACTURE	255	N. VERT	165	MINERALIZED	TV
2374	2375			FRACTURE	295	N. VERT	205		TV
2374	2374			FRACTURE	220	N. VERT	130		TV
2374	2379			FRACTURE	245	80	155	OPEN	AT/TV
2379	2379			FRACTURE	245	VERTICAL	155		TV
2379	2379			FRACTURE	250	SHALLOW	160		TV
2379	2380			FRACTURE	200	N. VERT	110		TV
2380	2381			FRACTURE	210	N. VERT	120		TV
2382	2385			FRACTURE	195	>77	105	MINERALIZED	TV
2421	2426			FRACTURE	275	81	185	OPEN	AT/TV
2422	2428			FRACTURE	270	82	180	OPEN	AT/TV
2424	2431			FRACTURE	275	83	185	OPEN	AT/TV
2430		BULLFROG	PW-NW	CONTACT					L
2430	2440			FRACTURE	275	83	185	OPEN	AT/TV
2443	2451			FRACTURE	260	83	170	OPEN	TV

TABLE 12. SUMMARY OF INFORMATION FROM LITHOLOGIC (L), TELEVISION (TV), ACOUSTIC TELEVIEWER (AT), CALIPER (C), AND TEMPERATURE (TEMP) LOGS FOR BOREHOLE UE-25C #3 --Continued

DEPTH BLW CASING (FEET)		GEOLOGIC UNIT	LITHOLOGIC ZONE	FEATURE	DIP AZIMUTH	DIP ANGLE	STRIKE AZIMUTH	REMARKS	LOG
TOP	BOTTOM								
2444	2448	BULLFROG	PW-NW	FRACTURE	255	72	165	OPEN	AT/TV
2445	2462			FRACTURE	255	87	165	OPEN	TV
2446	2464			FRACTURE	268	87	178	OPEN	TV
2447	2465			FRACTURE	262	87	172	OPEN	TV
2450	2452			FRACTURE	85	>62	355		TV
2454	2456			FRACTURE	280	N. VERT	190	MINERALIZED	TV
2470	2475			FRACTURE	260	80	170		TV
2476	2478			FRACTURE	270	>67	180		TV
2480	2480			FRACTURE	200	SHALLOW	110		TV
2503	2504			FRACTURE	285	VERTICAL	195		TV
2511	2525			FRACTURE	275	87	185	OPEN AT DOWNTOE	TV
2520	2521			FRACTURE	285	VERTICAL	195		TV
2521	2527			FRACTURE	265	80	175	OPEN	TV
2556	2557			FRACTURE	115	42	25	OPEN	TV
2563	2563			FRACTURE	270	N. VERT	180		TV
2611	2612			FRACTURE	265	N. VERT	175	MINERALIZED	TV
2619	2620			FRACTURE	85	49	355		TV
2650			BEDDED	CONTACT				SMOOTHER TEXTURE, NO LITHICS	L/TV
2670		TRAM	UPPER (NW-PW)					COARSER TEXTURE, SMALL WHITE CLASTS	L/TV
2685	2686			FRACTURE	125	49	35	OPEN	AT/TV
2690	2691			FRACTURE	54	38	324		TV
2690	2691			FRACTURE	50	42	320		TV
2692	2692			FRACTURE	50	34	320		TV
2692	2693			FRACTURE	50	29	320		TV
2693	2693			FRACTURE	50	34	320		TV
2694	2697			FRACTURE	155	69	65		TV
2695	2696			FRACTURE	10	N. VERT	280		TV
2696	2696			FRACTURE	265	N. VERT	175		TV

TABLE 12. SUMMARY OF INFORMATION FROM LITHOLOGIC (L), TELEVISION (TV), ACOUSTIC TELEVIEWER (AT), CALIPER (C), AND TEMPERATURE (TEMP) LOGS FOR BOREHOLE UE-25C #3 --Continued

DEPTH BLW CASING (FEET)		GEOLOGIC UNIT	LITHOLOGIC ZONE	FEATURE	DIP AZIMUTH	DIP ANGLE	STRIKE AZIMUTH	REMARKS	LOG
TOP	BOTTOM								
2697	2698	TRAM	UPPER (NW-PW)	FRACTURE	255	N. VERT	165		TV
2702	2702			FRACTURE	355	39	265		TV
2703	2704			FRACTURE	125	24	35	OPEN	AT/TV
2704	2704			FRACTURE	305	19	215		TV
2708	2709			FRACTURE	355	24	265		TV
2711	2711			FRACTURE	80	24	350		TV
2711	2713			FRACTURE	55	67	325		TV
2713	2713			FRACTURE	350	38	260		TV
2720	2721			FRACTURE	350	42	260		TV
2728	2730			FRACTURE	100	55	10		TV
2734	2735			FRACTURE	340	34	250		TV
2735	2735			FRACTURE	340	24	250		TV
2740	2741			FRACTURE	335	24	245		TV
2740	2741			FRACTURE	335	38	245		TV
2742	2743			FRACTURE	335	29	245		TV
2742	2743			FRACTURE	78	53	348		TV
2744	2745			FRACTURE	330	33	240		TV
2747	2748			FRACTURE	85	24	355		TV
2749	2749			FRACTURE	90	29	0	MINERALIZED	TV
2750	2751			FRACTURE	90	33	0		TV
2752	2752			FRACTURE	280	34	190		TV
2753	2754			FRACTURE	82	51	352		TV
2753	2754			FRACTURE	325	38	235		TV
2753	2754			FRACTURE	98	45	8		TV
2755	2755			FRACTURE	315	34	225		TV
2758	2759			FRACTURE	315	38	225		TV
2760	2761			FRACTURE	90	42	0		TV
2760	2761			FRACTURE	90	25	0		TV
2762	2763			FRACTURE	335	N. VERT	245		TV

TABLE 12. SUMMARY OF INFORMATION FROM LITHOLOGIC (L), TELEVISION (TV), ACOUSTIC TELEVIEWER (AT), CALIPER (C), AND TEMPERATURE (TEMP) LOGS FOR BOREHOLE UE-25C #3 --Continued

DEPTH BLW CASING (FEET)		GEOLOGIC UNIT	LITHOLOGIC ZONE	FEATURE	DIP AZIMUTH	DIP ANGLE	STRIKE AZIMUTH	REMARKS	LOG
TOP	BOTTOM								
2763	2763	TRAM	UPPER (NW-PW)	FRACTURE	315	19	225		TV
2763	2765			FRACTURE	95	64	5		TV
2764	2765			FRACTURE	90	60	0		TV
2764	2765			FRACTURE	270	N. VERT	180		TV
2765	2767			FRACTURE	170	61	80		TV
2766	2767			FRACTURE	90	54	0		TV
2770	2772			FRACTURE	85	72	355		TV
2771	2773			FRACTURE	90	60	0		TV
2772	2773			FRACTURE	92	65	2		TV
2773	2774			FRACTURE	90	60	0		TV
2774	2774			FRACTURE	290	N. VERT	200		TV
2776	2777			FRACTURE	95	65	5		TV
2777	2778			FRACTURE	90	>49	0		TV
2777	2778			FRACTURE	95	>56	5		TV
2777	2778			FRACTURE	280	61	190		TV
2777	2778			FRACTURE	305	STEEP	215		TV
2782	2783			FRACTURE	85	53	355		TV
2783	2784			FRACTURE	92	64	2		TV
2785	2788			FRACTURE	110	70	20		TV
2787	2788			FRACTURE	85	>59	355		TV
2790	2792			FRACTURE	280	59	190		TV
2791	2793			FRACTURE	82	65	352		TV
2793	2794			FRACTURE	85	>51	355		TV
2793	2795			FRACTURE	270	62	180		TV
2796	2798			FRACTURE	80	>58	350		TV
2798	2799			FRACTURE	330	SHALLOW	240	MINERALIZED	TV
2801	2801			FRACTURE	195	N. VERT	105		TV
2803	2804			FRACTURE	345	N. VERT	255	BOREHOLE WALLS SHATTERED 2803-2804	TV
2803	2804			FRACTURE	345	N. VERT	255		TV
2803	2804			FRACTURE	92	56	2		TV

TABLE 12. SUMMARY OF INFORMATION FROM LITHOLOGIC (L), TELEVISION (TV), ACOUSTIC TELEVIEWER (AT), CALIPER (C), AND TEMPERATURE (TEMP) LOGS FOR BOREHOLE UE-25C #3 --Continued

DEPTH BLW CASING (FEET)		GEOLOGIC UNIT	LITHOLOGIC ZONE	FEATURE	DIP AZIMUTH	DIP ANGLE	STRIKE AZIMUTH	REMARKS	LOG
TOP	BOTTOM								
2803	2804	TRAM	UPPER (NW-PW)	FRACTURE	90	SHALLOW	0		TV
2804	2804			FRACTURE	270	N. VERT	180		TV
2804	2805		TUFF BRECCIA	CONTACT	W	51	S	TEXTURE BECOMES VERY COARSE (PATCHY)	TV
2805	2806			FRACTURE	230	STEEP	140		TV
2807	2808			FRACTURE	90	SHALLOW	0	PAINTBRUSH CN? FAULT ZONE 2807-2828 ON LITH LOG	TV
2811	2811			FRACTURE	170	SHALLOW	80		TV
2814	2814			FRACTURE	265	STEEP	175		TV
2814	2814			FRACTURE	90	SHALLOW	0		TV
2814	2816			FRACTURE	80	65	350		TV
2819	2820			FRACTURE	75	STEEP	345		TV
2820	2821			FRACTURE	305	51	215	OPEN	AT/TV
2824	2825			FRACTURE	285	58	195	OPEN	AT/TV
2824	2825			FRACTURE	75	49	345		TV
2824	2825			FRACTURE	70	SHALLOW	340		TV
2825	2825			FRACTURE	335	N. VERT	245		TV
2825	2825			FRACTURE	60	SHALLOW	330		TV
2825	2826			FRACTURE	307	55	217		AT
2827	2828			FRACTURE	270	58	180		AT
2830	2830			FRACTURE	50	43	320	MINERALIZED	TV
2830	2831			FRACTURE	240	STEEP	150		TV
2830	2832	TRAM	TUFF BRECCIA	FRACTURE	300	62	210		AT
2831	2832			FRACTURE	65	STEEP	335		TV
2831	2838			FRACTURE	285	>78	195	CAVERNOUS; HOLE FOLLOWS FRACTURE	TV
2839	2841			FRACTURE	305	66	215	BOREHOLE WALLS SHATTERED	AT/TV
2843	2843			FRACTURE	75	34	345	MINERALIZED; HOLE ENLARGED BY FRACTURES 2839-2872	TV

TABLE 12. SUMMARY OF INFORMATION FROM LITHOLOGIC (L), TELEVISION (TV), ACOUSTIC TELEVIEWER (AT), CALIPER (C), AND TEMPERATURE (TEMP) LOGS FOR BOREHOLE UE-25C #3 --Continued

DEPTH BLW CASING (FEET)		GEOLOGIC UNIT	LITHOLOGIC ZONE	FEATURE	DIP AZIMUTH	DIP ANGLE	STRIKE AZIMUTH	REMARKS	LOG
TOP	BOTTOM								
2849	2849	TRAM	TUFF BRECCIA	FRACTURE	210	SHALLOW	120		TV
2849	2850			FRACTURE	10	37	280		TV
2849	2850			FRACTURE	95	STEEP	5		TV
2850	2851			FRACTURE	35	54	305	OPEN; ROCK VERY BRECCIATED 2850-2877	TV
2865	2868			FRACTURE	265	N. VERT	175		TV
2869	2870			FRACTURE	265	N. VERT	175		TV
2871	2872			FRACTURE	78	49	348		TV
2872	2877			FRACTURE	270	>79	180		TV
2880	2881			FRACTURE	122	56	32	MINERALIZED	TV
2881	2881			FRACTURE	68	35	338	MINERALIZED	TV
2881	2883			FRACTURE	120	63	30	MINERALIZED	TV
2881	2882			FRACTURE	55	49	325	MINERALIZED	TV
2884	2885			FRACTURE	65	49	335		TV
2884	2885			FRACTURE	47	49	317	MINERALIZED	TV
2886	2886			FRACTURE	60	42	330		TV
2886	2887			FRACTURE	55	49	325		TV
2886	2887			FRACTURE	75	58	345		TV
2886	2887			FRACTURE	65	45	335	MINERALIZED	TV
2887	2888			FRACTURE	70	51	340	MINERALIZED	TV
2887	2888			FRACTURE	65	55	335	MINERALIZED	TV
2888	2889			FRACTURE	45	51	315	MINERALIZED	TV
2888	2889			FRACTURE	45	38	315	MINERALIZED	TV
2888	2889			FRACTURE	45	38	315	MINERALIZED	TV
2892	2893			FRACTURE	45	54	315	MINERALIZED	TV
2892	2893			FRACTURE	45	54	315	MINERALIZED	TV
2895	2896			FRACTURE	40	49	310	MINERALIZED	TV
2895	2896			FRACTURE	40	58	310	MINERALIZED	TV
2896	2897			FRACTURE	40	53	310	MINERALIZED	TV
2898	2899			FRACTURE	65	51	335	MINERALIZED	TV
2899	2900			FRACTURE	60	52	330	MINERALIZED	TV

TABLE 12. SUMMARY OF INFORMATION FROM LITHOLOGIC (L), TELEVISION (TV), ACOUSTIC TELEVIEWER (AT), CALIPER (C), AND TEMPERATURE (TEMP) LOGS FOR BOREHOLE UE-25C #3 --Continued

DEPTH BLW CASING (FEET)		GEOLOGIC UNIT	LITHOLOGIC ZONE	FEATURE	DIP AZI-MUTH	DIP ANGLE	STRIKE AZI-MUTH	REMARKS	LOG
TOP	BOT-TOM								
2899	2900	TRAM	TUFF BRECCIA	FRACTURE	65	STEEP	335		TV
2900	2901			FRACTURE	85	52	355		TV
2900	2901			FRACTURE	95	46	5	MINERALIZED	TV
2902	2904			FRACTURE	80	52	350		TV
2903	2903			FRACTURE	5	SHALLOW	275		TV
2904	2905			FRACTURE	80	52	350		TV
2904	2905			FRACTURE	45	56	315		TV
2906	2907			FRACTURE	0	25	270		TV
2906	2907			FRACTURE	90	30	0		TV
2907	2908			FRACTURE	70	42	340		TV
2907	2907			FRACTURE	65	30	335		TV
2908	2908			FRACTURE	40	30	310		TV
2908	2908			FRACTURE	175	SHALLOW	85		TV
2908	2909			FRACTURE	40	35	310		TV
2909	2909			FRACTURE	40	43	310		TV
2910	2910			FRACTURE	155	43	65		TV
2923	2924			FRACTURE	112	46	22		TV
2926	2928			FRACTURE	5	67	275		TV
2932	2933			FRACTURE	260	VERTICAL	170		TV
2937	2940			FRACTURE	85	>76	355		TV
2940	2942			FRACTURE	95	62	5		TV
2944	2945			FRACTURE	90	54	0		TV
2950	2954			CABLE				RESTING ON BOTTOM OF HOLE	TV
2954				BOTTOM				HOLE CAVED TO ORIGINAL TD AT 3000	TV/C